Epstein Barr Virus: Environmental Trigger and Therapeutic Target in Autoimmune Diseases

---

Dissertation

zur

Erlangung der naturwissenschaftlichen Doktorwürde

(Dr. sc. nat.)

vorgelegt der

Mathematisch-naturwissenschaftlichen Fakultät

der Universität Zürich

von

Kristina Krasimirova Kakalacheva

aus Bulgarien

Promotionskomitee

Prof. Dr. rer. nat. Christian Münz (Vorsitz)

Prof. Dr. med. Jan Lünemann (Leitung der Dissertation)

Prof. Dr. rer. nat. Burkhard Becher

Prof. Dr. med. Burkhard Ludewig

Zürich, 2014

TABLE OF CONTENTS

DISCLAIMER

This thesis is partly based on the following two published original articles and one review paper:

Kakalacheva K, Maurer MA, Tackenberg B, Münz C, Willcox N, Lünemann JD. Intrathymic Epstein-Barr virus infection is not a prominent feature of myasthenia gravis. *Ann Neurol*. 2011 Sep;70(3):508-14

Comabella M, Kakalacheva K, Río J, Münz C, Montalban X, Lünemann JD. EBV-specific immune responses in patients with multiple sclerosis responding to IFN-β therapy. *Mult Scler*. 2012 May;18(5):605-9

Kakalacheva K, Münz C, Lünemann JD. Viral triggers of multiple sclerosis. *Biochim Biophys Acta*. 2011 Feb;1812(2):132-40

SUMMARY

Epstein-Barr virus (EBV) is a ubiquitous pathogen that infects more than 95% of the human adult population. Most people acquire the virus asymptomatically early in their childhood, while a small percentage who acquire the virus later in life would develop symptomatic primary infection called infectious mononucleosis (IM). After lytically replicating in the early stages of the primary infection, EBV establishes latency in B cells and is maintained for a lifetime. Even though the majority of EBV carriers are not affected by the virus, EBV infection and particularly a history of IM have been associated with a number of malignancies such as Burkitt's and Hodgkin's lymphoma, posttransplant proliferative disease, and nasopharyngeal carcinomas among others. Moreover, accumulating evidence points towards an association of the virus with several autoimmune diseases such as multiple sclerosis (MS) and myasthenia gravis (MG). Despite a plethora of conflicting studies implicating EBV in the immuno-pathogenesis of these autoimmune diseases, the exact mechanism of causation has not yet been clearly elucidated. To address this issue we designed three studies that respectively looked at the association of the virus with autoreactivity during IM, EBV responses in IFN-β treated MS patients, and involvement of EBV in MG.

In the first study, we hypothesized that during the fulminant infection of IM, persistent autoreactive humoral and cellular immune responses are generated that eventually lead to autoimmune-pathologies later in life. We discovered considerable humoral poly-autoreactivity that positively correlated with EBV viral load. These results suggest a potential role of EBV-associated humoral immune responses in contributing to immunopathologies later in life.

Next, we investigated whether IFN-β treatment affects EBV-specific immune responses in MS patients. We observed decreased cellular responses to EBNA1 but not to other EBV antigens in MS patients who responded to IFN-β treatment, which hinted at the role of EBNA1-specific T cells in the pathogenesis of the disease.

Our third study aimed at clarifying the controversial association of EBV in MG. Despite reports of active EBV infection in MG thymi, we found only rarely signs of EBV infection on DNA and protein level. Therefore, we could not confirm that active EBV infection is implicated in the pathogenesis of MG.

Despite the considerable number of diseases associated with EBV, currently no treatment exists that targets latent EBV infection. In the last study described in this thesis, we targeted EBNA1, a viral antigen expressed during all latency stages of the virus. With a high-throughput screening we were able to identify Tilorone as an inhibitor of EBNA1's functions to maintain and replicate latent EBV infection. The compound had cytotoxic and anti-

proliferative effects on EBV-positive but to a lesser extent on EBV-negative lymphoma cell lines and reduced EBV-associated tumor burden in immunodeficient mice, but only marginally decreased EBV viral load in EBV-infected mice with reconstituted human immune system components. The compound might nevertheless constitute a promising lead compound to develop small molecules for the treatment of not only EBV infection but also EBV-associated diseases.

In conclusion, our observations in IM patients and IFN-β treated MS patients have reinforced the association of EBV and autoimmunity pointing at early involvement of EBV in the development of autoreactive poly-specific humoral immune responses. Our high-throughput screen on the other side has led to the identification of a compound that is a promising candidate against latent EBV infection and EBV-associated diseases.

In the mid 1980s, de Thé named EBV the ”Rosetta stone for understanding the role of viruses in human carcinogenesis” [2]; with the work described in this doctoral thesis we believe we have gone one step closer to deciphering the Rosetta stone of virus-associated autoimmune diseases and the strategies to treat them.

ZUSAMMENFASSUNG

Das Epstein-Barr-Virus (EBV) ist ein ubiquitäres Virus, mit welchem über 95% aller Menschen infiziert sind. Die meisten Träger des Pathogens bleiben während ihrer frühen Kindheit asymptomatisch. Eine Minderheit derer, die zu einem späteren Zeitpunkt infiziert werden, durchlaufen als symptomatische Primärinfektion die infektiöse Mononukleose (IM). Nach einer lytischen Replikation während der Primärinfektion bleibt EBV latent und lebenslang in B-Zellen des betroffenen Organismus. Die Mehrheit der EBV-Träger ist durch das Virus nicht beeinträchtigt. Allerdings ist für einen Teil der EBV-Infektionen und im besonderen der IM eine Assoziation mit einer Vielzahl von Krankheiten beschrieben. Zu diesen Erkrankungen zählen das Burkitt- und Hodgkin-Lymphom, proliferative Krankheiten nach Transplantationen und das Nasopharynxkarzinom. Zusätzlich liegen zahlreiche Hinweise für einen Zusammenhang von EBV mit verschiedenen Autoimmunkrankheiten wie beispielsweise der Multiplen Sklerose (MS) und Myasthenia Gravis (MG) vor. Der genaue Mechanismus von EBV in diesen autoimmun mediierten Erkrankungen ist noch nicht vollständig geklärt. Um die Rolle des Virus im Pathomechanismus dieser Erkrankungen zu verstehen, führten wir drei Studien durch, die den Zusammenhang zwischen EBV Infektion und Autoimmunität untersuchen sollten. Hierbei konzentrierten wir uns auf die drei Erkrankungen IM, MS und MG.

Grundlage der ersten Studie war die Hypothese, dass während einer fulminanten IM-Infektion anhaltende autoreaktive humorale und zelluläre Reaktionen generiert werden, die zu Autoimmunpathologien im späteren Leben führen. Wir fanden eine erhöhte humorale Immunantwort, die mit der EBV-Viruslast positiv korrelierte. Dies legt nahe, dass die mit EBV in Verbindung stehende humorale Antwort zur Immunpathologie im späteren Leben beiträgt.

Als nächstes untersuchten wir, ob eine Behandlung mit IFN-β bei MS-Patienten die EBV-spezifische Immunantwort beeinflusst. Wir fanden in MS-Patienten eine reduzierte zelluläre Antwort auf EBNA1, jedoch keine Veränderung der Immunantwort auf andere EBV Antigene. Dies ist ein Indiz dafür, dass EBNA1-spezifische T-Zellen in der Pathogenese der MS eine Rolle spielen.

Unsere dritte Studie hatte zum Ziel, die Kontroverse um den Zusammenhang von EBV und MG zu klären. Trotz Berichten über aktive EBV-Infektionen im Thymus von MG Patienten konnten wir nur geringe Anzeichen von EBV-Infektionen auf DNA- und Proteinlevel finden. Folglich konnten wir nicht bestätigen, dass eine aktive EBV-Infektion in der Pathogenese der MG eine Rolle spielt.

Trotz zahlreicher Krankheiten, die mit EBV assoziiert sind, gibt es derzeit keine Behandlung, welche auf latente EBV-Infektionen abzielt. In der letzten in dieser Arbeit beschriebenen Studie lag der Fokus auf EBNA1, welches während der latenten Virusphase exprimiert wird. Mit einem Hochdurchsatz-Screening identifizierten wir die Substanz Tiloron als einen Inhibitor von EBNA1-Funktionen, der die Erhaltung und Replikation des Virus während EBV-Infektionen reduziert. Die Substanz zeigte zytotoxische und antiproliferative Effekte auf EBV-positive, jedoch nur in geringem Maß auf EBV-negative Lymphom-Zelllinien. Des Weiteren führte Tiloron zu reduzierter EBV-assoziierter Tumorlast in immungeschwächten Mäusen und wenig reduzierter EBV-Viruslast in EBV-infizierten Mäusen mit einem humanen Immunsystem. Tiloron hat vielversprechendes Potential, nicht nur im Hinblick auf eine Behandlung von EBV-Infektionen, sondern auch im Hinblick auf EBV-assoziierte Erkrankungen.

Zusammenfassend bekräftigen unsere Beobachtungen, dass es bei IM-Patienten und bei IFN-β behandelten MS-Patienten eine Assoziation von EBV und Autoimmunität gibt. Unsere Daten betreffend autoreaktiven poly-spezifischen humoralen Immunantworten während der IM deuten darauf hin, dass EBV bereits vor dem Krankheitsausbruch eine Rolle spielt. Das Hochdurchsatz-Screening hat eine Substanz identifiziert, die das Potential hat, bei latenten EBV-Infektionen und EBV-assoziierten Krankheiten eingesetzt zu werden.

Mitte der 80er-Jahre nannte de-Thé EBV den „Stein von Rosette für Verständnis von der Rolle von Viren in menschlicher Karziogenese“ [2]. Mit den in dieser Doktorarbeit gewonnen Erkenntnissen glauben wir einen Schritt näher an die Entschlüsselung vom Stein von Rosette gekommen zu sein im Bereich von virus-assoziierten Autoimmunerkrankungen und deren Behandlungen.

ABBREVIATIONS

aa	Amino acid
7-AAD	7-Aminoactinomycin D
AChR	Acetylcholin receptor
ADP	Adenosine diphosphate
APC (cell type)	Antigen-presenting cells
APC (FACS)	Allophycocyanin
BART	*BamHI* A rightward transcript
Bax	Bcl-2 associated X protein
Bcl-2	B-cell lymphoma 2
BCR	B cell receptor
bp	Base pair
CD	Cluster of differentiation
CFSE	Carboxyfluorescein succinimidyl ester
CIS	Clinically isolated syndromes
CMV	Cytomegalovirus
CNS	Central nervous system
CTL	Cytotoxic T lymphocytes
Da	Dalton
DC	Dendritic cells
DMSO	Dimethyl sulfoxide
DNA	Deoxyribonucleic acid
DS	Dyad symmetry
DTT	Dithiothreitol
EAE	Experimental allergic encephalomyelitis
EBER	EBV-encoded RNA
EBNA1	EBV nuclear antigen 1
EBV	Epstein-Barr virus
E. coli	Escherichia coli
EDSS	Expanded Disability Status Scale
ELISA	Enzyme-linked immunosorbent assay
ELISPOT	Enzyme-linked immunosorbent spot
EMSA	Electrophoretic mobility shift assay
EOMG	Early onset myasthenia gravis
FCS	Fetal calf serum
FR	Family of repeats
g	Gravitational force
GC	Germinal center
Gd	Gadolinium
gp	Glycoprotein
HCl	Hydrogen chloride
HEK	Human Embryonic Kidney
HHV	Human herpes virus
His	Histidine
HL	Hodgkin's lymphoma
HLA	Human leukocyte antigen
HRP	Horseradish peroxidase
HTS	High-throughput screen
IFN-β	Interferon beta
IFN-γ	Interferon gamma
IM	Infectious mononucleosis
IRF	IFN regulatory factors

Ion	Ionomycin
i.p.	Intraperitoneal
IPTG	Isopropylthio-β-galactoside
ITAM	Immunoreceptor tyrosine-based activation motifs
i.v.	Intravenously
kbp	Kilobase pairs
KSHV	Kaposi's sarcoma virus
LB	Lysogeny broth
LCL	Lymphoproliferative cell line
LD_{50}	Lethal dose, 50 percent kill
LMP	Latency membrane protein
MACS	Magnetic-activated cell sorting
MFI	Mean fluorescence intensity
MG	Myasthenia gravis
MHC	Major histocompatibility
MHV-68	Murine gamma-herpesvirus 68
MOG	Myelin Oligodendrocyte glycoprotein
MOI	Multiplicity of infection
MRI	Magnetic resonance imaging
MS	Multiple sclerosis
Nab	Neutralizing antibody
NaCl	Sodium chloride
NFkB	Nuclear factor kappa B
NK	Natural killer
NOD	Non-obese diabetic
NPC	Nasopharyngeal carcinoma
NSG	NOD-SCID-gamma-chain-deficient
OD	Optical density
ORC	Origin recognition complex
OriP	Origin of plasmid replication
OriLyt	Origin of lytic replication
PBMC	Peripheral blood mononuclear cell
PCNA	Proliferating cell nuclear antigen
PCR	Polymerase chain reaction
PerCP	Peridinin chlorophyll
PHA	Phytohaemagglutinin
PMA	Phorbol 12-myristate 13-acetate
pp	peptide pool
PRR	Pattern recognition receptor
RA	Rheumatoid arthritis
RANA	Rheumatoid arthritis nuclear antigen
RANK	Receptor activator of nuclear factor kappa B
RIU	Raji infectious units
RNA	Ribonucleic acid
RRMS	Relapsing-remitting multiple sclerosis
RS	Reed-Sternberg
SCID	Sever combined immunodeficiency
SDS-PAGE	Sodium dodecyl sulfate polyacrylamide gel electrophoresis
SFU	Spot forming units
SLE	Systemic lupus erythematosus
TAP	Transporter associated with antigen processing
TBM	3,3',5,5'-Tetramethylbenzidine
TCR	T cell receptor
TMEV	Theiler's murine encephalomyelitis virus

TMEV IDD	TMEV induced demyelinating disease
TNF	Tumor necrosis factor
TRAF	Tumor-necrosis-factor-receptor-associated factors
TR-FRET	Time resolved fluorescence energy transfer
VCA	Viral Capsid Antigen
VZV	Varicella-zoster virus
wo	Without stimulation

1. INTRODUCTION

1.1. Human Herpesvirus Family

Herpesviridae comprises of a family of enveloped, double-stranded DNA viruses with large complex genomes. Eight varieties have been isolated from humans and have been grouped into three subfamilies (Table 1.1). The neurotropic alpha herpesvirus subfamily includes herpes simplex virus (HSV) type 1 and 2, and varicella-zoster virus (VZV). To the beta herpesviruses group belong cytomegalovirus (CMV) and human herpesvirus 6 and 7. Epstein-Barr Virus (EBV) and Kaposi's sarcoma herpesvirus (KSHV) form the gamma subfamily that establishes infection in B lymphocytes [3]. The gamma viruses are divided into two genera, gamma-1 and gamma-2. The gamma-2 genus comprises of KSHV and its relative murine gamma-herpesvirus 68 (MHV-68), which establish latency in B cell, however they have no independent capacity to drive B cell proliferation. On the other hand, the more recently evolved gamma-1 viruses, which EBV belongs to, are characterized by B cell growth transforming potential [4].

Table 1.1. Human herpesvirus subfamilies members, their tropism, and the diseases they cause.

Subfamily	Scientific name	Common name	Tropism	Associated Diseases
Alpha	HHV-1	HSV-1	Neurotropic	Facial, labial, ocular lesions
	HHV-2	HSV-2		Genital lesions
	HHV-3	VZV		Chickenpox and shingles
Beta	HHV-5	CMV	Myelotropic	Infectious mononucleosis
	HHV-6	-		Mild early childhood roseola
	HHV-7	-		Mild early childhood roseola
Gamma	HHV-4	EBV	Lymphotropic (B, T and NK cells), epithelial cells	Infectious mononucleosis, cofactor in human cancers
	HHV-8	KSHV		Cofactor in Kaposi's sarcoma

1.2. Virion Structure of EBV

All herpesvirus virions are comprised of four basic structures (Figure 1.1). A single linear double-stranded DNA molecule is wrapped around a toroid-like protein core. The core is

surrounded by an icosahedral capsid composed of 162 capsomeres. The tegument fills up the space between the capsid and the envelope. The envelope is the outermost layer of the virion and consists of host membrane and viral transmembrane glycoproteins such as gp350/220 that mediate attachment and entry of the virus.

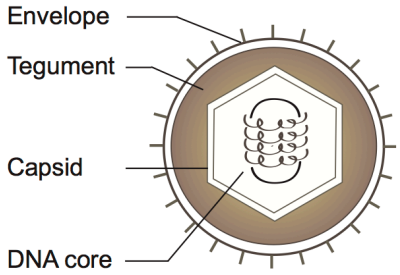

Figure 1.1. *Herpesviridae* virion structure.

1.3. EBV Genome

EBV has a linear double-stranded genome of approximately 172 kilobase pairs (kbp) with 85 to 95 open reading frames, and was the first large DNA virus to be sequenced [5]. The sequenced genome, B95-8, was derived from a EBV-infected marmoset cell line [6] which was later determined to contain a 12 kb deletion, that involves three open reading frames [7]. Still this EBV genome is the one used most often in laboratory experiments. While the genes expressed during lytic replication are highly conserved among the *Herpesviridae* family, those expressed during EBV latency are not found in other human herpesviruses.

Two types of closely related EBV genomes, which differ predominantly in the sequence of their latency gene EBNA2, have been identified: EBV-1 and EBV-2 [8]. While EBV-1 isolates are more common in the United States, Europe, and Southeast Asia, EBV-2 is largely restricted to equatorial Africa and Papua New Guinea. Interestingly, HIV patients in the United States and Europe have higher frequency of EBV-2 infection [9].

1.4. EBV Life Cycle

EBV infection usually occurs through salivary contact early in childhood and results in asymptomatic primary infection. After oral transmission, the virus lytically replicates in a permissive cell type of contested origin in the oropharynx (Figure 1.2). EBV gains entry into B cells by binding to CD21 (C3d complement receptor) through its major glycoprotein gp350 [10]. Additionally, glycoprotein gp42 interacts with MHC Class II, which functions as an

EBV co-receptor. Epithelial cells do, however, not express CD21 and therefore it is thought that EBV enters epithelial cell through CD21-independent pathways. Tugizov *et al*. have shown that EBV entry could be mediated through three such pathways: (1) direct cell-to-cell contact of apical cell membranes with EBV-infected lymphocytes, (2) entry of cell-free virions through basolateral membranes that is mediated through the interaction of β1 or α5β1 integrin and the EBV protein BMRF-2, (3) virus spread across lateral membranes to adjacent epithelial cells [11].

The lytic replication of the virus leads to large amounts of shed virus in the throat. The virus reaches mucosal B cells, infects them and initiates a latent growth-transforming program, which leads to substantial expansion of the EBV-transformed B cells many of which are later on killed by the immune response. However, EBV-infected B cells that downregulate viral antigen expression and enter into a resting state would be spared by the immune system and would persist as long-lived memory B cells that recirculate in the blood and pharyngeal lymphoid tissues. These latent EBV infection-harboring cells might be pushed towards lytic reactivation through antigen stimulation or plasma cell differentiation signals, which can lead to low-level virus shedding and novel infection of B cells [4].

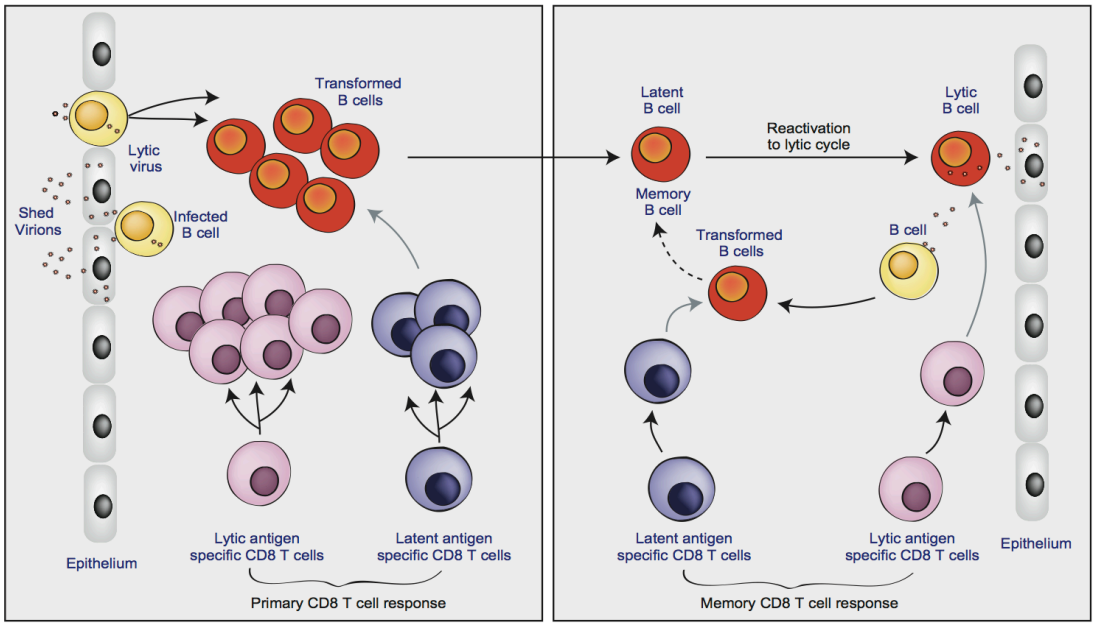

Figure 1.2. Cellular responses to EBV infection. (Figure drawn based on Hislop *et al*. [4])

1.4.1. Lytic Infection

1.4.1.2. Lytic Viral Replication

EBV is one of the few known viruses that have two completely independent genome replication systems: one system that is used by most herpesviruses to actively replicate the linear genome during lytic infection, and a second system that is unique to EBV and is essential to facilitate circular viral genome replication in synchrony with cellular replication during viral latency [12].

Viral replication during lytic infection leads to the generation of thousands of viral copies produced in concatemers, which are subjected to further processing to generate cleaved, packaged, linear genomes bound to capsid polyamides [13], [14]. While the virus is dependent on cellular factors for the initiation phase, the process of replication itself is mainly self-reliant and homologous but not identical to the replication process of HSV. The EBV genome contains two lytic replication origins, *oriLyt*, located opposite each other on the viral episome, and characterized by 1055-bp core element, composed of two identical duplicate segments [15]. It should be noted that the commonly used laboratory EBV strain B95-8 has only one *oriLyt* copy due to a deletion (Figure 1.3A).

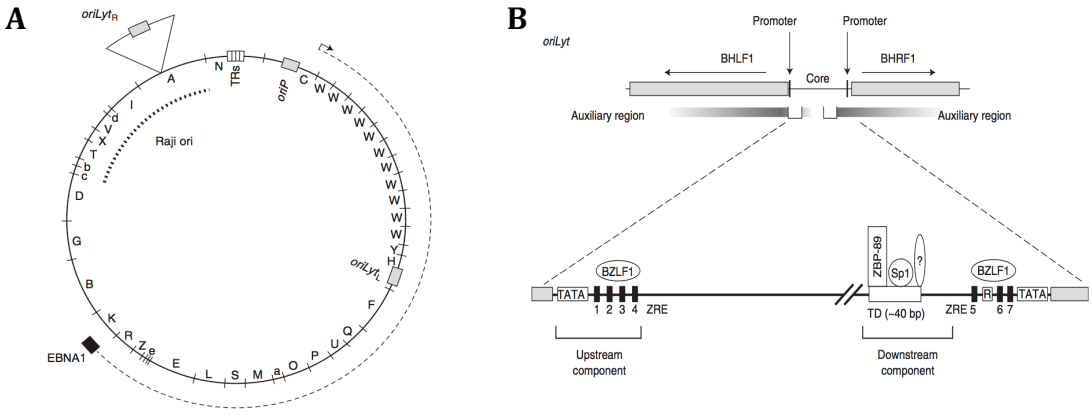

Figure 1.3. (**A**) Physical map of B95-8 laboratory strain. The triangle designates the deletion site of B95-8 compared to other EBV strains. (**B**) *OriLyt* and its expanded core domain. (Figures adapted from Hammerschmidt and Sugden [16])

BZLF1, the master switch between latent and lytic EBV infection, is a key transcriptional regulator that binds to several sites on *oriLyt* (Figure 1.3B) and initiates lytic replication by supporting the expression of viral factors of lytic amplification. Moreover, BZLF1 interacts with members of the replication complex such as helicases and primases and

the viral polymerase accessory factor BMRF1 [17], [18], [19], [20]. The mechanisms initiated at *oriLyt* include DNA replication and homologous recombination [21], and initiation of the recruitment of cellular recombination and DNA repair factors [22], [23], [24].

In summary, not only is lytic replication at *oriLyt* intricate because it involves two distinct but interdependent mechanisms of DNA replication and homologous recombination, but also because it uses a complex repertoire of viral and poorly defined cellular components to execute these processes.

1.4.1.2. Lytic Gene Expression

The EBV genome encodes about 90 genes expressed during lytic viral replication. Their products are classified as immediate-early, early, and late proteins. Immediate-early proteins such as BZLF1 and BRLF1 function as transcriptional activators of viral genes. Early genes involved in the viral DNA replication include DNA polymerase and thymidine kinase, proteins involved in apoptosis inhibition, soluble cytokine receptors, and activators of early gene expression. Late proteins such as viral capsid antigen (VCA), gp350, gp42, and gp85 are major components of the viral capsid and envelope and are essential for viral entry into B cells. One interesting late EBV protein is BCRF1, also termed viral IL-10 for its close homology to human IL-10. This protein provides the virus with an immune evasion strategy not only to reduce dendritic cell (DC) activation and subsequent $CD8^+$ T cells responses, but also to stimulate growth of B cells [25].

1.4.2. Latent Infection

1.4.2.1. Origin of Latent Replication

OriP, the origin of latent EBV replication is a DNA fragment of 1.7 kbps that supports the autonomous replication and maintenance of the latent EBV episome. Latent viral replication is initiated in synchrony with the tightly regulated replication of the host cell chromosomal DNA and is mediated by the cellular replication machinery [12]. Even though EBV's genome encodes more than 100 gene products, EBV nuclear antigen 1 (EBNA1) is the only viral protein that is essential for latent EBV replication and maintenance. EBNA1 binds site-specifically to *OriP* and is instrumental for episome maintenance, recruitment of the cellular replication machinery and initiation of latent replication. EBNA1 and its DNA binding sites are discussed in detail in the following three sections.

1.4.2.2. Family of Repeats Region

The Family of repeats (FR) is an array of 20 non-conserved tandem repeats of 30bp size that is located on the *OriP* and is essential for episomal maintenance (Figure 1.4) [12]. EBNA1 can bind with high affinity as a dimer to 20 motifs in the FR; however, only seven of the 20 motifs need to be occupied by EBNA1 for efficient episomal maintenance to occur [12]. The carboxyl terminus of EBNA1 binds specifically to FR, while its amino terminus bind AT-rich chromosomal sequences. In this way EBNA1 tethers the episome to condensed mitotic chromosomes as they segregate during mitosis and ultimately it minimizes episomal loss in proliferating cells. Recent live-cell image studies have shown that 88% of newly synthesized episomes are segregated equally to the daughter cells, while the rest are segregated in a poorly understood random manner [26].

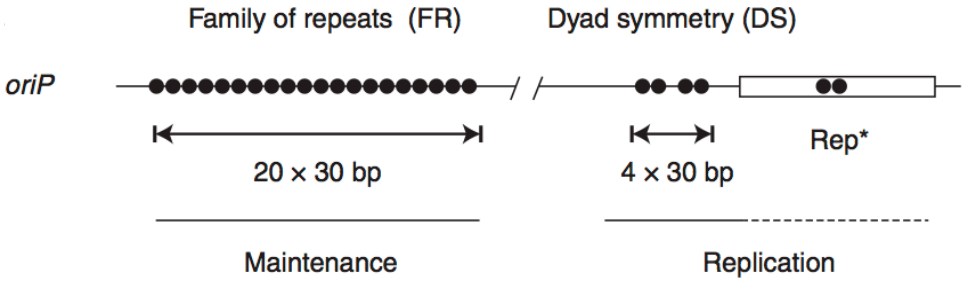

Figure 1.4. Depiction of OriP and its EBNA1 binding sites. (Figure drawn based on Hammerschmidt *et al*. [16])

1.4.2.3. Dyad Symmetry Region

The dyad symmetry (DS) is a 65 bp region on *OriP* located about 1 kbps downstream of FR and is the minimal replicator element of episomal EBV. The region consists of two pairs of low affinity EBNA1-binding sites [12], [16]. The sites within one pair are spaced exactly 21 bp apart so that they fall in the same helical phase, a characteristic essential for their function as replicator that is not required for EBNA1 binding at the FR region [27]. It was shown that only one pair of binding sites is sufficient to initiate replication, however, the upstream presence of FR region is indispensable for the initiation of bidirectional DNA synthesis at the DS element [12], [28], [29]. The efficacy of initiation of replication at DS has been linked, but not fully understood, to the presence of proximal auxiliary elements one of which has been shown to bind telomere-associated proteins [30], [31].

Downstream of DS lies the Rep* element (Figure 1.4), which is a 300 bps motif that was identified as an alternative EBNA1-dependent lower activity replicator [32], [16]. Rep* maintains only short-term replication of plasmids, however multimers of the motif have been shown to support long-term plasmid replication [33].

Interestingly, chromatin structure is suspected to influence replication at *OriP* since spacing and modification of the nucleosomes surrounding DS have been observed to be cell cycle-dependent [34], [35].

1.4.2.4. EBV-Nuclear Antigen 1 (EBNA1)

During latency EBV dramatically reduces the number of expressed viral gene products. EBNA1 is the only viral protein that is expressed in all forms of viral latency and in all EBV-associated tumors, which reinforces its position as one of the most essential viral products. It has three essential functions: (1) to maintain the EBV genome in dividing cells, (2) to initiate latent episomal replication by recruiting the cellular replication machinery at *OriP*, (3) to transactivate gene expression. Purified EBNA1 has been shown, however, to lack ATPase or DNA helicase activity [36] suggesting that the functions of EBNA1 are mediated through its interaction with cellular components [12]. Learning more about the structure of EBNA1 can facilitate the understanding of its properties and interactions.

A 160 amino acid stretch at the carboxyl terminus of EBNA1 facilitates the dimerization of the protein and enables site-specific DNA binding to *OriP* (Figure 1.5) [37]. Crystallographic studies have revealed the presence of four antiparallel beta strands that when dimerized form eight-stranded beta barrels with projecting alpha helices that establish DNA contacts [38], [39]. The structure of the carboxyl terminus of EBNA1 closely resembles the dimerization and DNA-binding domain of the E2 protein of papillomaviruses [40], [39]. Additional similarity between the two proteins lies in their ability to bend DNA upon site-specific binding [27], [33].

UR1 is another functional component of EBNA1 that bears resemblance to a similar domain of the E2 protein and spans 25 amino acids between the glycine-arginine and the glycine-alanine repeat motifs. This region contains two cysteine residues that facilitate the coordinated binding of two EBNA1 monomers to Zinc, a process that is instrumental for the transcriptional transactivation potential of EBNA1 [41], [42].

Moreover, clusters of DNA-bound EBNA1 dimers, such as at the FR region, have the propensity to adhere to other EBNA1/DNA complexes forming a DNA loop [43], [44]. This linking and looping activity of EBNA1 is mediated by the LR1 and LR2 that are segments rich in arginine and glycine residues. In addition, the presence of arginine-glycine repeats promotes the binding of EBNA1 to AT-rich DNA sequences [45]. This binding promotes the

attachment of EBNA1 to AT-rich chromosomal DNA and the maintenance of the EBV episome in latently infected cells. A third function of the LR1 and LR2 regions is to bind G-rich RNA, which facilitates the recruitment of the human origin recognition complex (ORC) at the DS segments, however the precise mechanisms of how that happens is not yet clearly understood [16].

A hallmark of EBNA1 is the 200 amino acid glycine-alanine repeat region that has no link to the genome maintenance and replication function of EBNA1 but has been shown to reduce EBNA1 antigen processing by limiting its proteasomal degradation, ribosomal translation and eventually minimizing MHC class I presentation of EBNA1 epitopes [46], [47]. This is presumably one of the main reasons for the success of EBV infection: EBNA1, an essential viral protein that is expressed during all latency stages of EBV is at the same time poorly recognized by $CD8^+$ T cells. Nevertheless, EBNA1 epitopes have been shown to be presented on MHC class II molecules after autophagosomal degradation, which resulted in the generation of EBNA1-specific $CD4^+$ T cell responses [48].

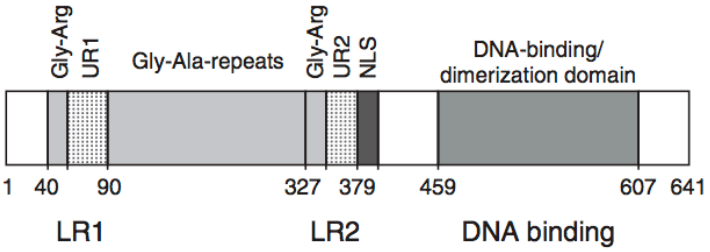

Figure 1.5. Schematic structure of EBNA1. (Figure adapted from Hammerschmidt *et al*. [16])

1.4.2.5. Latency Programs and Latency-Associated Proteins

Characteristic for EBV latency is the drastic reduction of viral gene expression from about 100 genes to only 11 latently expressed genes. These include six EBNA genes (EBNA1, EBNA2, EBNA3A, EBNA3B, EBNA3C, and EBNA-LP), two latent membrane proteins (LMP1 and LMP2), two EBV-encoded RNAs (EBER1 and EBER2), and *BamHI* A rightward transcript (BART). Among these, only EBNA1 and LMP1 are also expressed during lytic infection. Depending on the number of expressed genes, EBV latency can be categorized into 4 programs (Table 1.2).

Table 1.2. EBV latency programs, associated protein expression pattern and diseases.

Latency Program	Proteins expressed	Affected B cell	Associated disease
0	EBER, BART	Memory B cell	Peripheral blood B lymphocytes
I	EBNA1, EBER, BART	Memory B cell	Burkitt lymphoma
II	EBNA1, LMP1, LMP2, EBER, BART	Germinal center centroblast	Nasopharyngeal carcinoma, Hodgkin's disease
III	EBNA1, EBNA2, EBNA3, LMP1, LMP2, EBER, BART	Immunoblast	Infectious mononucleosis, LCLs

LMP1 and LMP2 are multiple-membrane spanning molecules that act as constitutively activated ligand-independent receptors and provide survival signals to stimulate B cells to enter into memory state [49], [50]. LMP1 has extensive functional homology with CD40 and is able to interact with a number of tumor-necrosis-factor-receptor-associated factors (TRAFs) that trigger downstream NFkB activation and promote survival and proliferation of B cells [51], [52], [53]. CD40 is expressed on germinal center B cells and is activated upon interaction with its T cell ligand, CD40L (CD154). LMP2, on the other hand, is a B cell receptor (BCR) homolog that contains immunoreceptor tyrosine-based activation motifs (ITAM) motifs [54]. It provided tonic survival signals in EBV-infected B cells that lack surface expression of immunoglobulins [49].

1.5. Immune Response to EBV Infection

The immune responses targeting EBV have been best studied in patients with primary symptomatic EBV infection, also known as infectious mononucleosis (IM). Therefore, the following sections will elucidate the innate and adaptive EBV-specific immune response in the setting of IM.

1.5.1. Innate Immune Responses

Natural killer (NK) cells provide the first defense against microbial invaders and are involved in tumor immunosurveillance through their ability to secrete IFN-γ. NK cells expand during IM and their number has been shown to inversely correlate with viral load [55]. Tonsillar NK cells are known to be particularly strong IFN-γ producers that can inhibit *in vitro* resting B cell transformation in the presence of DCs as IL-12 producers [56].

Moreover, NK cells may provide a defense against the virally induced HLA class I donwregulation on infected cell [57].

1.5.2. Adaptive Immune Responses

1.5.2.1. $CD8^+$ T Cell Responses

Oligoclonal populations of EBV-specific $CD8^+$ T cells arise early in IM, reaching frequencies of 1-40% of total $CD8^+$ T cell population that are mainly directed against immediate early and early antigens [58], [4]. Reactivity to latent proteins is minor, accounting for 0.1-5 % of the $CD8^+$ T cell population and mainly directed against members of the EBNA3 family [4]. Characteristic of the EBV-directed $CD8^+$ T cells is their strong cytotoxicity and activation state. These cells are positive for perforin and exhibit cytotoxic activity *ex vivo* [59], [58], [60]. The cells express molecules that characterize them as cells that recently encountered antigen such as the activation marker CD38, cell cycling marker Ki-67, and CD45RO isoform [60], [61], [4]. If no antigen stimulation is provided *in vitro*, these cells will undergo rapid apoptosis since they express low levels of anti-apoptotic molecules such as Bcl-2 and Bcl-x and high levels of the pro-apoptotic Bax molecules [60], [62]. This explains the rapid reduction in $CD8^+$ T cell numbers in late IM when the antigen availability becomes scares. $CD8^+$ T cells directed against lytic antigens are reduced dramatically both in absolute numbers and in percentages. On the other hand the latent antigen-specific $CD8^+$ T cells are also reduced in numbers but to a much lower extend than the T cells targeting lytic antigens [4]. The surviving $CD8^+$ T cells then lose their activation status, i.e. they lack CD38 and CD69 expression, and upregulate Bcl-2 [63], [64].

Long-term asymptomatic EBV carriers who did not develop IM shed very low or absent levels of virus and carry 1-50 EBV-infected B cells per million total B cells. These healthy carriers develop $CD8^+$ memory responses to an array of epitopes: 0.2-2% of all $CD8^+$ T cells are directed against lytic antigens, while 0.05-1% against latent epitopes [4], which signifies the importance of $CD8^+$ T cells in controlling asymptomatic EBV infection even in EBV healthy carriers.

Curiously, characteristic for EBV-specific $CD8^+$ T cell responses is that despite the variety of HLA types, infected people develop immune responses towards a limited number of immunodominant antigens. Among the lytic antigens the immunodominant epitopes are derived from the immediate early BZLF1 or BRLF1, from some of the early proteins such as BMLF1, BMRF1, BALF2, or BALF5, and very rarely from late lytic proteins [4]. This

skewing of the immune responses towards immediate early and early epitopes and away from late proteins together with the observation of reduced HLA class I surface levels on lytically infected cells [65] suggests of an immunoevasion strategy by the virus. Indeed, the early EBV protein BNLF2a has been shown to interfere with HLA class I antigen presentation by blocking TAP1/TAP2 peptide transport [4].

1.5.2.2. $CD4^+$ T Cell Responses

EBV-specific $CD4^+$ T cell responses have been much less well characterized than the $CD8^+$ responses mostly due to the difficulty of generation of MHC class II tetramers and the lack of massive oligoclonal expansion of $CD4^+$ T cells during IM [66], [67]. Nevertheless, EBV-directed $CD4^+$ T cell responses are of a comparable magnitude to $CD4^+$ responses to other viral infections and peak during acute IM. The responses are directed to both lytic and latent antigens and are rapidly reduced few weeks post the peak of disease. One study that evaluated responses to a limited set of antigens determined that most common in the lytic antigen repertoire were epitopes from the immediate early BZLF1 protein, while responses to EBNA1 were less frequent [68]. Another study that looked at the $CD4^+$ memory T cells determined that these cells secrete IFN-γ and TNF-α, limited levels of IL-2 and express CD45RO, CD27 and CD28, which significantly differs from the phenotype of CMV-specific memory T cells which lack CD27 and CD28 [67].

In contrast to the $CD8^+$ T cell responses, $CD4^+$ memory lytic T cell responses encompass immediate early, early, and late proteins along with envelope glycoproteins that rarely elicit CD8 responses [4]. The latent antigens are derived similarly to the CD8 responses from EBNA3 proteins, however the largest proportion of CD4 responses is targeted to EBNA1 and EBNA2, proteins that elicit only limited CD8 responses [4].

Interestingly, the virus has developed an evasion strategy to prevent infected cells from CD4 responses by shedding large amounts of a truncated form of gp42, an envelope protein that binds MHC class II and serves as a co-receptor for viral entry. The truncated form masks MHC class II molecules on the surface of infected cells and interferes with $CD4^+$ T cell recognition [69].

1.5.2.3. B Cell Responses

Generation of EBV-specific antibody responses has been best studied during acute IM and the detection of IgM and IgG targeted against the viral capsid antigen (VCA), early antigen, and EBNA1 are used in the clinical diagnosis of IM [70]. IgM responses to VCA appear at the time of IM symptoms presentation and resolve 1-2 months after (Figure 1.6). While no IgM

responses can be detected in chronic viral carriers, IgG response to VCA develop at the time of IM diagnosis and persist at reduced levels for life [70].

Antibodies against the early lytic protein, early antigen D, develop during the peak of IM and resolve 3-6 months later, however in about 20% of individuals they can persist for life. EBNA1 IgG antibodies appear only several weeks after IM and persist for life [70].

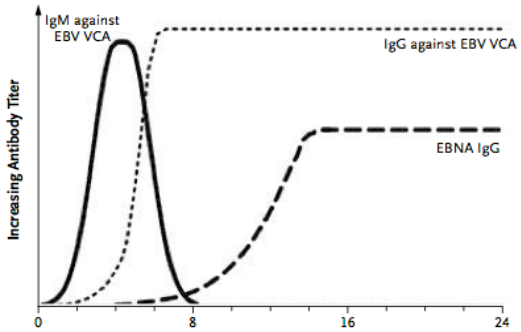

Figure 1.6. EBV-specific antibody responses during and after infectious mononucleosis. (Figure copied from Luzuriaga *et al*. [70])

1.6. EBV-Associated Diseases

1.6.1. Infectious Mononucleosis

More than 95% of the adult population is carrier of latent EBV infection. The majority of individuals acquire EBV infection during the first 5 years of life. However, in the industrialized and developed world about 50% of the population acquires the virus later in life [70]. That predisposes between 30-50% of the individuals who acquire EBV between 15 and 24 year of age to develop symptomatic primary infection or infectious mononucleosis (IM) [70]. IM symptoms appear 30-50 days post viral exposure and constitute of pharyngitis, fever, and lymphadenopathy [70]. The symptoms typically resolve one month after diagnosis. However, cervical lymph node enlargement and fatigue might persist for a longer time period. IM is associated with a risk of mild hematologic complications as well as rare severe neurological complications. The disease is rarely fatal, however, male patients with X-linked lymphoproliferative disease, who carry a mutation that results in uncontrolled $CD8^+$ T cell expansion, suffer from very severe or even fatal IM [71].

Interestingly, a history of IM has been associated with four-fold increased risk of development of Hodgkin's lymphoma, and a two-fold risk for development of multiple sclerosis later in life. The suspected molecular mechanisms behind these associations are discussed below.

1.6.2. EBV-Associated Malignancies

Even though animal studies from the early 1900s had already implicated the role of viruses in tumorigenesis, it was not until the identification of EBV in Burkitt lymphoma biopsies in 1964 that established the role of viruses in human cancer [72]. This is why EBV is commonly referred to as the Rosetta stone of viral tumorigenesis. The virus encodes for proteins that share close homology to anti-apoptotic factors, cytokines, and signal transducers that are used by the virus to promote infection, transformation and immortalization of the infected cells. Due to these characteristics the virus is associated with a number of lymphoproliferative disorders that include B cell, as well as T/NK cell malignancies, and carcinomas some of which will be briefly reviewed below.

1.6.2.1. Burkitt's Lymphoma

Three variants of Burkitt's lymphoma exist: endemic, affecting children in equatorial Africa and New Guinea; sporadic, affecting children and young adults worldwide; and immunodeficiency-related, affecting mainly HIV patients. The majority of endemic cases are EBV-associated, while only 15-20% of the sporadic cases, and 30-40% of the immunodeficiency-related cases are linked to EBV [73]. The lymphoma is highly proliferative and is a result of translocation of the c-*myc* oncogene under the control of the immunoglobulin heavy or light chain loci [74]. The exact mechanism of the association of EBV and the c-*myc* translocation has not yet been elucidated, however it has been suggested that the translocation happens as an error to somatic hypermutation in the germinal centers [74]. Yet, EBV genes, associated with induction and maintenance of proliferation, are not expressed in EBV-infected Burkitt's lymphoma cells. Being in latency I, these cells express constitutively only EBNA1. Moreover, Kennedy *et al*. determined that EBNA1 provides survival signals to the infected cells since inhibition of EBNA1 led to decreased cell survival [75].

1.6.1.2. Hodgkin's Lymphoma

Hallmarks of the classical form of Hodgkin's lymphoma (HL) are giant multinuclear Hodgkin's and Reed-Sternberg (RS) cells, which are transformed B cells that originated from

pre-apoptotic germinal center B cells [73]. They are characterized by constitutive NFkB activation that provides survival signals to the transformed cells. The activation can be induced by members of the classical NFkB activation pathway such as CD30, CD40, and the receptor activator of nuclear factor kB (RANK) all of which are expressed on RS cells. About 40% of all classical HL cases are associated with EBV infection. EBV infected cells express LMP1, which acts as a CD40 homolog and stimulates NFkB activation [73].

1.6.1.3. Non-B Cell Lymphomas

Besides B cell lymphomas, EBV is also associated with a number of T and NK cell malignancies such as peripheral T-cell lymphomas, angioimmunoblastic T cell lymphoma, extranodal nasal type NK/T-cell lymphoma, enteropathy-type T cell lymphoma, gamma delta T cell lymphomas, T cell lymphoproliferative disorders after chronic EBV infection, EBV-associated cutaneous T cell lymphoproliferative disorders, and aggressive NK cell leukemia [73].

The virus is also associated with 95% of nasopharyngeal carcinoma (NPC) cases. NPC is a squamous cell carcinoma that is predominant among isolated populations such as in southern Chinese, the Inuits of Alaska, and native Greenlanders [76].

1.6.1.4. Other Lymphoproliferative Diseases

There are three main categories of EBV-associated lymphoproliferative lymphomas: ones that occur in primary immunodeficiencies such as X-linked lymphoproliferative disease, ones that occur due to immunosuppressive treatment post organ transplantation, and lymphomas associated with AIDS.

1.6.3. EBV-Associated Autoimmune Diseases

1.6.3.1. Mechanisms of EBV-Induced Autoimmunity

The following text is adapted from Kakalacheva et al., 2011 and partially from Münz et al., 2009.

Several mechanisms have been proposed to explain how pathogens such as viruses might trigger autoreactive immune responses in autoimmune diseases. These include virus-induced general activation of the immune system and the provision of viral gene products that specifically stimulate immune responses that cross-react with self-antigen (Figure 1.7).

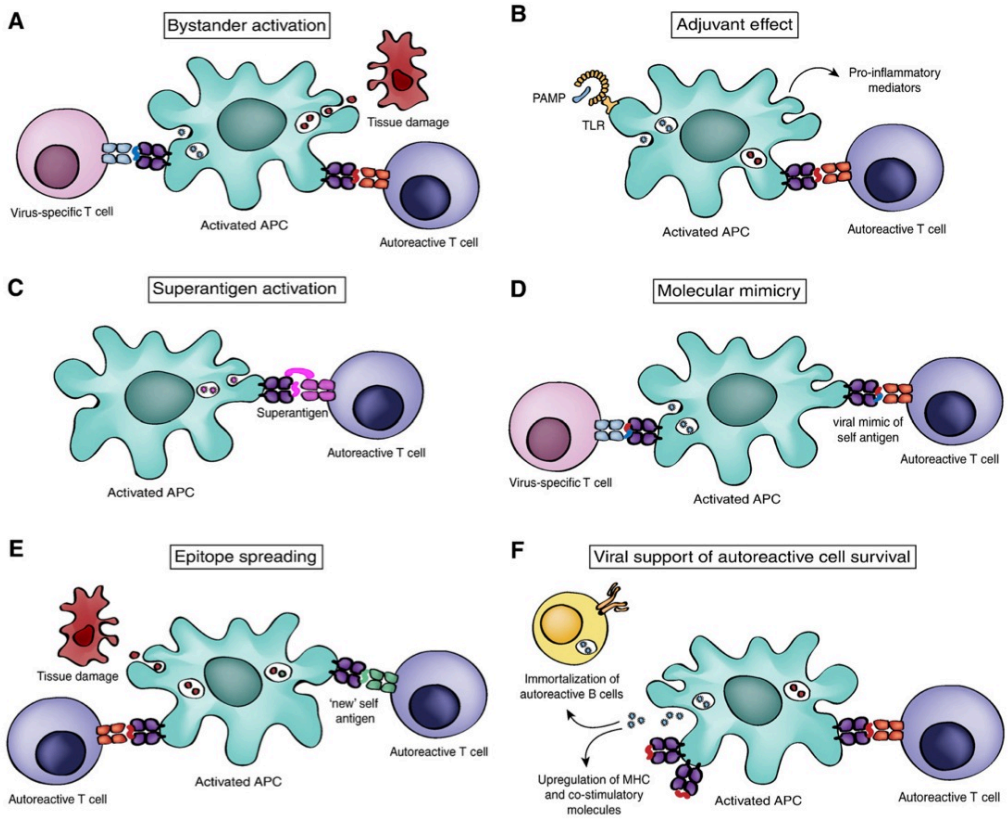

Figure 1.7. Molecular mechanisms of pathogen-induced autoimmunity. (Figure adapted from Kakalacheva *et al*. [77])

1.6.3.1.1. Mechanisms of Bystander Activation

Infectious agents express specific pathogen-associated molecular patterns (PAMPs). These are recognized by immune cell receptors leading to cellular activation, which increases the antigen-presenting capacity and the expression of costimulatory molecules of antigen-presenting cells (APCs). This also leads to APC production of type I interferons, pro-inflammatory cytokines and chemokines, which in turn initiate and direct the immune response against the invading pathogen. Thus, EBV, when recognized by the immune system can mediate activation of APCs that at the same time contain self-antigens obtained from dying cells or damaged tissue. In this way the activated APCs can not only activate EBV-specific lymphocytes but also cross-activate autoreactive T and B cells. Alternatively, the Th1-driven environment during viral infection could facilitate activation of autoreactive bystander T and B cells via proinflammatory cytokine production. One would assume that that is the case during acute IM infection when massive activation of virus-specific T cells leads to bystander activation of EBV non-specific lymphocytes (Figure 1.7A and B).

1.6.3.1.2. Mechanisms of Molecular Mimicry

Polyspecific antigen recognition has emerged as a fundamental feature of adaptive cellular immune responses. Mathematical models indicated that the TCR repertoire is not large enough to give functional protection against all possible foreign epitopes on the basis of a one TCR–one epitope model, and several groups consistently have demonstrated that there can be considerable flexibility in TCR recognition of peptide–major histocompatibility complex (MHC) complex, [78], [79], [80]. Polyspecific or so-called degenerate TCR recognition is considered to represent a compromise between the need to provide host protection against virtually any pathogen-derived epitope and, at the same time, the need to ensure thymic positive selection and peripheral maintenance of this T cell repertoire via intermediate affinity recognition of self-peptides that are presented by self-MHC molecules. Such degenerate specificity, however, also carries a certain risk for autoimmunity under special circumstances, e.g., strong innate immune activation (Figure 1.7D).

1.6.3.1.3. Mechanisms of Epitope Spreading

In addition to one TCR being engaged by different MHC/peptide complexes, one TCR specificity can set free epitopes for other TCRs and lead to a process called epitope spreading. Epitope spreading describes the phenomenon observed in animal models of autoimmune diseases and cancer patients in which responses to immunodominant epitopes are elicited first, followed by responses to less dominant epitopes [81], [82], [83], [84], [85]. Although these examples document epitope spreading within autoantigens and to additional autoantigens, the inflammatory environment of EBV infection could also support these immune response cascades by increasing the presentation of autoantigens, thereby spreading immune responses from foreign to self-antigens (Figure 1.7E).

1.6.3.1.4. Emerging Mechanisms

The mechanisms of bystander activation, polyspecific antigen recognition/molecular mimicry, and epitope spreading are not the only ways by which EBV might trigger or accelerate autoimmunity. Viral infections could also directly maintain autoreactive effector T cells or autoantigen-presenting cells. For example, Theiler's murine encephalomyelitis virus (TMEV)-induced demyelinating disease (TMEV-IDD) is a model of MS in which intracerebral TMEV infection of mice leads to an autoimmune demyelinating disorder 30–40 days after infection [86]. Persistent infection of microglial cells with TMEV has been shown to upregulate expression of MHC and costimulatory molecules and to enhance the ability of these cells to function as effective APCs [87]. Furthermore, EBV immortalizes B cells and assists in their

differentiation into long-lived memory B cells. These mechanisms could support the survival of autoreactive B cells or of a reservoir of APCs that can present autoantigens to promote autoimmunity [88], [89].

The evidence for a biological role of these mechanisms mainly stems from experimental autoimmune disease models. Testing whether these mechanisms are indeed relevant in human autoimmune diseases is challenging because of a number of reasons including the following: (1) Chronic autoimmune diseases are likely to become clinically apparent only after a considerable period of subclinical autoreactivity, at which time the pathogen might have already been cleared and/or the antiviral immune responses might have subsided. (2) The proposed mechanisms by which a pathogen or a number of pathogens potentially initiate and sustain MS are likely dynamic, not mutually exclusive and might occur simultaneously or sequentially. A simple 'one organism–one disease' or 'one mechanism–one disease' paradigm might not apply to complex and heterogeneous diseases. (3) The flip side of the idea that autoimmunity is driven by viral infections is that autoreactive immune responses, or even only a predisposition to the development of these responses, might affect the ability of the host to control infections and to regulate antiviral immune responses. (4) The argument that infections contribute to disease development is strong for autoimmune conditions associated with one or two specific infectious agents such as Guillain–Barré syndrome, which is frequently preceded by *Campylobacter jejuni* infection or Rheumatic fever after Streptococcus infection. In contrast, other complex autoimmune diseases have been associated with a number of infectious agents and the data is still inconclusive.

The suggested role of EBV in multiples sclerosis, myasthenia gravis, systemic lupus erythematosus, and rheumatoid arthritis is extensively discussed in the following sections.

1.6.3.2. Multiple Sclerosis

The following text is adapted from Kakalacheva et al. 2011.

Evidence for a potential role of EBV in the development of multiple sclerosis (MS) arises from reports on the positive correlation between clinical history of IM and MS occurrence [90], [91]. The risk of MS has been suggested to increase after IM and to persist for at least 30 years post infection [92]. Ramagopalan *et al.* compared more than 14 000 MS cases and 7 000 spouse controls. Their study found a positive correlation of MS disease with history of IM, while no such association was observed for history of symptomatic measles, mumps, rubella, and varicella infections, or with history of measles, mumps, rubella, hepatitis B, and influenza vaccination [93]. A recent meta-analysis confirmed these findings by reviewing 14 studies, 11 case–control and 3 cohort studies, which investigated the association of IM and

MS. The analysis concluded that the combined relative risk for development of MS after IM was 2.3-fold and in HLA-DR2-positive individuals even 7-fold [94], suggesting that symptomatic EBV infection is a risk factor for MS [95].

Serological studies have demonstrated close to 100% EBV seropositivity in MS patients. However, high seropositivity, ranging between 90% and 95%, is also detected in the healthy adult population. A more prominent difference in seropositivity was observed in children with MS, 83% of which were reported to be seropositive for EBV, compared to 42% of healthy age-matched controls [96]. Moreover, no significant difference in seropositivity was observed between the two groups for cytomegalovirus, parvovirus B19, and VZV. These results were confirmed by a German study, showing 98.6% EBV seropositivity in children with MS in contrast to 72.1% in age-matched healthy controls [97]. Comparable results were observed by a more recent study that identified broadened and augmented recognition of the latency-associated EBV nuclear antigen 1 (EBNA1), suggesting dysregulation of EBV-specific immune responses in pediatric MS [98].

An age-dependent relationship was suggested between alterations in EBV-specific immune responses and clinical manifestation of MS [99]. A longitudinal study in 69 matched case–control sets of US military personnel investigated the presence of EBV antibodies before MS onset. While EBV-specific antibody titers were similar between people who developed MS before the age of 20, a two- to three-fold increase in EBV-specific antibody titers was observed in MS cases after the age of 25. The strongest risk factor, rising MS susceptibility ten-fold, was increased titers of serum antibodies to EBV-derived nuclear antigens (EBNA) and in particular to EBNA1 [99], [100]. A recent study confirmed these results by reporting that EBNA1-specific antibody responses occurred 15 to 20 years before the onset of symptoms in MS patients [101]. Although these observations suggest an EBV-specific immune dysregulation preceding MS onset, one limitation of the abovementioned studies is that they compared EBV-specific responses only to CMV responses and not to those towards other viruses, suspected in MS association.

A more recent study determined immune responses to EBV, HHV-6, CMV, influenza virus, and measles virus antigens in a cohort of 147 patients with clinically isolated syndromes suggestive of MS (CIS) with a mean follow-up of 7 years compared to 50 demographically matched controls [102]. CIS patients showed increased humoral and cellular immune responses to EBNA1 but not to other EBV-derived proteins. IgG responses to other viral antigens and frequencies of T cells specific for CMV and influenza virus gene products were unchanged in CIS patients. Furthermore, EBNA1 was the only viral antigen with which immune responses correlated with number of clinical disability and MRI metrics during the follow-up period. The authors therefore concluded that increased EBNA1-specific IgG

responses in CIS patients predicted conversion to clinically definite MS. Higher IgG responses to EBNA1 in patients with CIS and relapsing-remitting MS (RRMS) were also reported to correlate with increased frequencies of EBV-specific $CD8^+$ T cells [103]. In line with the results of the former study, Farrell *et al*. found higher IgG responses to EBNA1 in CIS and RRMS patients, whereas responses to lytic EBV capsid antigens, CMV, and measles-virus encoded proteins were unchanged compared to healthy blood donors. In these patients, elevated EBNA1-specific IgG responses were associated with the development of gadolinium-enhancing (Gd^+) lesions and predictive for T2 lesion volume change and clinical disability for a period of 5 years [104].

EBNA1 is the most consistently recognized EBV-specific antigen, which stimulates $CD4^+$ T cell responses in healthy virus carriers and selective expansion of T cells specific for EBNA1 was observed in MS patients [105], [98]. Moreover, a small subset of these cells has been shown to cross-react with myelin antigens, supporting the hypothesis that clonally expanded EBNA1-specific T cells could be actively involved in MS immunopathology by stimulating cross-recognition through molecular mimicry [106].

Molecular mimicry is one of the classical paradigms for infection-induced autoimmunity and there is solid evidence from a number of animal models transgenic for human autoreactive T cell receptors that microbial peptides can induce MS-like disease through mechanisms of molecular mimicry [107], [108], [109]. An alternative hypothesis for the association of EBV infection and autoimmune diseases is based on the virus' ability to immortalize B cells and to assist in their differentiation into long-lived memory B cells. Indeed, there is evidence that the EBV-encoded proteins LMP1 and LMP2 mimic signals of T cell help and B cell receptor engagement, respectively, possibly rendering autoreactive B cells less susceptible to tolerance control in the periphery [110]. These mechanisms could support the survival of autoreactive B cells or of a reservoir of APCs that can present autoantigens to promote autoimmunity [88], [89].

B cells are now recognized to play a critical role in the pathogenesis of MS, and an increasing number of compounds that deplete B cells or target pathways essential for B cell development and function are currently being tested for their potential use as MS therapeutics. Serafini *et al*. found that EBV-infected B cells expressing viral antigens are significantly enriched in postmortem brain samples from patients with MS, but not in brain samples from patients with other inflammatory CNS diseases [111]. Activated $CD8^+$ T cells were also present close to EBV-infected B cell foci, suggesting that EBV-specific lymphocyte responses may be involved in MS immunopathologies. However, these findings could not be reproduced in several subsequent studies [112], [113], [114]. Further research should clarify the source of this discrepancy. At present, the aforementioned conflicting data on the

presence of EBV in MS brain tissue do not allow to draw definite conclusions on the frequency and potential function of EBV-infected B cells in the CNS of patients with MS.

Taken together, there is strong epidemiological evidence for a link between symptomatic EBV infection and MS development. The immune-modifying function of EBV suggests that this virus is, indeed, a major candidate for triggering MS. The mechanisms responsible for this association are, however, far from understood.

1.6.3.3. Myasthenia Gravis

The following text is adapted from Kakalacheva et al. 2011.

Myasthenia gravis (MG) was the first neurological disease to be classified as antibody-mediated. It is characterized by loss of acetylcholine receptors (AChR) on the neuro-muscular junction. This antibody-mediated loss results in reduced muscle contraction and even life-threatening muscle weakness [115]. More than 80% of patients with early onset myasthenia gravis (EOMG; age <40 years) show medullary thymic infiltrates. They include T cell areas and lymphoid follicles closely resembling those found in reactive lymph nodes, with germinal centers (GC) and rare native AChR-expressing myeloid cells nearby [115], [116]. The EOMG thymus behaves like a target organ. Not only is production of pathogenic autoantibodies to the AChR selectively activated there, but AChR-specific B cells undergo antigen-driven clonal proliferation and somatic hypermutation and thus help to maintain and diversify the patients' autoimmune responses [117]. Infections with common viruses are long-suspected environmental risk factors for MG but no specific candidates have yet been firmly implicated [115], [118], [119]. EBV is an interesting candidate since it is able to infect and transform B cells. Cavalcante and colleagues investigated recently thymi from 17 MG patients including 12 with hyperplasia and reported high frequencies of EBV-infected thymus-infiltrating B cells [120]. All the investigated MG thymi showed evidence of active, i.e. replicative, EBV infection as defined by the presence of lytic and latent viral transcript and protein expression [120]. Their findings however were contested by others and us and will be further explained in the Sections 3.3. and 4.3 of this thesis.

1.6.3.4. Systemic Lupus Erythematosus

Similarly to MS, Systemic lupus erythematosus (SLE) is a complex multifactorial autoimmune disease with heterogeneous clinical presentation, which affects more often women than men. It is characterized by the generation of autoantibodies targeting nuclear components that form immunocomplexes which interfere with the function of vital organs.

The disease has been associated with genetic predisposing factors, however environmental factors are also thought to play a role.

SLE patients have been shown to have increased frequency of EBV early antigen antibodies and high but comparable to healthy donors titers to EBNA1 [121], [122]. Interestingly, it was shown that EBNA1-specific antibodies produced in immunized mice cross-react with common SLE antigens such as dsDNA and Sm [123], [124]. One study showed elevated EBV-specific $CD69^+$ $CD4^+$ T cells producing IFN-γ post EBV stimulation [125]. A different study looked at a larger cohort of patients determined significantly higher EBV viral loads in both active and inactive SLE patients compared to healthy controls [126]. Interestingly, the authors observed that less EBV-specific $CD8^+$ T cells have polyfunctional characteristics in terms of secretion of IFN-γ, TNF-α, IL-2, and MIP-1beta and have reduced cytotoxic function as measured by CD107a and granzyme B expression. The authors, however, observed that contrary to expectations EBV reactivation is an aggravating consequence rather than a cause to SLE since EBV reactivation followed disease flares. Moreover, longitudinal studies that looked at patients with history of IM, found no elevated risk in those patients for development of SLE [127].

EBV has been suggested to play different roles in SLE predisposition; however, many of the studies led to inconclusive conclusions. SLE patients have higher level of early antigen antibody titers and elevated EBV viral load after disease activity peak, which might suggest more frequent viral reactivation as a result of the disease, rather than a causative function of EBV in SLE.

1.6.3.5. Rheumatoid Arthritis

Rheumatoid arthritis (RA) is a complex autoimmune disease characterized by chronic joint inflammation that leads to bone erosion and cartilage destruction. RA has been historically linked to EBV since RA patient serum was found to react to an antigen expressed on EBV-infected B cells that was termed rheumatoid arthritis nuclear antigen (RANA) that was later on determined as EBNA1 [128]. Interestingly, the glycine-alanine repeat typical for EBNA1 are also expressed in cytoskeletal proteins such as cytokeratin and type 2 collagen [129]. This finding suggests that molecular mimicry could be a hypothetical mechanism of EBV and RA association.

The virus has been shown to be found in RA PBMCs, saliva, synovial fluid or synovial membrane more frequently than for healthy donors [128]. Moreover, patients who had both the susceptibility allele HLA-DR4 and presence of EBV DNA in the synovium had 41-fold increased risk for development of RA compared with subject with no EBV DNA [130]. Similarly to SLE patients, RA patients have elevated, about ten-fold higher, levels of

EBV DNA compared to healthy controls. However, yet again it is hard to say whether the elevated levels of EBV are sign of causation or rather due to the high inflammatory environment in the course of both diseases. The question remains unanswered if EBV is reactivated and functions as additional exacerbator of the disease, but not as its cause.

1.6.4. Treatment Strategies

In the majority of individuals EBV infection is asymptomatic, however, commonly it leads to fulminant symptomatic infection called infectious mononucleosis that has been associated with the development of malignant and autoimmune diseases. Furthermore, immunocompromised individuals such as post-transplantation patients, and individuals with hereditary or acquired immunodeficiency syndrome are at particular risk of developing EBV-associated diseases like lymphoproliferative diseases. Currently, there is no medication that inhibits latent EBV infection. EBV associated disease are commonly treated with antiviral agents such as aciclovir, ganciclovir, and vidarabine, which are general inhibitors of herpes viral DNA polymerases [128]. Table 1.3 summarizes the most common treatment strategies against EBV-associated diseases.

Table 1.3. Therapeutic strategies for EBV-associated diseases. (Table adapted from Toussirot *et al.* [128])

EBV-Associated Disease	Pathogenic Mechanism	Therapeutic Strategies
Burkitt lymphoma, Nasopharyngeal carcinoma	Proliferation of latently infected cells	Surgery; chemotherapy; irradiation
Primary or hereditary immunodeficiency syndrome (X-linked lymphoproliferative syndrome, Wiskotte Aldrich syndrome)	Proliferation of latently infected cells	Immunoglobulin; monoclonal antibodies targeting B cells (anti-CD20); hematopoietic stem cell transplantation; EBV-specific CTL
Acquired immunodeficiency syndrome: transplant recipients, AIDS	Proliferation of latently infected cells	Cessation or decrease of immunosuppressive drugs; antiviral agents; monoclonal antibodies against CD20, CD21, CD24, and IL-6; Hydroxyurea
Oral hairy leukoplakia (in AIDS)	Replication of EBV in infected cells	Aciclovir; ganciclovir; vidarabine
Severe infectious mononucleosis in immunocompromised hemophagocytic lymphohistiocytosis	Immune response against EBV-infected cells	Corticosteroids; immunoglobulin; cyclosporine; etoposide; plasmapheresis; bone marrow transplantation, monoclonal antibodies against CD20 and TNF-α

As seen from Table 1.3 very few of the agents target EBV specifically and the ones that do so affect only lytic EBV infection and have no effect on the latent maintenance or replication of the virus. It is tempting to say that a drug that targets latent infection would provide a very effective treatment strategy for all EBV-associated disease. However, that should be speculated with caution since EBV might be the initiator early on during the disease onset, while the role of the virus in the late stages of the EBV-associated diseases is unclear.

1.6.5. Vaccination Strategies

A major difficulty for the design and testing of an EBV vaccination strategy is the lack of appropriate animal models and the scarcity of knowledge on immune correlates of protection against EBV infection. Another challenge for performing preventive clinical trials is the long period of time between EBV infection and occurrence of malignancies. Despite these difficulties there are few EBV vaccination strategies that show limited promise.

Vaccination trials performed in the cotton-top tamarin, now an endangered species, with the major viral protein, gp350, showed remarkable protection capacity of the vaccine from EBV-associated B cell lymphomas post parenteral challenge [131]. However, several caveat of this model organism are that EBV is not a natural pathogen of the cotton-top tamarin and the animals cannot be infected orally, they do no develop persistent infection and lack expression of MHC class I molecules [132].

Another good model for EBV vaccine efficacy studies is the rhesus macaque, whose natural virus, the rhesus lympocryptovirus is genetically homologous to EBV. Infection with the virus leads to viral persistency and long-term viral shedding and if immunosuppressed the animals can acquire virus-associated malignancies [133]. This model was used to compare three types of EBV vaccines: soluble gp350, virus-like replicon particles that express gp350, and a combination of gp350-expressing virus-like replicon particles and EBNA3A and EBNA3B. The study concluded that soluble gp350 provided the optimal protection from oral EBV challenge [134].

Not many EBV vaccine trials have been done in humans. One study performed with nine EBV seronegative children in China showed that only one-third of the gp350-expressing vaccinia virus immunized children became seropositive at 16 months compared to 100% of the unvaccinated children [135]. The only double-blind randomized Phase 2 clinical trial performed to date involved 181 seronegative adults who received either soluble gp350 in alum and monophosphoryl lipid A or placebo. The gp350-vaccinated individuals showed 78% reduction in the rate of IM, however there was no difference in the infection rate between the groups [136].

As mentioned earlier, a major burden for the development of an EBV vaccine is the lack of appropriate model organism. However, the development of severely immunosuppressed mice with reconstituted human immune system components poses new opportunities for study and development of novel EBV vaccine as well as therapeutic agents.

2. MATERIALS AND METHODS

2.1. Generation of Autoreactive Humoral and Cellular Immune Responses during Infectious Mononucleosis

2.1.1. EBV Viral Load Quantification

Quantitative analysis of serum EBV DNA was performed by the Medical Virology department at the University of Zurich using a TaqMan® (Applied Biosystems) real-time PCR technique [137] with modified primers for the BamHI W fragment (5'-CTTCTCAGTCCAGCGCGTTT-3' and 5'-TCTAGGGAGGGGGACCACTG-3') and the fluorogenic probe (5′-(FAM)-CGTAAGCCAGACAGCAGCCAATTGTCAG-(TAMRA)-3′). PCR of duplicate samples were performed using ABI Prism 7700 Sequence Detector (Applied Biosystems).

2.1.2. VCA and Vimentin ELISAs

Viral capsid antigen (VCA)-specific IgG and anti-vimentin IgM and IgG antibodies were assessed using commercially available ELISA kits: VCA (p23/p28) IgG (Immunolab GmbH), and anti-vimentin IgM and anti-vimentin IgG (VIDIA). Standards and controls provided by the ELISA kits were used to quantitatively evaluate the results in arbitrary units (U/mL) for the VCA kit and as positivity index for the vimentin ELISA as recommended by the manufacturers.

2.1.3. Quantification of Serum Antibodies Reactive to Myelin Oligoglycoprotein

Human oligodendroglial cell line MO3.13 lentivirally transduced with human full-length MOG and protocols were generously provided by Fabienne Brilot-Turville (University of Sydney). MO3.13 cells lentivirally transduced with a MOG-negative vector were used as control cell line. The cells were cultured in high-glucose DMEM media (Gibco) supplemented with 10% FCS (Sigma), 1:100 GlutaMax (Invitrogen), and 1:100 Penicillin/Streptomycin (Sigma). The cells were washed with PBS and harvested using Versene (Invitrogen) and seeded at $5x10^4$ cells per well in a V-bottom 96-well plate. Human sera at a 1:50 dilution was added to the cells diluted in PBS + 2% FCS and incubated for one hour at room temperature. The cells were then washed with PBS + 2% FCS and 50 μl of secondary antibody goat anti-human IgG Alexa Fluor 647 (Invitrogen) 1:100 dilution was added and incubated for 1 hour at room temperature in the dark. The cells were then stained

with a Live/Dead Fixable APC-Cy7 Dead Cell Stain Kit (Invitrogen) and acquired on a FACS Canto (BD Biosciences). The results are presented as delta MFI that was calculated as the MFI signal obtained for the MOG expressing cell line minus the MFI signal obtained for the control MOG-negative cell line. The positivity threshold was determined as three standard deviations above the mean of the healthy control samples. 818C5 anti-MOG antibody was used as positive control, while secondary antibody only was used as negative control of the assay.

2.1.4. Serum Autoreactivity

Human anti-nuclear antibodies were detected by indirect immunofluorescence microscopy, using slides coated with HEp2 cells and cryostat tissues of rat kidney, liver and stomach (Eurommun), that were incubated at room temperature with patients' serum samples at an starting dilution of 1:40, followed by incubation with FITC – labeled conjugates: anti-IgG/A/M, anti-IgM, anti-IgG (Euroimmun). The reaction was visualized by fluorescence microscopy, and subsequent titration was performed for positive samples. Background was adjusted for with negative control samples. Slides were viewed with a LEICA DLMB microscope using Leica objectives HC PL Fluotar 20x/0.5 and HCX PL Fluotar 40/0.75. Images were acquired using a Leica camera DFC 420C and were processed with Application Suite 3.4.0 imaging software (Leica). Additionally, serum reactivity to SS-A (anti-Ro) and citrullinated protein (CCP2) was quantified according to the standard protocols of the Clinical Immunology Unit at the University Hospital Zurich.

2.1.5. IFN-γ ELISPOT

Frozen PBMCs were thawed and seeded at $2x10^5$ cell density per well on MultiScreen 96-well plate (Millipore) pre-coated with human IFN-γ antibody 1D1K (Mabtech). The cells were then stimulated with peptide pools of EBNA1 (Tables 2.2.1), latent EBV (Tables 2.2.2), lytic EBV (Tables 2.2.3), myelin, and pro-insulin with concentration of individual peptides at 5 μM. PMA/Ionamycin was used as positive control, while 0.01% DMSO was used as negative control. After 18-20 hours of incubation at 37ºC, the wells were washed and incubated with detection antibody 7B6-Biotin (Mabtech) at 1:1 000 dilution in PBS + 0.5% FCS. After 2 hours incubation at room temperature, the plate was washed and incubated with Streptavidin-ALP at a 1:2 000 dilution. After one hour of incubation and thorough washing, BCIP/NBT substrate (Mabtech) was added and developed for 45 minutes before the reaction was stopped by washing the plate with water. The plate was read and analyzed 24 hours later with an ELISpot reader and software (AID).

2.1.6. Cloning of EBNA1-Reactive T Cells

Frozen PBMCs were thawed and resuspended in H5 media composed of RPMI 1640 (PAA) containing 5% pooled human AB-serum (Invitrogen) and Penicillin/Streptomycin (1:100). First, the EBNA1-reactive T cells, seeded at $2x10^5$ cells per well in a 96-well U bottom plate, were expanded for 12 days according to the schedule in Table 2.1.1 and as described by Scherrenburg *et al*. [138]. On day 12 the cells were washed and rested for 24 hours.

Table 2.1.1. Schedule for IL-2 and EBNA1 peptide pool addition for expansion of EBNA1-reactive clones.

Time	IL-2 concentration (U/mL)	EBNA1 (μM, concentration of individual peptides)
Day 0	-	2.5
Day 2	10	-
Day 6	10	10
Day 9	10	-
Day 12	-	-

The EBNA1-reactive cells were then stimulated again with EBNA1 peptide pool with individual concentration of each peptide at 2.5 μM and the IFN-γ secreting cells were captured using the IFN-γ Secretion Assay – Detection Kit (Miltenyi) according to manufacturer's recommendations. The selected cells were then seeded at cell densities of 0.03 cells/well, 0.3 cells/well, 3 cells/plate, or 30 cells/plate and cultured with irradiated feeders comprising of three types of LCLs (irradiated with 200 Gray) and 3 different PBMC donors cells (irradiated with 60 Gray) and pre-pulsed with EBNA1 peptide pool. The wells that proliferated were checked for EBNA1-reactivity through IFN-γ ELISA. The selected EBNA1-reactive cells were supplemented with 100 U/mL IL-2 every 5 days and every 2 weeks with new feeders pre-pulsed with EBNA1 peptides. All assays measuring antigen-specific activity were performed 2 weeks after the addition of feeders to minimize the background signal.

2.1.8. IFN-γ ELISA

T cell clone cultures were stimulated with EBNA1, EBV latent, EBV lytic, myelin, and pro-insulin peptide pools (as described in Section 2.1.5) over 18-20 hours. The culture supernatants were then collected and incubated on MaxiSorb plate (Nunc) that was pre-coated with anti IFN-γ antibody (Mabtech). Serial dilutions of human IFN-γ (Mabtech) at a concentrations ranging from 2000 pg/mL to 31.25 pg/mL were incubated on the same plate as the samples and were used as standards in the assay. After 2 hours of incubation at room

temperature, the plate was washed and incubated with biotinylated anti-IFN-γ antibody (Mabtech) for one hour at room temperature, then washed again and incubated with Streptavidin-HRP antibody at 1:1 000 dilution. After 30 minutes incubation the plate was thoroughly washed and TBM substrate was added to the plates and incubated for 40 minutes until blue color developed. Then the reaction was stopped with 1M HCl and the plate was immediately measured at OD_{450}.

2.1.9. Statistical Analysis

The non-parametric Mann Whitney test was used unless otherwise stated. A *p*-value of less than 0.05 was considered significant. Correlation analysis and graphs were generated by Prism software (GraphPad Software).

2.2. EBV-Specific Immune Responses in Patients with Multiple Sclerosis Responding to IFN-β Therapy

The following section is adapted from Comabella, Kakalacheva et al. Mult Scler. 2012 May;18(5):605-9.

2.2.1. Patient Demographics

In total, 28 patients with MS who showed a clinical response to IFN-β were included in the study. A clinical response to IFN-β was defined by the absence of relapses and lack of progression on the Expanded Disability Status Scale (EDSS) score during the first 2 years of treatment. Since paired peripheral blood mononuclear cells (PBMC) and serum samples were not available in all of the 28 patients included in this study, we determined antibody responses in a total of 24 patients and cellular immune responses in a total of 18 patients. The study was approved by the local ethics committee and patients gave their informed consent.

2.2.2. CFSE Proliferation

Immune responses were evaluated at baseline before application of IFN-β and after 1 year of treatment. T cell responses were determined by CFSE dilution as described previously [139]. Overlapping peptides of 12–22 aa length (average of 15 aa length) with 11 aa overlap were designed for the $EBNA1_{400–641}$ sequence of the B95-8 EBV strain (Table 2.2.1). For $CD8^+$ T cell epitopes from EBV and CMV, we synthesized nonamer peptides that are part of the CEF control peptide pool of the National Institutes of Health AIDS Research and Reference Reagent Program (Table 2.2.2). Peptides were used at a 5 μM individual concentration. Samples were measured on an LSRFortessa (BD Biosciences) flow cytometer. Gating and calculations for precursor frequencies were performed with FlowJo software. The frequencies of proliferating antigen-specific T cells were determined by subtracting the background frequency from the frequency of antigen-stimulated positive samples. A positive response was defined as a stimulation index of at least two-fold increase in peptide-stimulated cells compared to non-stimulated cells.

2.2.3. ELISA for Detection of Antiviral Immune Responses

Virus antigen-specific IgG antibodies were assessed using commercially available ELISA kits: EBV-encoded nuclear antigen 1 (EBNA1) (p72 encoded by BKRF1) IgG (Biotest), viral capsid antigen (VCA) (p23/p28) IgG (Immunolab GmbH), and human cytomegalovirus (CMV) IgG antigens in lysates of infected versus control cells (Diamedix Corporation).

Standards and controls provided by the VCA and EBNA1 ELISA kits were used to quantitatively evaluate the results in arbitrary units (U/mL), while antibody (Ab) indices were calculated by dividing the OD_{450} value of each sample by the control cut-off value, as recommended by the manufacturer.

Table 2.2.1. EBNA1 peptide pool.

Antigen	Sequence	Length (aa)
EBNA1 (400-414)	PGRRPFFHPVGEADY	15
EBNA1 (405-418)	FFHPVGEADYFEYH	14
EBNA1 (409-422)	VGEADYFEYHQEGG	14
EBNA1 (413-429)	DYFEYHQEGGPDGEPDV	17
EBNA1 (420-434)	EGGPDGEPDVPPGAI	15
EBNA1 (425-439)	GEPDVPPGAIEQGPA	15
EBNA1 (430-451)	PPGAIEQGPADDPGEGPSTGPR	22
EBNA1 (435-451)	EQGPADDPGEGPSTGPR	17
EBNA1 (442-458)	PGEGPSTGPRGQGDGGR	17
EBNA1 (449-461)	GPRGQGDGGRRKK	13
EBNA1 (452-465)	GQGDGGRRKKGGWF	14
EBNA1 (456-469)	GGRRKKGGWFGKHR	14
EBNA1 (460-474)	KKGGWFGKHRGQGGS	15
EBNA1 (465-478)	FGKHRGQGGSNPKF	14
EBNA1 (469-482)	RGQGGSNPKFENIA	14
EBNA1 (473-487)	GSNPKFENIAEGLRA	15
EBNA1 (478-491)	FENIAEGLRALLAR	14
EBNA1 (482-496)	AEGLRALLARSHVER	15
EBNA1 (487-503)	ALLARSHVERTTDEGTW	17
EBNA1 (494-508)	VERTTDEGTWVAGVF	15
EBNA1 (499-510)	DEGTWVAGVFVY	12
EBNA1 (501-514)	GTWVAGVFVYGGSK	14
EBNA1 (505-518)	AGVFVYGGSKTSLY	14
EBNA1 (509-522)	VYGGSKTSLYNLRR	14
EBNA1 (513-527)	SKTSLYNLRRGTALA	15
EBNA1 (519-532)	NLRRGTALAIPQCR	14
EBNA1 (523-536)	GTALAIPQCRLTPL	14
EBNA1 (527-541)	AIPQCRLTPLSRLPF	15
EBNA1 (532-544)	RLTPLSRLPFGMA	13
EBNA1 (535-548)	PLSRLPFGMAPGPG	14
EBNA1 (539-554)	LPFGMAPGPGPQPGPL	16
EBNA1 (545-559)	PGPGPQPGPLRESIV	15
EBNA1 (549-563)	PQPGPLRESIVCYFM	15
EBNA1 (554-566)	LRESIVCYFMVFL	13
EBNA1 (557-571)	SIVCYFMVFLQTHIF	15
EBNA1 (562-576)	FMVFLQTHIFAEVLK	15
EBNA1 (566-580)	LGTHIFAEVLKDAIK	15
EBNA1 (571-584)	FAEVLKDAIKDLVM	14
EBNA1 (575-588)	LKDAIKDLVMTKPA	14
EBNA1 (579-593)	IKDLVMTKPAPTCNI	15

EBNA1 (584-597)	MTKPAPTCNIRVTV	14
EBNA1 (588-600)	APTCNIRVTVCSF	13
EBNA1 (591-604)	CNIRVTVCSFDDGV	14
EBNA1 (595-609)	VTVCSFDDGVDLPPW	15
EBNA1 (600-614)	FDDGVDLPPWFPPMV	15
EBNA1 (605-619)	DLPPWFPPMVEGAAA	15
EBNA1 (610-625)	FPPMVVEGAAAEGDDG	16
EBNA1 (616-629)	EGAAAEGDDGDDGDE	15
EBNA1 (620-634)	EGDDGDDGDEGGDGD	15
EBNA1 (625-639)	DDGDEGGDGDEGEEG	15
EBNA1 (630-641)	GGDGDEGEEGQE	12

Table 2.2.2. Latent EBV peptide pool.

Antigen	Sequence	HLA restriction	Virus
EBNA3A (158-166)	QAKWRLQTL	HLA-B8	EBV
EBNA3A (325-333)	FLRGRAYGL	HLA-B8	EBV
EBNA3A (379-387)	RPPIFIRRL	HLA-B7	EBV
EBNA3A (458-466)	YPLHEQHGM	HLA-B35	EBV
EBNA3A (603-611)	RLRAEAQVK	HLA-A3	EBV
EBNA3B (416-424)	IVTDFSVIK	HLA-A11	EBV
EBNA3C (258-266)	RRIYDLIEL	HLA-B27	EBV
EBNA3C (281-290)	EENLLDFVRF	HLA-B44	EBV

Table 2.2.3. Lytic EBV peptide pool.

Antigen	Sequence	HLA restriction	Virus
BZLF1 (190-197)	RAKFKQLL	HLA-B8	EBV
BRLF1 (28-37)	DYCNVLNKEF	HLA-A24	EBV
BRLF1 (134-143)	ATIGTAMYK	HLA-A11	EBV
BRLF1 (148-156)	RVRAYTYSK	HLA-A3	EBV
BMLF1 (259-267)	GLCTLVAML	HLA-A2	EBV

Table 2.2.4. CMV peptide pool.

Antigen	Sequence	HLA restriction	Virus
pp65 (417-426)	TPRVTGGGAM	HLA-B7	HCMV
pp65 (495-503)	NLVPMVATV	HLA-A2	HCMV
pp65 (512-521)	EFFWDANDIY	HLA-B44	HCMV

Table 2.2.5. Myelin peptide pool.

Peptide	Sequence	Number of amino acids
$MBP_{13–32}$	KYLATASTMDHARHGFLPRH	20
$MBP_{83–99}$	ENPVVHFFKNIVTPRTP	17
$MBP_{111–129}$	LSRFSWGAEGQRPGFGYGG	19
$MBP_{131–155}$	ASDYKSAHKGLKGVDAQGTLSKIFK	25
$MBP_{146–170}$	AQGTLSKIFKLGGRDSRSGSPMARR	25
$PLP_{40–60}$	TGTEKLIETYFSKNYQDYEYL	21
$PLP_{89–106}$	GFYTTGAVRQIFGDYKTT	18
$PLP_{139–154}$	HCLGKWLGHPDKFVGI	16
$PLP_{178–197}$	NTWTTCQSIAFPSKTSASIG	20
$PLP_{190–208}$	SKTSASIGSLCADARMYGVLP	20
$MOG_{1–20}$	GQFRVIGPRHPIRALVGDEV	20
$MOG_{11–30}$	PIRALVGDEVELPCRISPGK	20
$MOG_{35–55}$	MEVGWYRPPFSRVVHLYRNGK	21
$CNP_{343–373}$	EVGELSRGKLYSLGNGRWMLTLAKNMEVRAI	31
$CNP_{356–388}$	GNGRWMLTLAKNMEVRAIFTGYYGKGKPVPTQG	33

2.2.4. Statistical Analysis

The non-parametric Wilcoxon test was used to compare antibody and T cell responses before and during IFN-β treatment. A *p*-value of less than 0.05 was considered significant.

2.3. Intrathymic Epstein-Barr Virus Infection in Patients with Myasthenia Gravis

The following section is adapted from Kakalacheva et al., Ann Neurol. 2011;70:508–514.

2.3.1. Patient Demographics

With informed consent and ethical committee approval, we cryo-stored patients' plasma, peripheral blood mononuclear cells (PBMCs), and thymic cells that were taken before any immunosuppressive drug treatments in 15 out of 16 cases. Thymi were dispersed mechanically in every case, and in 7 out of 16 cases dispase and/or collagenase were used to maximize recovery of GC, stromal and plasma cells [140]. After washing, thymic cells were frozen and stored at –180°C, and later thawed for testing as described below. Antiviral immune responses in patients were compared to those in 15 demographically matched healthy subjects (mean age 28 ± 4; 8 female, 7 male).

2.3.2. Flow Cytometry Staining and MACS Separation of Thymi Suspensions

Cryo-preserved thymic suspensions were thawed and then stained according to manufacturers' recommendations with Live/Dead Fixable Aqua Stain (Invitrogen), CD45-Pacific blue (BD Biosciences), CD3-APC (BD Biosciences), CD19-PeCy7 (BD Biosciences), CD27-PE (BD Biosciences) and acquired on FACSCanto (BD Biosciences). B cells were identified as live, $CD45^+CD3^-CD19^+$ cell population. Memory B cells were identified as the frequency of $CD27^+$ cells from total $CD19^+$ cell population.

In order to separate $CD19^+$ B cells from total thymi cells, we incubated the thymi suspensions with $CD19^+$ MicroBeads (Miltenyi) and isolate them by positive selection with an AutoMACS Pro Separator (Miltenyi) according to manufacturer's recommendation.

2.3.2. EBV Detection by Real-Time PCR

DNA was extracted using QIAamp DNA Blood Mini Kit (Qiagen). EBV DNA was quantified from thymic cells, cell lines, and EBV-positive tonsil samples by quantitative PCR using a TaqMan PCR kit (Roche) and a Model 7500 Sequence Detector (Applied Biosystems) as described previously [105]. All samples were tested at least in triplicates, and mean results were determined.

2.3.3. Histochemistry

Serial cryo-sections of EOMG thymi were *in situ* stained for EBV-encoded RNA (EBER), EBNA2, and CD20. The staining was performed independently at the Department of Pathology at the University Hospital Zurich. For *in situ* hybridization the slides were pretreated with Enzyme 1 (Leica). FITC-labeled EBER-Probe (Leica) was used and detected

with anti-FITC antibody (Dako) and detection-kit Refine-AP (Leica).

Sections for CD20 and EBNA2 staining were pretreated at 100°C with EDTA-Buffer (Leica). Rabbit anti-mouse IgG $F(ab)^2$ (Epitomics) was used as secondary antibody. All incubations were performed on BondMax (Leica) with the detection Kit Refine HRP according to the manufacturer's guidelines. EBV-positive tonsil samples were used as positive controls.

2.3.4. ELISA for Detection of Antiviral Immune Responses

Virus antigen-specific IgG antibodies were assessed using commercially available ELISA kits: EBNA1 (p72 encoded by BKRF1) IgG (Biotest), viral capsid antigen (VCA) (p23/p28) IgG (Diamedix Corporation), VCA IgM (Immunolab GmbH), human cytomegalovirus (CMV) IgG (Immunolab GmbH). Values are presented as antibody indices, which were calculated by dividing the OD_{450} value of each sample by the cut-off value as recommended by the kit manufacturers. IgG reactivity towards EBV-encoded VCA antigen defined persistent EBV infection, i.e. EBV carrier status. The majority of individuals tested for EBV-specific T cell responses as well as for EBV viral loads had detectable levels of VCA-specific IgG antibodies.

2.3.5. Intracellular Cytokine Staining

PBMC at a cell density of 2×10^6 cells per 0.5 ml were cultured in RPMI 1640 medium (PAA) containing 5% pooled human AB-serum (Invitrogen) and were stimulated with (or without) viral peptide mixtures (final concentration of 5 μM per peptide per reaction) or PMA/Ionomycin (Sigma) for 6 hours in the presence of 1 μg/mL of co-stimulatory monoclonal antibodies to CD28 and CD49d (BD Biosciences), and Brefeldin A (Sigma) at a concentration of 10 μg/mL as previously described [105], [141]. The peptide mixtures included EBV latent- (n =8) (Table 2.2.2.) and lytic- (n = 5) (Table 2.2.3.) as well as CMV phosphoprotein 65- (n = 3) (Table 2.2.4.) derived immunodominant epitopes for $CD8^+$ T cells, as well as overlapping peptides (n = 51) derived from the most consistently recognized EBV-encoded $CD4^+$ T-cell antigen, the EBNA1 (Table 2.2.1.) [105], [141]. Positive responses were characterized as frequencies at least 2-fold above background (no antigen) and at least 10 IFN-γ^+ events. The frequencies of antigen-specific T-cells were determined by subtracting background frequencies from those of antigen-stimulated positive samples

2.4 Identification of a Novel Inhibitor of Latent EBV Infection

2.4.1. EBNA1 Protein Expression

DE3BL21 bacteria expressing recombinant $EBNA1_{458-641}$ were streaked from frozen stock onto LB-Ampicillin plates and grown overnight at 30ºC. The next day, two colonies were picked and grown separately in 100 mL LB-Ampicillin pre-culture. The flasks were left overnight shaking at 30ºC. The next day, 2.5 mL flasks were taken containing 500 mL fresh LB-Ampicillin media. 5 mL of the pre-culture was added and grown at 30ºC. OD_{600} measurements were taken at every hour, and the cultures were induced with 1 mM IPTG once an OD_{600} of 0.6-0.7 was reached. The cultures were then left overnight to express the recombinant protein. Next day, the cultures were spun for 30 minutes at 5 500g at 4ºC. The supernatant was removed and the pellet was resuspended in PBS, and then again spun at 4 000 g for 40 minutes at 4ºC. Then, every mL of pellet was resuspended in 5 mL of lysis buffer including 1 mg/mL freshly added lysozyme and protease inhibitor (Roche) in 20 mM Imidazole in PBS. The mixture was incubated for 30 minutes on ice and then the cells were lysed with cell harvester. The cell lysate was then spun at 30 000g for 60 minutes at 4ºC. The supernatant was then filtered through a 0.4 μm filter without applying high pressure.

2.4.2. EBNA1 Protein Purification

A 5 mL nickel-chelated HiTrap HP column (GE Healthcare) was used with a maximal flow of 5 mL/min and maximal back pressure of 0.3 MPa. All buffers were filtered before use. 100 mL lysate was loaded at 2.5 mL/min flow rate. The flow-through was collected and later re-loaded on the column. 40 mM Imidazole was used as washing buffer until the UV signal was clean. Three-step elusion was then performed. Unspecific bacterial products were eluted with 100 mM Imidazole in 7 fractions of 10 mL volume. Then, 2 fractions of 3 mL volume with 250 mM Imidazole were used to eliminate all other leftover contaminants. The EBNA1 recombinant protein was eluted with 500 mM Imidazole in 15 fraction of 5 mL volume. The fractions with the highest protein concentrations, based on the UV signal, were selected and dialyzed overnight in PBS buffer. The purity of the fractions was then determined through SDS-PAGE and Silver stain (Pierce Silver Stain Kit, used according to manufacturers recommendations) of pre-purification bacterial lysate, flow-through while loading, flow-through during washing, and all elution fractions. After determination of purity and specificity, the fractions of interest were aliquoted and stored at -20ºC.

2.4.3. Sodium Dodecyl Sulfate Polyacrylamide Gel Electrophoresis (SDS-PAGE)

30 μl of each purification fraction was incubated with loading dye for 5 minutes at 95ºC and loaded onto a 0.75 mm 12.5% resolving gel containing 1 cm long 4% stacking gel. The gel was run for 2 hours at 100V. The reagents used for the SDS-PAGE are enlisted below and in Table 2.4.1.

Table 2.4.1. Chemical reagents used for SDS-PAGE gel preparation.

Reagent	**Resolving Gel (12.5%), Volume for 2x 0.75 mm gels**	**Stacking gel (4%), Volume for 2x 0.75 mm gels**
Acrylamide/Bis 30:8 (w/v)	4.17 mL	650 μL
1.5M Tris pH 8.8	2.5 mL	418 μL
10% SDS	100 μL	50 μL
d H_2O	3.14 mL	3.9 mL
10% APS	75 µL	37.5 µL
TEMED	15 µL	7.5 µL

SDS-PAGE Buffer Recipes:

1.5 M Tris pH8.8 (150ml):

27.23 g Tris base
add dH_2O until ~80ml and adjust pH to 8.8 with 6N HCl

1.5 M Tris pH6.8 (100ml):

18.17 g Tris base
add dH_2O until ~60ml and adjust pH to 6.8 with 6N HCl

6N HCl

50ml dH_2O + 50ml 37% HCl solution

1x Running buffer:

25 mM Tris base (3.03g/L)
192 mM Glycine (14.4g/L)
0.1% SDS
Set pH to 8.3 (with HCl)

2.4.4. EBNA1 Western Blot

After the SDS-PAGE run was completed, the gel was removed from the chamber, incubated for 10 minutes in 1x Transfer buffer and blotted onto 0.45 μm nitrocellulose membrane (Biorad) for 1 hour at 10V. EBNA1 was detected by Western blot using 1:10 diluted EBNA1-specific 5F12 hybridoma supernatant followed by 1:10 000 diluted goat-anti rabbit HRP-labeled secondary antibody (Biorad). The signal was developed by SuperSignal WestPico Chemiluminescent Substrate (Pierce) and developed onto an Amersham Hyperfilm ECL film (GE Healthcare).

Western Blot Buffer Recipes:

10x Transfer buffer:

250 mM Tris base (30.3 g/L)
1920 mM Glycine (144g/L)
pH should be 8.3, do not adjust!

1x Transfer buffer:

20% Methanol
10% 10x transfer buffer
70% distilled water

2.4.5. TR-FRET High-Throughput Screening Assay

300 nM of $EBNA1_{458-641}$ were incubated together with 25 nM biotin-labeled DNA oligonucleotide (Biotin-TEG-5'-GGGTAGCATATGCTATCTAGATAGCATATGCTACCC-3'), 2 nM Eu3+ Cryptate-conjugated mouse monoclonal anti-6 His antibody, and 12.5 nM Streptavidin-d2. All components were mixed together in a total volume of 10 μl in reaction buffer comprising of 200 mM NaCl, 20 mM Tris, 1 mM DTT, and 0.5% w/v BSA. The 384 well plates were incubated for 120 minutes at 30ºC and read using Perkin Elmer EnVision reader at 340 nm excitation and 665 nm emission. The HTS assay was performed by the European Screening Port, a company specialized in establishing, optimizing, performing and analyzing HTS assays.

2.4.6. Chemical Libraries Used in HTS

Table 2.4.2. Names of libraries, number and concentration of compounds used in the HTS.

Library	Number of compounds	Concentration used for initial screening
ChemBioNet	16 671	20 μM
ComGenex	2 133	20 μM
KiWiZ	140	20 μM
UHH	421	20 μM
ChemBridge	2 240	20 μM
Analyticon Discovery	2 040	10 μM
ENZO	640	4 μg/mL
HYPHA Discovery	8 783	unknown

2.4.7. HTS Hit Quality Control

Optically interfering compounds were removed as follows: The average Eu signal intensity was calculated and compounds that had values of 2-times below the average were excluded as quenching compounds, while compounds that had a value 2-times higher than the average were excluded as fluorescent compounds.

2.4.8. HTS Hit Profiling

The identified Group 1 hits showing 30% or more inhibition of the TR-FRET signal were tested in 11-point dose response studies. ActivityBase XE analysis was used to calculate the fit of the compounds. DsDNA intercalating compounds were identified by the Quant-iT PicoGreen dsDNA Assay Kit (Invitrogen). Identification of cell cytotoxic molecules was performed by 11-point compound dose response with HEK 293 cells incubated with the compounds for 24h in 0.1% v/v DMSO concentration. The cells were then lysed and intracellular ATP was measured with CellTiter-Glo Kit (Promega) used according to the manufacturer's recommendations.

2.4.9. Virtual HTS Screen

Virtual screen was performed with 1.1 M compounds from ZINC Lead-like library. TrixX^{BMI} Software was used to analyze the binders through two different scoring functions (ChemScore and ScreenScore). 4 400 binding models were used for the visual analysis.

2.4.10. Electrophoretic Mobility Shift Assay (EMSA)

120 μg/mL of EBNA1 were incubated for 30 minutes at 30ºC with 12 nM of biotinylated oligonucleotide (as used in the HTS assay) in 100 μL of reaction buffer (200 mM NaCl, 20 mM Tris, 1 mM DTT, and 0.5% w/v BSA). The reaction was the aliquoted into 8 tubes with 15 μL volume to which 0, 10, 25, 50, 100, 500, 1 000, or 10 000 μL of Tilorone were added. The reactions were incubated at 30ºC for additional 120 minutes. EBNA1 only and oligonucleotide only were used as controls and underwent the same procedure as the samples. Non-denaturing loading dye was added to the samples, which were then loaded on a 1.5mm 6% non-denaturing polyacrylamide gel (4 mL 30% Acrylamide, 600 μL Glycerol, 15 mL 0.5 TBE buffer, 300 μL 10% APS, 20 μL TEMED). Before the addition of the samples the gel was pre-run for 30 minutes at 100 V in cold 0.5 M TBE buffer. The gel was then run at 70V for 2 hours and then transferred for 45 minutes at 12V onto a Biodyne B positively charged Nylon membrane (Pall Corporation). The membrane was then immediately UV-cross-linked for 15 minutes and blocked overnight in 5% skimmed milk in PBS buffer. The oligonucleotide was then detected by incubation of the membrane with 1:1 000 diluted Streptavidin-HRP antibody (eBioscience) and the signal was detected by SuperSignal West Femto (Pierce) and developed onto an Amersham Hyperfilm ECL film (GE Healthcare).

EMSA Running Buffer

10X TBE Buffer Recipe

1 M Tris

0.9 M boric acid

0.01 M EDTA

2.4.11. Cell Line Culturing and Cytotoxicity Assay

LCL and Ramos cell lines were cultured in R10 media (10% FCS, Penicillin/Streptomycin diluted 1:100 in RPMI) at an initial cell density of 0.3 x 10^6 cells per mL T75 flasks or 6-well plate. 0, 10, 15, 20, or 25 μM of Tilorone were added to the cultures. Respective volume of 0.1% DMSO was added to the sample with 0 μM of Tilorone, which served as a no-treatment control. The samples were counted at least 3 times per week using Trypan Blue (Gybco), counting chamber and a microscope to discern dead cells. The samples that reached a cell density of 1 x 10^6 cells per mL or higher were split to the original cell density of 0.3 x 10^6 cells per mL. The cultures were kept for at least 17 days and the cell splitting was taken into account for the final calculation of total cell numbers versus time of culture.

2.4.12. Cell Viability Assay

Similarly to the cell cytotoxicity assay (above) the LCLs and L428 cell lines were incubated at an initial cell density of 0.3 x 10^6 cells per mL in 6-well plates and 0, 10, 15, 20, or 25 μM of Tilorone were added to the cultures. Respective volume of 0.1% DMSO was added to the sample with 0 μM of Tilorone, which served as a no-treatment control. Measurements were taken at day 1, 3, 5, and 7, stained with Live/Dead Fixable Death Cell Kit APC-Cy7 dye (Invitrogen), and the frequency of live cells from all cells was measured by flow cytometry on an LSR Fortessa (BD Biosciences). The frequency was then related to the frequency of live cells of the 0 μM Tilorone sample at the respective time points.

2.4.13. Cell Proliferation Assay

LCLs or L428 cells were stained with Cell Trace Violet (Invitrogen) at a final dye concentration of 1 μM. The cells were cultured as described in section 2.4.12. and stained with Live/Dead Fixable Death Cell Kit APC-Cy7 to eliminate dead cells. Cell Trace Violet was detected in the Pacific Blue channel by flow cytometry on an LSR Fortessa (BD Biosciences). The relative mean fluorescence intensity (MFI) of Cell Trace Violet was normalized to LCL or L428 conditions incubated with 0 μM Tilorone at the respective time point. Dilution of the Cell Trace Violet MFI signal signified proliferation of the cells.

2.4.14. Annexin V Apoptosis Staining

LCL and L428 cell lines were cultured and incubated with 0, 5, 10, 15, 20, or 25 μM Tilorone concentrations as described above (Section 2.4.12.). 24 hours later the cell samples were harvested, washed in PBS, resuspended in 1x Binding Buffer, and stained with 0.5 μl Annexin V (Biolegend) per 100 μl staining volume. 0.5 μl 7-AAD (Biolegend) per 100 μl staining volume was added to discern dead cells. The samples were then incubated for 30 minutes at 4°C and measured within one hour by flow cytometry on an LSR Fortessa (BD Biosciences). Annexin V was detected in the APC channel while 7-AAD was detected in the PerCP channel.

2.4.15. Caspase 3/7 Activation Assay

Caspase-Glo 3/7 Assay (Promega) was used for measurement of apoptosis through the activation of Caspase 3 and 7. LCLs and L428 cells were resuspended in fresh R10 and seeded in 96-well plate at 15 000 cells per well in a total volume of 100 μL together with 0, 5, 10, 15, 20, 25 μM Tilorone. The cells were incubated with the inhibitor for 3, 8 and 24 hours and the Caspase 3/7 activity was measured according to the manufacturer's recommendation.

100 μM Ionamycin was used as positive control, while 0 μM Tilorone served as negative control of the assays.

2.4.16. Lytic Infection Inhibition Assay

AKBM cells that express GFP upon switch from latent to lytic EBV replication were grown in R10 media supplemented with Hygromycin. On the day of the assay the cells were washed in R10 media only to remove the Hygromycin from the cell culture. 200 μL of cell culture with a cell density of 4 x 10^6 per mL was distributed in 24-well plates and incubated for 2 hours with 3.5 μL F(Ab) IgG cross-linking antibody at 37ºC. As negative control, no F(Ab) IgG was added to the cultures. Concomitantly, Tilorone at a concentration of 0, 10, 15, 20 or 25 μM was added to the cell cultures. After two hours of incubation, 800 μL of R10 was added to the wells and the cells were left overnight at 37ºC. On the next day, the cells were stained with Live/Dead APC-Cy7 Fixable Death Cell Stain (Invitrogen). The GFP expression was used as a quantification marker of lytic reactivation. The flow cytometry analysis was performed on an LSR Fortessa (BD Biosciences). Beforehand, the cells were counted in a counting chamber to determine Tilorone- or induction-related cell death.

2.4.17. *Ex Vivo* EBV Transformation of B Cells

$CD19^+$ cells were MACS separated from freshly isolated PBMCs and stained with Cell Trace Violet (Invitrogen) as described in Section 2.4.13. 2x10^5 $CD19^+$ cells were plated per well in a U-bottom 96-well plate and infected with 0.5 MOI of EBV (1x10^5 RIU per well). Then 0, 1, 10, and 20 μM of Tilorone we added to the cultures and the cellular proliferation was analyzed with FlowJo cell proliferation tool at day 4, 6, and 11 post infection. The relative frequency of divided cells was normalized to the frequency of cells incubated with 0 μM of Tilorone for four days.

2.4.18. Luciferase Transduction of Cell Lines

pLenti CMV Puro LUC (w168-1) (Addgene) supernatants were used for transfection of LCLs or L428 with firefly luciferase. LCLs were diluted at a 1:1 ratio in pLenti supernatant and R10 at a cell density of 0.5x10^6 per mL. The cells were then plated in 24-well plates at 2 mL per well. Puromycin antibiotic selection was started with 0.7 μg/mL and continued for at least 14 days. Then serial dilution of cells was performed ranging from 1x10^3 to 1x10^5 cells per well in a 96-well plate. D-Luciferin (Caliper Lifesciences) was added to the cells and the luciferase signal was detected in Xenogen IVIS 100 (Caliper Lifesciences) imaging system.

The cells, LCL-luc or L428-luc, were then cultured without Puromycin selection in R10 media and used for further experiments.

2.4.19. Non-Reconstituted NSG Mouse Tumor Model

Non-reconstituted NOD Cg-Prkdc^{scid} Il2rg^{tm1Wjl}/SzJ (NSG) mice (The Jackson Laboratory) were injected with 10x10^6 luciferase-expressing LCLs (LCL-luc) or control (L428-luc) cells i.v. into the tail vein. The mice were treated with 50 mg/kg Tilorone or PBS thrice a week for the continuation of four weeks. The weight and the general health status of the mice were observed thrice a week. Mice whose weight dropped below 15% of the highest weight were sacrificed. The proliferation and localization of the injected cells was measured weekly as follows: 150 mg/kg D-Luciferin (Caliper Lifesciences) was injected i.p. and the animals were anesthetized with 2% isofluran, and then transferred in the dark chamber of a Xenogen IVIS 100 (Caliper Lifesciences) imaging system where the anesthesia was maintained via nose cones. The luminescence was recorded 10 minutes post the D-Luciferin injection. The photo flux was measured in a rectangular region of interest of the same size around the whole body of the individual mice using Living Image 2.5 software (Caliper Lifesciences).

2.4.20. EBV Infection in Humanized NSG Mice

Sublethally-irradiated NOD Cg-Prkdc^{scid} Il2rg^{tm1Wjl}/SzJ (NSG) or NSG HLA-A2 transgenic pups (The Jackson Laboratory) were injected intrahepatically with 1-2 x10^5 CD34$^+$ MACS-isolated hematopoietic progenitor cells derived from human fetal liver tissue (Advanced Bioscience Resources). The preparation of the human fetal tissue and the isolation of the CD34$^+$ cells were performed as previously described by Strowig et al. [142]. The animal protocols were approved by the Cantonal Veterinary Office Zürich (protocol nos. 116/2008 and 148/2011). Three months post injection, the mice were bled and the reconstitution of the human immune system compartments was analyzed with the flow cytometry panel presented in Table 2.4.3.

Table 2.4.3. Flow cytometry panel for determination of human lymphocyte subsets in reconstituted humanized NSG mice.

Marker	Fluorophore	Clone	Dilution	Company
Live/Dead	Aqua	-	1:1000	Invitrogen
CD45	Pacific Blue	HI30	1:200	Biolegend
CD19	PE-Cy7	HIBI9	1:100	Biolegend
CD3	PE-Cy5.5	S4.1 (7D6)	1:50	Invitrogen
CD4	APC-Cy7	RPA-T4	1:50	Biolegend
CD8	PerCP	RPA-T8	1:100	BD Biosciences
CD45RO	AlexaFluo700	UCHL1	1:100	Biolegend
HLA-DR	FITC	L243	1:200	Biolegend
NKp46	APC	9E2	1:50	BD Biosciences

The mice were then distributed in two cohorts so that the median reconstitution rates of the human lymphocyte subsets were comparable. The mice were pre-treated with 50 mg/kg Tilorone i.p. and 24 hours later infected i.p. with $1x10^5$ Raji Infecting Units (RIU) GFP-EBV (B95-8); the titration of the virus was performed on Raji cells in serial dilutions and calculated as RIU using flow cytometry of GFP-positive Raji cells 3 days after cells infection. The mice were treated 3 times per week with 50 mg/kg Tilorone for the following 5 to 7 weeks. The weight and general health state of the mice was monitored thrice a week, while the whole blood viral load and the lymphocyte composition was evaluated once a week. The mice were sacrifice 5 to 7 weeks post infection or when a mouse lost 15% or more of its highest weight. The spleens and livers of the mice were harvested and the lymphocytes isolated through Collagenase D (Roche) and DNase (Roche) digestion. The cells were counted and stained with the panel in Table 2.4.3. and analyzed on an LSR Fortessa (BD Bioscences).

2.4.21. EBV Quantification from Tissue and Whole Blood

Tissue pieces were measured and digested by QIAmp DNA mini kit (Qiagen) and the EBV viral load per mg of tissue was determined by the Medical Virology department at the University of Zurich as follows: DNA isolated from the organs was eluted in 50 µl Tris-EDTA and stored at 4°C. Quantitative analysis of EBV DNA was performed by a TaqMan® (Applied Biosystems) real-time PCR technique [137] with modified primers for the BamHI W fragment (5'-CTTCTCAGTCCAGCGCGTTT-3' and 5'-TCTAGGGAGGGGGACCACTG-3') and the fluorogenic probe (5′-(FAM)-

CGTAAGCCAGACAGCAGCCAATTGTCAG-(TAMRA)-3′). PCRs of duplicate samples were performed using ABI Prism 7700 Sequence Detector (Applied Biosystems).

2.4.22. Statistical Analysis

Unless otherwise stated, all data was analyzed with two-tailed student's *t* test. A P value of <0.05 was considered statistically significant. Prism software (GraphPad Software) was used for the statistical analysis and graphs generation.

3. RESULTS

3.1. Generation of Autoreactive Humoral and Cellular Immune Responses during Infectious Mononucleosis

3.1.1. Demographics of IM Patients and Controls

Since patients with a history of IM have 2.3 times higher relative risk of developing MS later in life [94], we hypothesized that during the fulminant phase of IM autoreactive cellular and humoral immune responses are generated that contribute to autoimmune pathologies later in life. To test this hypothesis we collected samples from IM patients taken at the time of first doctor visit post occurrence of IM symptoms. In our cohort of IM patients the onset of symptoms was between 3 and 21 days before first doctor visit. PBMCs and serum samples were collected from these patients and compared to adolescents who suffered from unrelated, i.e. non-inflammatory medical conditions or were healthy. The control patients visited doctors in the same hospital and suffered from the following conditions with the respective number of patients written in brackets: migraine (3), healthy (2), sunstroke (2), chronic headache (1), tonsillitis (1), Lumbago (1), congenital facial paralysis (1), Melkersson–Rosenthal syndrome (1), and vocal cord dysfunction (1). Table 3.1.1 presents the demographics of the IM patients and controls.

Table 3.1.1. Demographics of IM patients and healthy controls.

	Controls	IM patients
Number	13	13
Gender (f/m)	9/4	5/8
Average age	15 (SD = 4)	16 (SD = 8)
Days with symptoms before doctor visit	NA	3-21
Symptoms (moderate/severe/ND)	NA	3/9/1

ND = Not determined, NA = Not available

3.1.2. Serum Analysis for Hallmarks of EBV Infection

To verify the infection status of the study participants we measured the EBV viral load in the serum of the patients and controls (Figure 3.1.1.). The serum viral load of the IM patients

varied between 200 and 35 700 viral particle per mL serum, while as expected none of the controls presented with detectable viral load in the serum.

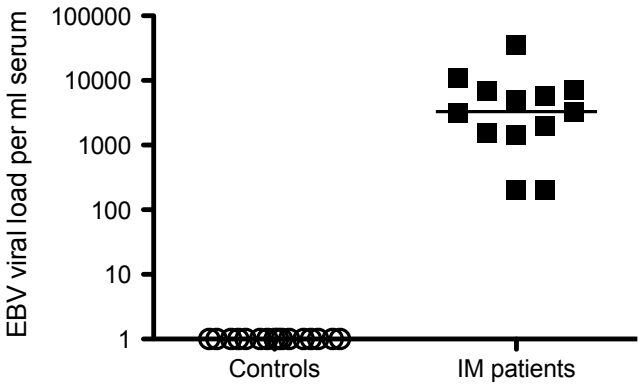

Figure 3.1.1. EBV viral load in the serum of control and IM patients. IM patients presented with high serum viral load with a variation between 200 and 35 700 viral particles per ml of serum, while no EBV viral load was detected in the control patients.

To verify the EBV seropositivity of our study participants we, then, performed ELISA for detection of anti-VCA IgG antibodies, which are a hallmark of latent EBV infection (Figure 3.1.2.). Since we wanted to compare latent EBV carriers as controls to active IM patients we eliminated from our analysis four of the initial control samples that were negative for VCA antibodies. These four controls were also excluded from the patient demographics table (Table 3.1.1). In contrast, all IM patients presented with anti-VCA IgG antibodies the median of which, however, was lower than that of the control patients.

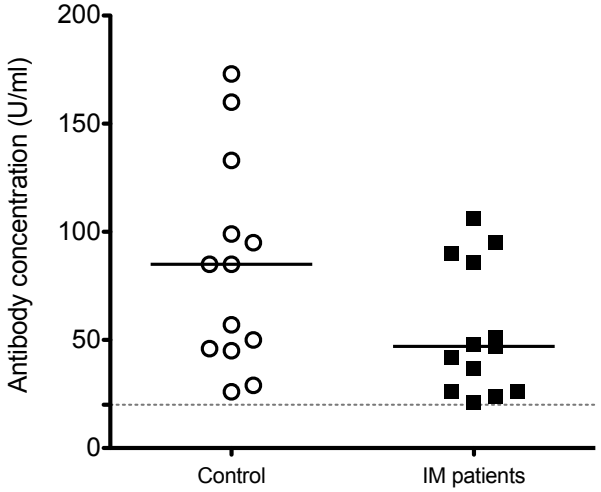

Figure 3.1.2. Presence of anti-VCA IgG antibodies in the serum of latent non-IM control EBV carriers and IM patients.

3.1.3. Investigation of Humoral Autoreactive Immune Responses

3.1.3.1. Reactivity Against Human MOG Antigen

The myelin oligodendrocyte glycoprotein (MOG) is expressed on the outer layer of the myelin sheath and therefore is easily accessible to attack by autoreactive antibodies. This antigen has been implicated in the pathology of MS since it is confined to the CNS and antibodies against MOG have been detected in MS patient serum, cerebral fluid, and brain lesions [143], [144]. Moreover, the mouse model of MS, experimental autoimmune encephalomyelitis (EAE), can be generated by induction of anti-MOG antibodies that infiltrate the CNS and cause MS-like pathologies [145], [146].

We investigated the presence of autoreactive anti-MOG antibodies in the control and IM patient sera by incubating the sera with an oligodendroglial cell line that constitutively expressed human MOG on its surface. The presence of bound serum antibodies was then determined through a secondary anti-human antibody bound to a fluorescent dye. A control oligodendroglial cell line transduced with a non-MOG lentivector was used to define the background fluorescence level. The anti-human MOG 818C5 antibody was used as positive control, and also to determine the detection limit of the assay (Figure 3.1.3.A). The MOG autoreactivity was measured as delta MFI of the MFI obtained by incubating the patient serum with the MOG-expressing cell line minus the MFI obtained with the non-MOG control cell line (Figure 3.1.3.B). Even though the median delta MFI of the IM patient group was higher than that of the control group, no statistical significance was observed. Interestingly, only one of the IM patients (IM15) but none of the controls had a delta MFI above the positivity threshold.

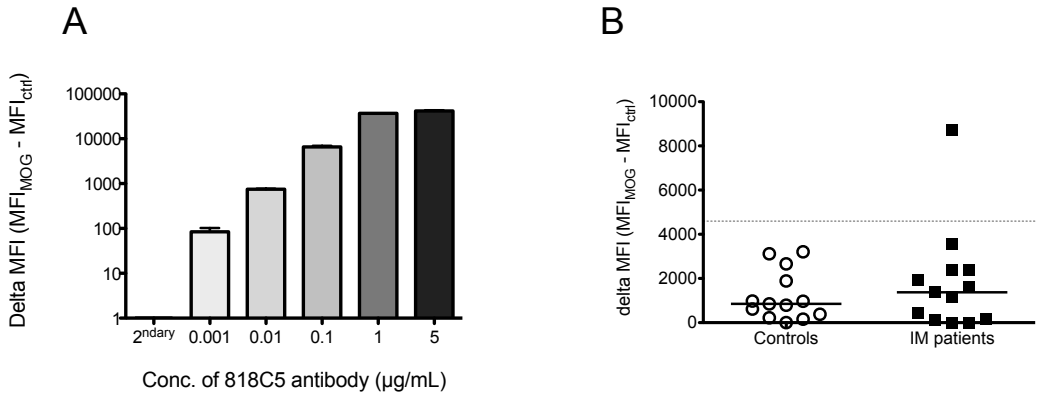

Figure 3.1.3. Serum reactivity to human MOG antigen. (**A**) Titration of MOG reactivity assay with different concentrations of anti-human MOG antibody. (**B**) Anti-MOG reactivity of controls and IM patient sera. The positivity threshold, designated with a grey dotted line, was determined as three standard deviations above the mean of the control samples.

3.1.3.2. Detection of Autoreactivity through HEp2 Immunofluorescence

Presence of anti-nuclear antibodies (ANA) is a hallmark of autoreactivity that is routinely tested in the clinic for diagnosis of autoimmune disease. In collaboration with the Clinical Immunology Department at the University Hospital Zurich, we analyzed the presence of autoantibodies by incubating control and IM patient sera with permeabilized HEp2 cells and performing immunofluorescence analysis to determine the binding pattern of potential autoreactive antibodies in the patient and control sera. 6 out of 13 IM patient samples were HEp2-staining negative, while 6 were borderline positive, and only 1 (IM12) was determined as positive. On the other hand, 11 out of 13 control samples were negative and 2 were considered as positive (CO9 and CO10). Interestingly, the HEp2 staining pattern observed for 8 of the 13 (62%) IM patient samples was determined as reticular cytoplasmic pattern that is similar to staining obtained with anti-vimentin autoantibodies (Figure 3.1.4.). None of the controls had such a vimentin-like pattern but rather a dense cytoplasmic staining for one of the controls (CO9), and a dense, homogeneous nuclear staining for the second positive control (CO10). The vimentin-like antibodies were determined by differential use of anti-IgG and anti-IgM secondary antibodies to be of IgM isotype.

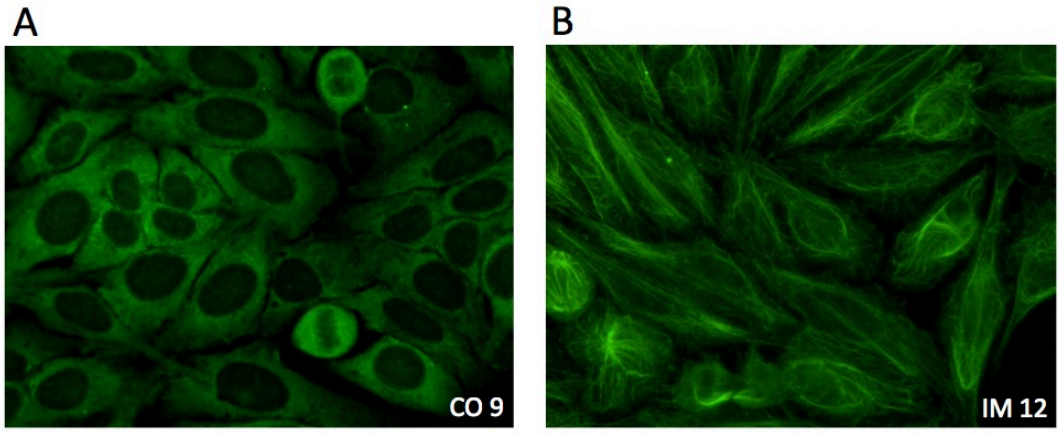

Figure 3.1.4. HEp2 immunofluorescence for detection of autoreactive antibodies. (**A**) Example of HEp2-positive control sample with dense cytoplasmic staining. (**B**) Representative HEp2-positive vimentin-like staining of an IM patient.

Additionally, we tested for presence of SS-A antibodies, characteristic of SLE, and citrullinated peptide antibodies (CCP2) that are typical for RA. All IM patients were negative for SS-A antibodies and only one (IM15) had borderline CCP2 positivity. Due to limited availability of serum from some of the control samples not all of them were tested for presence of SS-A and CCP2 antibodies. None of the tested control samples was positive for

SS-A or CCP2 autoantibodies. A summary of the HEp2 staining results obtained from the IM patient sera is presented in Table 3.1.2.

Table 3.1.2. Summary of HEp2 staining results with IM patient sera.

Patient number	SS-A	CCP2	HEp2 (ANA) quantitative	HEp2 (ANA) qualitative	HEp2 (ANA) binding pattern
IM5	ND	ND	40	Negative	None
IM6	1.8	6.1	160	Borderline	Reticular cytoplasmic pattern, vimentin-like
IM7	2.2	5.3	160	Borderline	(1) Nuclear speckled; (2) Reticular cytoplasmic pattern, vimentin-like
IM9	0.9	1.9	160	Borderline	(1) Reticular cytoplasmic pattern, vimentin-like; (2) Faint nuclear fine speckled pattern
IM10	0.2	1.7	160	Borderline	Reticular cytoplasmic pattern, vimentin-like
IM12	0.8	2.2	320	Positive	Reticular cytoplasmic pattern, vimentin-like
IM14	ND	ND	40	Negative	None
IM15	1.1	7.6	160	Borderline	Reticular cytoplasmic pattern, vimentin-like
IM16	0.5	2.8	40	Negative	Reticular cytoplasmic pattern, vimentin-like
IM17	0.9	3	40	Negative	Nuclear speckled
IM18	0.4	2.8	40	Negative	None
IM19	0.7	1.7	40	Negative	Faint nucleolar binding
IM20	0.3	2.9	160	Borderline	Reticular cytoplasmic pattern, vimentin-like

For SS-A values >7 were considered negative, 7-10 borderline, and >10 positive. For CCP2 values >7 were considered negative, 7-10 borderline, and >10 positive. Negative values are colored in green, borderline in orange, and positive in red. ND = Not determined

3.1.3.3. Detection of Anti-Vimentin Autoantibodies

To verify that the observed HEp2 staining pattern in the IM patietns is derived due to presence of anti-vimentin antibodies, we performed ELISA to detect and quantify the anti-vimentin IgM and IgG antibodies in the control and IM patient sera (Figure 3.1.5.). Indeed, the IM patients had significantly higher levels of anti-vimentin IgM antibodies compared to the controls (p=0.002). 9 out of 13 (69%) IM patients were positive for vimentin, while only 1 out of 13 (8%) control samples had an IgM anti-vimentin signal above the positivity threshold (Figure 3.1.5.A). Anti-vimentin IgG was detected in only 4 out of 13 (31%) IM patients, while none of the controls was positive. The difference between the two groups, however, did not reach statistical significance. We analyzed additionally one MS (n=18) and one MG

(n=12) patient cohorts for presence of anti-vimentin antibodies (Figure 3.1.5.A). The MS patient cohort was the same as described in Section 2.2.1., while the MG cohort was the same as described in Section 2.3.1. Interesting, 6 out of 18 (33%) of the MS patients were positive for anti-vimentin IgM, compared to only 1 MG patient out of 12 (8%). Similarly to our observation for the IM patients and controls, the IgG anti-vimentin reactivity was greatly decreased compared to the IgM responses. Only 1 MS patient (6%) and none of the MG patients had detectable IgG antibodies to vimentin (Figure 3.1.5.B).

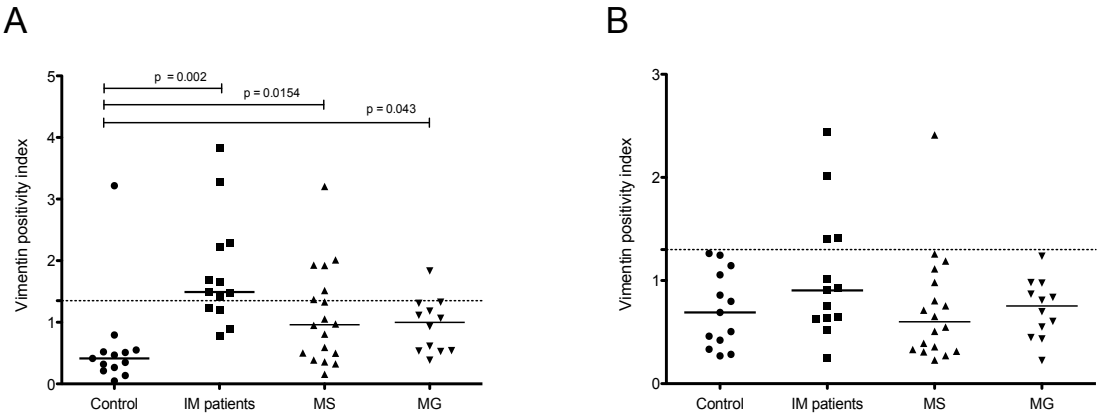

Figure 3.1.5. Detection of anti-vimentin IgM (**A**) and IgG (**B**) autoantibodies in control, IM patient, MS patient, and MG patient sera.

3.1.3.4. Correlation Between EBV Viral Load and Humoral Autoreactivity Responses

To determine whether there is a link between EBV viral load and humoral autoreactivity responses during acute IM, we correlated the serum viral load of the IM patients with their respective autoreactivity values to MOG, ANA, SS-A, CCP2, and the anti-vimentin IgM and IgG antibody levels (Figure 3.1.6.). Only MOG (Figure 3.1.6.A) and CCP2 (Figure 3.1.6.C) reactivity reached statistical significance. EBV viral load did not correlate with anti-vimentin IgM (Figure 3.1.6.E) or IgG (Figure 3.1.6.F) antibody levels. Curiously, the IM patients with the highest EBV viral load (IM15) presented with borderline positivity for CCP2 and ANA autoreactivity as well as the highest value for MOG reactivity. The IM patient with the second highest viral load (IM12) was clearly positive for ANA and had a relatively high but not above the positivity threshold value for MOG reactivity. These two patients were further analyzed for presence of autoreactive T cells.

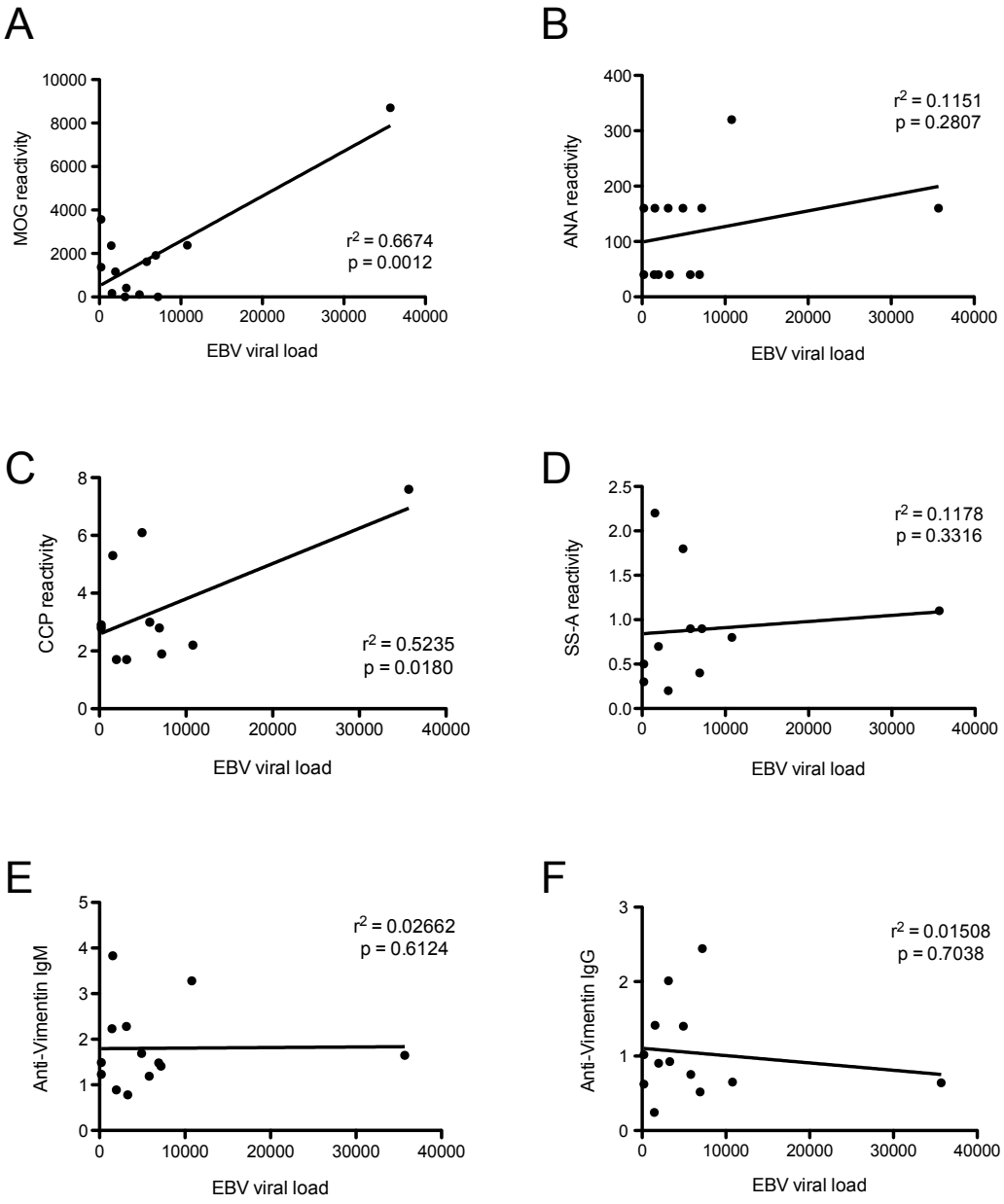

Figure 3.1.6. Correlation analysis between EBV viral load and autoreactive antibody levels in IM patient sera. (**A**) EBV viral load correlated to MOG reactivity. (**B**) EBV viral load correlated to HEp2 (ANA) reactivity. (**C**) EBV viral load correlated to CCP2 reactivity. (**D**) EBV viral load correlated to SS-A reactivity. (**E**) EBV viral load correlated to anti-vimentin IgM antibody levels. (**F**) EBV viral load correlated to anti-vimentin IgG antibody levels.

3.1.4. Investigation of Cellular Autoreactive Immune Responses

3.1.4.1. Reactivity to EBV and Autoantigen Peptide Pools

Next, we investigated the presence of autoreactive T cell responses during acute IM. Frozen PBMCs were thawn and stimulated with pools of 51 overlapping peptides of the C-terminal region of EBNA1, 5 lytic EBV peptides, 8 latent EBV peptides, 15 myelin peptides, or 15 pro-insulin peptides. As a negative control and baseline response determinant we used unstimulated PBMCs, while PMA/Ionomycin stimulation served as positive control for the assay. The myelin peptide pool that was used comprised of peptides that have been described to be immunodominat in MS patients and encephalytogenic in mice [147]. The pro-insulin peptide pool served as a control autoimmune reponse peptide pool unrelated to MS pathogenesis. The IM patients had reduced reactivity to stimulation with EBV antigens, however that was not surprising since hypotetically this is due to T exhaustion and lowered thresold of responsiveness in the setting of fulminant infection. Nevertheless, the IM patients had augmented responses to lytic and to a lesser extend to the latent EBV peptide pool compared to the controls. However, the IM patients did not differ in their reactivity to myelin nor to the pro-insulin autoantigens (Figure 3.1.7.).

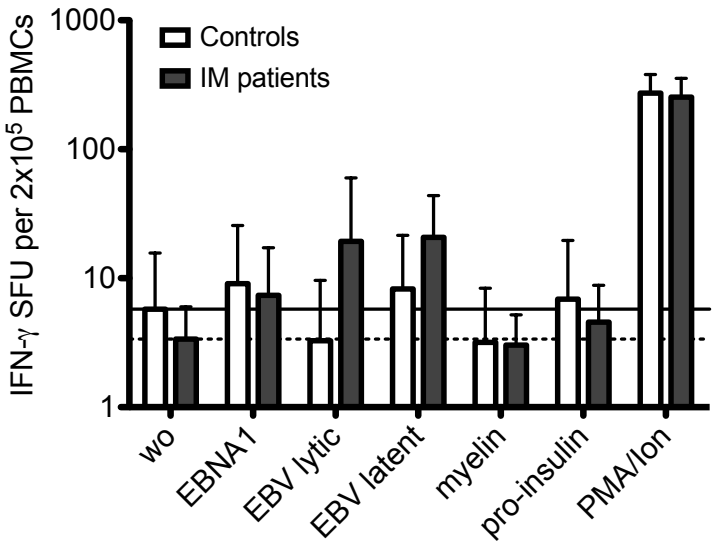

Figure 3.1.7. IFN-γ ELISPOT with IM patient and control PBMCs. The cells were stimulated with peptide pools of EBNA1, lytic or latent EBV antigens, myelin, pro-insulin. PMA/Ionomycin served as positive control, while no stimulation served as a negatice control. The baseline of IFN-γ response for each patient set was determined based on the SFU in the non-stimulated condition (wo). The straight line represents the baseline of response of the control patients, while the dotted line represent the baseline of response of the IM paient group.

3.1.4.2. Cross-Reactivity Analysis of EBNA1-Reactive T Cells from IM Patients

Since we did not find any signs of augmented autoreactivity to myelin or pro-insulin antigens in bulk PBMCs from acute IM patients, we deicded to chose the two patients with highest EBV viral load and to clone out EBNA1-reactive T cells in order to check whether these T cells would cross-react to autoantigens.

EBNA1-reactive T cells were expanded from bulk PBMCs and separated by cytokine capture assay, then single-cell seeded and outgrown. The cells were stimulated only with irradiated feeders and EBNA1 peptide pool, and supplemented with IL-2. No unspecific phytohaemagglutinin (PHA) stimulation was used during the expansion and clone maintenance.

34 EBNA1-reactive $CD4^+$ T cell clone cultures were outgrown from patient IM12, while 10 EBNA1-reactive $CD4^+$ T cell clone cultures could be outgrown from patient IM15. As control 5 EBNA1-reactive $CD4^+$ T cell clone cultures were isolated from control patient CO15.

The reactivity of the clone cultures was measured by IFN-γ , GM-CSF, and IL-2 cytokine production as well as expression of T cell activation markers, HLA-DR and CD69, post stimulation with 5 μM EBNA1 peptides, 5 and 25 μM of myelin peptide pool, or 5 and 25 μM of pro-insulin peptide pool (Table 2.2.5.). Stimulation with medium alone was used to determine the baseline cytokine secretion and activation marker expression of the clone cultures. The EBNA1-reactive clones secreted IFN-γ, GM-CSF, but no IL-2, and upregulated HLA-DR and CD69 in response to EBNA1 peptide pool stimulation. None of the clone cultures stimulated with myelin or proinsulin peptide pool, however, was observed to significantly upregulate T cell activation markers or secrete IFN-γ, GM-CSF, nor IL-2. Figure 3.18 presents IFN-γ production as result of stimulation with increasing concentrations of EBNA1, myelin, or proinsulin peptide pool stimulation.

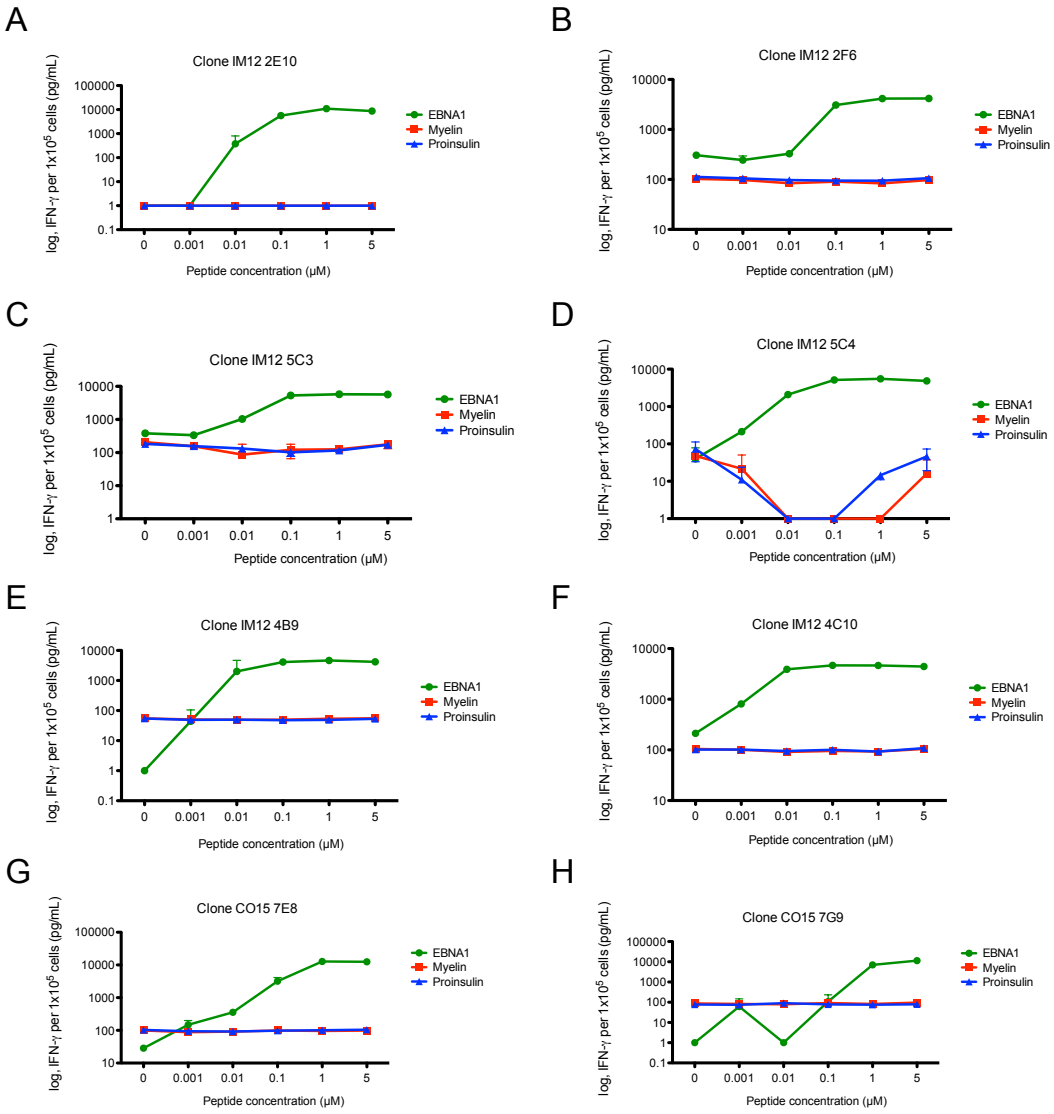

Figure 3.1.8. IFN-γ secretion as result of EBNA1, myelin, or proinsulin peptide pool stimulations of six representative EBNA1-reactive clones from IM12 (A-F), and two representative clones from CO15 (G-H).

3.2. EBV-Specific Immune Responses in Patients with Multiple Sclerosis Responding to IFN-β Therapy

The following section is adapted from Comabella, Kakalacheva et al. Mult Scler. 2012 May;18(5):605-9.

3.2.1. Patient Demographics

Symptomatic primary infection with the human γ-herpesvirus Epstein–Barr virus and elevated immune responses to EBV are associated with the development and progression of multiple sclerosis. Interferon-beta (IFN-β), first-line treatment for relapse-onset MS, exhibits complex immunoregulatory and antiviral activities. The objective of this study was to determine EBV-specific immune responses in patients with MS during IFN-β therapy. In order to do that we evaluated cellular and humoral immune responses to EBV- and cytomegalovirus (CMV)-encoded antigens in patients with MS before and 1 year after IFN-β treatment. Twenty-eight patients with MS who showed a clinical response to IFN-β as defined by the absence of relapses and lack of progression on the Expanded Disability Status Scale (EDSS) score during the first 2 years of treatment were included. Since paired peripheral blood mononuclear cells (PBMC) and serum samples were not available in all of the 28 patients included in this study, we determined antibody responses in a total of 24 patients and cellular immune responses in a total of 18 patients. A summary of the demographic and baseline clinical characteristics is shown in Table 3.2.1.

Table 3.2.1. Demographics and baseline clinical characteristics of MS patients treated with IFN-beta. (Table copied from *Comabella, Kakalacheva et al.* [148])

Characteristics	Whole group	Antibody responses	T-cell responses
n	28	24	18
Age (years)	34.0 (8.0)	34.6 (8.3)	33.4 (7.9)
Female/male (% women)	18/10 (64.3)	15/9 (62.5)	12/6 (66.7)
Clinical form (RR/SP)	26/3	22/2	15/3
Duration of disease (years)	5.3 (5.0)	4.4 (4.7)	5.4 (4.7)
EDSS[a]	2.0 (1.5–2.8)	2.0 (1.5–2.8)	2.0 (1.0–3.0)
Number of relapses in the two previous years	2.3 (0.9)	2.3 (1.0)	2.2 (0.8)
Type of IFNb [*n* (%)]			
IFNβ 1a IM	8 (28.6)	8 (33.3)	5 (27.8)
IFNβ 1b SC	11 (39.3)	10 (41.7)	8 (44.4)
IFNβ 1a SC	9 (32.1)	6 (25.0)	5 (27.8)

Data are expressed as mean (standard deviation) unless otherwise stated. [a]Data are expressed as median (interquartile range).
RR, relapsing–remitting MS; SP, secondary progressive MS; EDSS, Expanded Disability Status Scale; IM, intramuscular; SC, subcutaneous.

3.2.2. Virus-Specific IgG Antibody Levels in Patients with MS Remain Unchanged before and during IFN-β Treatment

We determined IgG responses specific for the EBV-encoded immunogenic C-terminal domain of the latent viral protein EBNA1 (p72) and towards pooled viral capsid antigens (VCA), expressed during productive viral replication. These responses were compared with IgG reactivity against lysates of the β-herpesvirus CMV. EBV-specific antibody responses were detectable in 96% (23/24) of the patients compared with a seropositivity rate of 50% (12/24) for CMV (Figure 3.2.1.). Antibody responses to EBNA1 tended to be lower after 1 year of therapy (median of 9062 U/mL before treatment compared with 5804 U/mL during treatment). However, this difference did not reach statistical significance (p = 0.2296). Humoral immune responses to lytic VCA antigens remained unchanged during IFN-β treatment, whereas IgG responses to CMV lysates slightly decreased (median of antibody index: 1.29 U/mL before treatment compared with 1.18 U/mL during treatment, p = 0.007).

Neutralizing antibody (NAb) data at baseline and after 12 and 24 months of treatment were available in 16 patients (57.2%). Only one patient out of 16 (6.3%) developed low titre of NAbs at 12 and 24 months of treatment. Humoral and cellular immune responses in this patient did not differ from the NAb-negative cohort and patients from whom NAb determinations were missing.

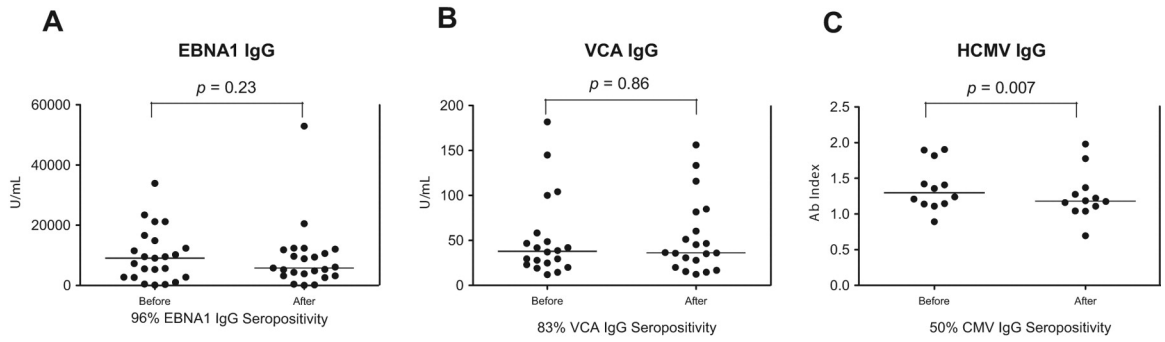

Figure 3.2.1. Virus-specific IgG antibody levels in patients with MS remained unchanged before and during IFN-β treatment. (**A**) Serum ELISA for IgG antibody responses to EBV-encoded nuclear antigen 1 (EBNA1). Median EBNA1 antibody concentration before treatment was 9062 U/mL, while after treatment 5804 U/mL. (**B**) Serum ELISA for IgG antibody responses to EBV-encoded lytic viral capsid antigens (VCA). Median VCA antibody concentration before treatment was 37.85 U/mL, while after treatment 36.21 U/mL. (**C**) Serum ELISA for IgG antibody responses to CMV lysates. Median CMV antibody index before treatment was 1.29, while after treatment 1.18. The frequencies of patients seropositive for the respective ELISAs are noted below the graphs. Seronegative individuals were excluded from the analysis. (Figure copied from *Comabella, Kakalacheva et al.* [148])

3.2.3. Viral Antigen-Specific T Cell Proliferation Is Altered in Patients with MS before and during IFN-β Treatment

Employing a multiparameter flow cytometry-based CFSE dilution assay, we next determined EBV- and CMV-specific $CD4^+$ and $CD8^+$ T cell responses in 18 patients before and during IFN-β therapy. PBMC were stimulated with either MHC class I-restricted epitopes from three latent (EBNA3A, EBNA3B, EBNA3C) and three lytic (BZLF1, BRLF1, BMLF1) antigens or an overlapping peptide library spanning the C-terminal domain of EBNA1 (400-641) [141]. The MHC class I-restricted T cell epitopes were selected based on their previous identification as immunodominant $CD8^+$ T cell epitopes [149], [149], whereas EBNA1 was chosen as a dominant EBV-encoded $CD4^+$ T cell antigen in healthy virus carriers [150]. MHC class I-restricted CMV pp65-derived peptides were used as control antigens [149]. IFN-β treatment was associated with a marked downregulation of EBNA1-specific $CD4^+$ T cell responses ($p = 0.0156$) (Figure 3.2.2.). In contrast, $CD8^+$ T cell responses towards other EBV-encoded antigens expressed during both B cell transformation and lytic replication did not change significantly during treatment. Although we observed a slight decrease of CMV-specific IgG levels (Figure 3.2.1.), CMV-specific proliferative $CD8^+$ T cell responses remained unchanged during clinically effective IFN-β therapy (Figure 3.2.2.).

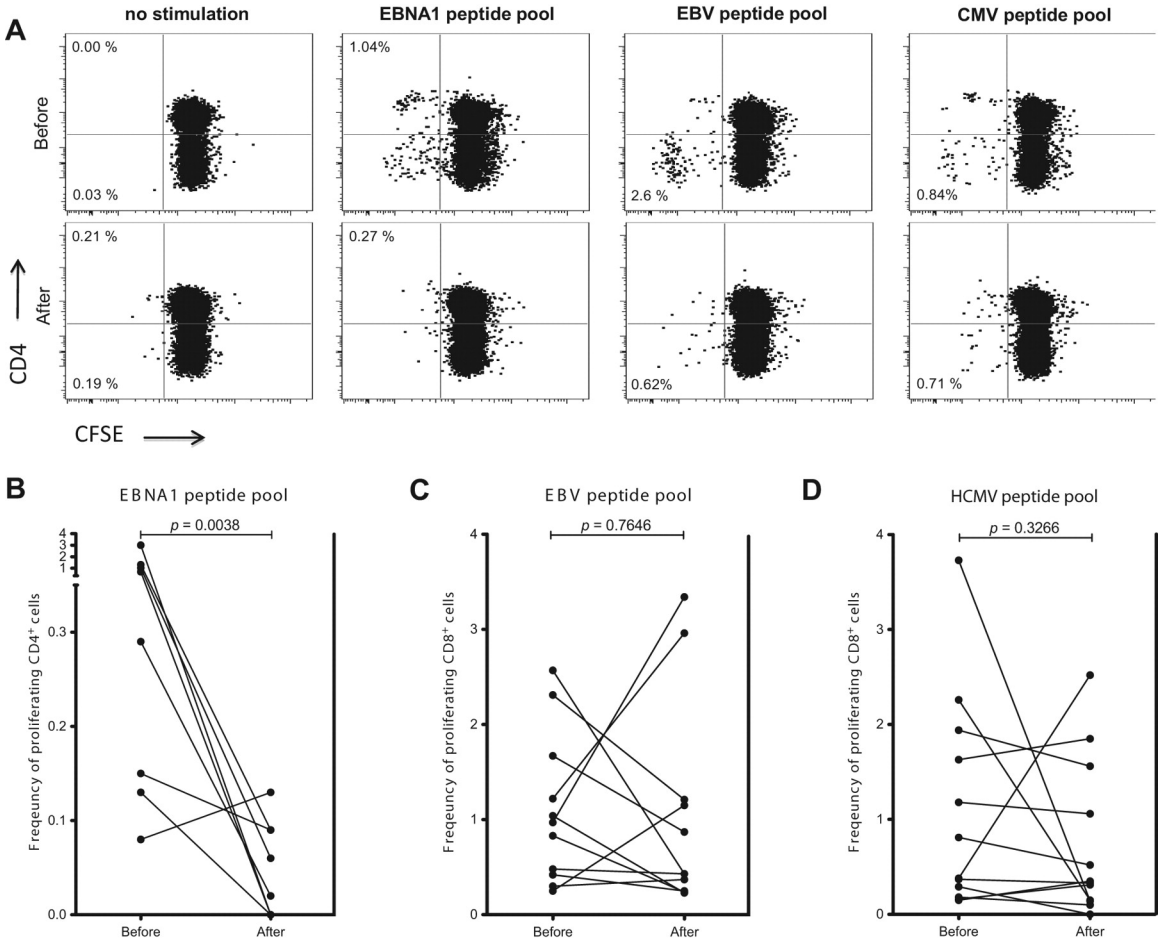

Figure 3.2.2. Viral antigen-specific T cell proliferation was altered in patients with MS before and during IFN-β treatment. (**A**) Antiviral T cell responses were quantified using a flow cytometry-based CFSE dilution assay. Peripheral blood mononuclear cells (PBMCs) were stimulated without or with EBNA1, EBV and CMV-derived peptides. The populations were pre-gated on single live $CD3^+$ cells and $CD4^+$ versus CFSE dilution is displayed in dot blots. Percentages in quadrants represent frequencies of $CFSE^{low}$ cells of the respective CD4-positive or CD4-negative populations. Data obtained from one representative patient before and after treatment is shown. (**B**) Percentage of proliferating $CD4^+$ T cells after stimulation with EBNA1 before and during IFN-β treatment. (**C**) Percentage of proliferating CD8 T cells after stimulation with MHC class I-restricted EBV peptide mix before and during IFN-β treatment. (**D**) Percentage of proliferating $CD8^+$ T cells after stimulation with CMV-pp65 before and during IFN-β treatment. 8/19, 11/19 and 12/19 patients showed proliferative responses to EBNA1, MHC-class I restricted EBV peptides and CMV pp65 peptides, respectively, at baseline. Patients not showing a proliferative T cell response were excluded from the analysis. (Figure copied from *Comabella, Kakalacheva et al*. [148])

3.3. Intrathymic Epstein-Barr Virus Infection Is Not a Prominent Feature of Myasthenia Gravis

The following section is adapted from Kakalacheva et al., Ann Neurol. 2011;70:508–514.

3.3.1 Rarity of B Cells Containing EBV DNA in EOMG Thymi

Recently, Cavalcante *et al.* reported presence of active EBV infection in thymi derived from Myasthenia Gravis patients [120]. The authors claimed that dysregulated EBV infection is common in the diseased thymi and could contribute to the immunological changes that initiate and/or perpetuate the disease [120]. To evaluate whether EBV infection is characteristic of early-onset Myasthenia Gravis (EOMG), we investigated thymus, plasma and PBMC samples from 16 patients. Thymic $CD19^+$ B cell frequencies ranged from 6.2 to 23.6%, of which 13 to 75% showed 'memory-type' $CD27^+$ phenotype.

Table 3.3.1. MG patient demographics at thymectomy. (Table copied from *Kakalacheva et al.* [1])

Patient	Gender	Age (Years) at:		MG Duration (Months)	Anti-AChR (nM)	Cortico-Steroids*	Frequency of Thymic $CD19^+$ B cells	
		MG Onset	Thymectomy				Of Total[$]	$CD19^+CD27^+$ Fraction[†]
MG1	F	13.0	14.1	12	24.1	No	15.5	32.8
MG2	F	13.5	15.0	18	117.0	No	9.6	41.0
MG3	F	16.5	18.1	19	60.0	No	8.0	69.7
MG4	F	17.6	18.4	11	1000.0	No	12.7	51.0
MG5	F	18.1	21.4	39	75.0	No	23.6	46.4
MG6	F	18.7	19.8	12	52.3	Yes[#]	5.3	52.7
MG7	M	19.0	22.1	37	34.8	No	13.1	81.0
MG8	F	19.2	20.6	16	29.5	No	10.6	47.8
MG9	F	19.7	21.3	19	627.5	No	10.0	37.0
MG10	F	21.0	21.7	9	71.7	No	6.2	13.4
MG11	F	22.0	22.6	6	110.0	No	13.2	19.1
MG12	F	23.5	24.4	11	3.4	No	7.1	24.7
MG13	F	23.7	24.7	12	1.2	No	13.4	46.8
MG14	F	25.1	27.3	26	8.5	No	8.9	60.1
MG15	F	33.1	35.6	30	24.6	No	7.9	63.8
MG16	M	39.3	41.5	27	20.2	No	20.4	74.7

Plasma and PBMC samples were taken on the day of thymectomy in 6 cases and within the next 9 months in the remainder.
*Before or during thymectomy and/or bleeding.
[#]MG6 had been on 5mg/day of prednisolone for the previous 12 months.
[$]% of total $CD45^+$ cells.
[†]% of total $CD45^+CD19^+$ lymphocytes that were $CD27^+$.

Real-time PCR was performed to quantify the content of genomic EBV DNA (BamHI W repeat region) in EOMG thymi. The lowest detection limit of the assay was 3

copies of BamHI-W-encoding plasmid as determined by serial plasmid dilutions (Figure 3.3.1.A). This high sensitivity was further confirmed by detection of as few as 20 EBV-positive Raji (human Burkitt's lymphoma cell line) cells in $1x10^7$ EBV-negative RAMOS cells (EBV-negative human Burkitt's lymphoma cell line); the same sensitivity was observed with Lymphoid cell lines (LCLs) that had been infected and transformed with EBV *in vitro* (data not shown).

Even with this highly sensitive PCR reaction, EBV was not detected in the majority of EOMG thymi; signals of EBV positivity barely reached the detection limit of the assay (mean ± SD of 3 ± 1 copies) in only 4 of all 16 samples (Figure 3.3.1C). That corresponds to approximately one viral genome, since the *Bam*HI-W sequence occurs in multiple repeats (5-11) in EBV genomes [151]. In order to increase sensitivity of the assay, we used immuno-magnetic beads to isolate $CD19^+$ B cells, the site of persistent EBV infection, from 10 thymic suspensions. In addition, to further maximize frequencies of GC and stromal cells, we tested enzymatically-dispersed cells, available from 7 of these 10 cases. Nevertheless, low EBV DNA signal was observed in 3 of the B-cell sorted samples (mean ± SD of 9 ± 5 viral copies) (Figure 3.3.1D). Demographic and individual data for each patient is presented in Table 3.3.1. and Table 3.3.2., respectively.

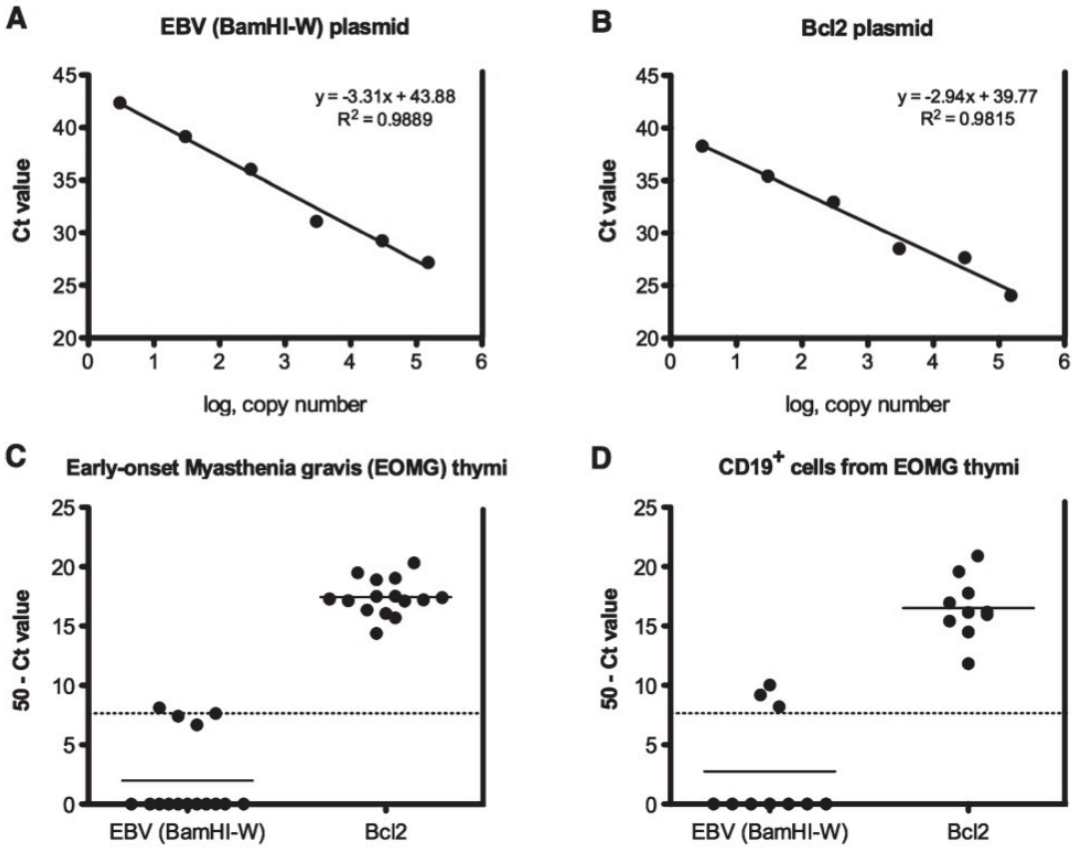

Figure 3.3.1. Infrequent detection of Epstein-Barr virus (EBV) in EOMG thymic cells, using real-time polymerase chain reaction to quantify the presence of genomic EBV DNA (EBV BamHI-W repeat region). Plasmids encoding EBV BamHI-W repeat (**A**) and Bcl2 (**B**) were used to plot the standard curves and to calibrate the sensitivity of the assay. Levels of EBV DNA in total (**C**) or B cell enriched (**D**) EOMG thymic cell suspensions; 1 of the 3 positive cases had also been positive in C. The bars in C and D represent mean values; the dotted lines indicate the EBV BamHI-W detection limit as determined with its plasmid. Mononuclear cells isolated from tonsils from 2 different EBV carriers with persistent throat infection were used as positive controls and yielded 50-Ct (cycle threshold) values of 14.7 and 14.6, respectively. (Figure copied from *Kakalacheva et al*. [1])

3.3.2. Rarity of B Cells Expressing EBV Markers in EOMG Thymi

Cryosections of the thymi samples from EOMG patients that presented with EBV-positive DNA signals in total thymi suspensions (n=3), and in $CD19^+$-sorted samples (n=3), as well as one EBV PCR-negative sample were stained for CD20, EBER, and EBNA2. All investigated section had large numbers of $CD20^+$ cells localized at foci (Figure 3.2.2.). However, no EBER or EBNA2 positive cells were found at regions of $CD20^+$ cell foci. Occasionally, we found individual EBER or EBNA2 positive cells localizing in regions that resemble

capillaries. However, the frequency of such EBV-positive cells was extremely rare. No EBV-positive cells were observed in the PCR-negative EOMG thymic section. Individual data for each patient is presented in Table 3.3.2.

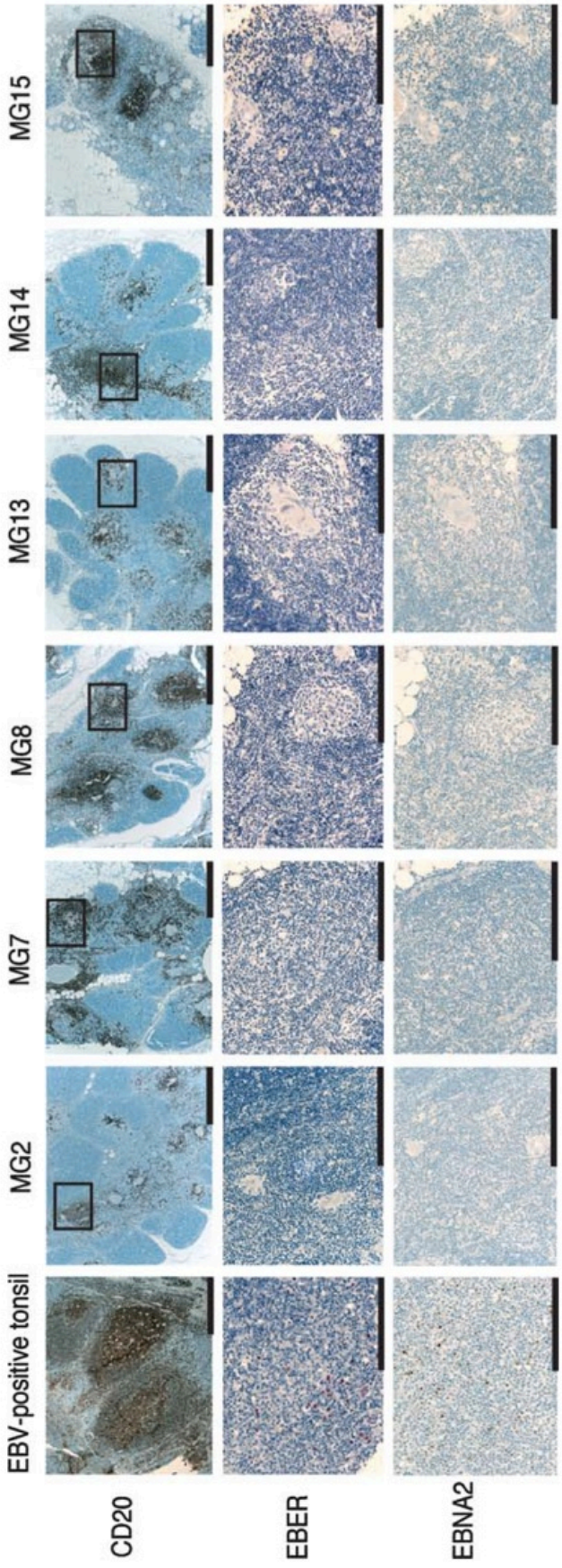

Figure 3.3.2. Staining for CD20, Epstein-Barr virus (EBV)-encoded RNA (EBER), and EBV-encoded nuclear antigen 2 (EBNA2) in myasthenia gravis thymus sections. Serial sections from 6 different early onset myasthenia gravis patient thymi were stained for CD20, EBER RNA, and EBNA2 protein. Sections of tonsils from chronic EBV carriers were used as positive control; they show numerous positive cells within and especially around the follicles. The overviews (top row; original magnification, x10) show highly cellular lobules of thymic cortex, which surround sparser medullary areas including tertiary lymphoid tissue infiltrates. The lower 2 rows show original magnifications of x40 of the areas highlighted in the upper panel. Bars in the upper row correspond to 500 μm. Bars in the middle and bottom rows correspond to 200 μm. (Figure copied from *Kakalacheva et al.* [1])

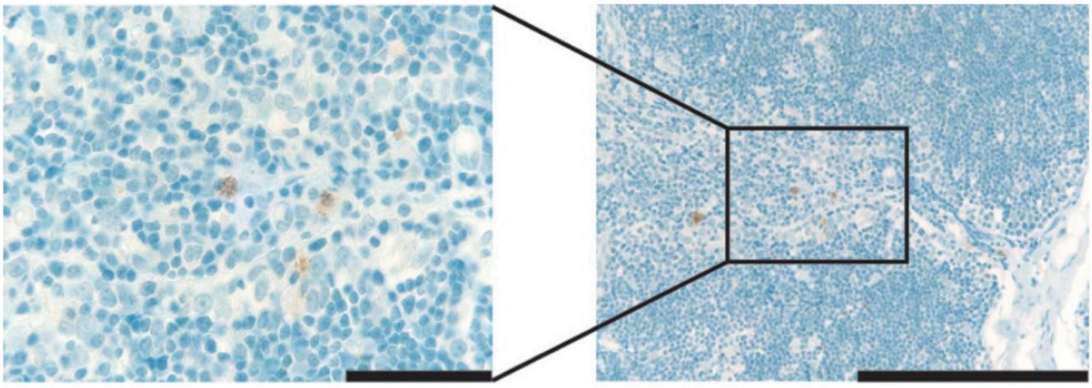

Figure 3.3.3. Occasional detection of Epstein-Barr virus (EBV)-encoded nuclear antigen 2 (EBNA2)-positive cells outside B cell follicles. EBV-encoded RNA (EBER) or EBNA2 signal was detected near high endothelial venules looping across this field, in thymic sections from patient MG2, who showed low but detectable viral DNA levels in thymic cell suspensions. No EBER- or EBNA2-positive signal was found in the polymerase chain reaction-negative early onset myasthenia gravis thymus. The bars correspond to 50 μm (left panel) and 200 μm (right). (Figure copied from *Kakalacheva et al.* [1])

3.3.3. No Evidence for Altered EBV-Specific Immune Responses in EOMG Patients

We next checked for circulating antibodies to EBV antigens, using commercially available ELISA kits to determine the levels of IgG specific for the EBV-encoded immunogenic C-terminal domain of EBNA1 (p72) and the lytic EBV viral capsid antigen (VCA). EBV-specific IgG antibodies were compared to those against viral lysates of cells infected with the ubiquitous human cytomegalovirus (HCMV). No significant differences were observed between levels or prevalence of IgG reactivity in EOMG and healthy controls (Figure 3.3.4.A). In order to investigate the occurrence of EBV reactivation, we measured IgM VCA antibodies in both the EOMG and healthy donor serum samples. Nevertheless, we could not detect any positive IgM VCA serum levels expect for one healthy donor who presented with borderline IgM VCA levels (data not shown).

Next, we investigated the presence of altered EBV and HCMV peptide-specific T cell responses, as measured by frequencies of IFN-γ-positive T lymphocytes by intracellular cytokine staining (ICS). No significant differences between EOMG patients and healthy controls were observed in response to EBNA1 or HCMV peptide pools (Figure 3.3.4.C). Moderate but not statistically significant elevation of IFN-γ-producing $CD8^+$ T lymphocytes was observed after stimulation with MHC class I-restricted EBV-encoded peptides, as compared to healthy controls (Figure 3.3.4.C).

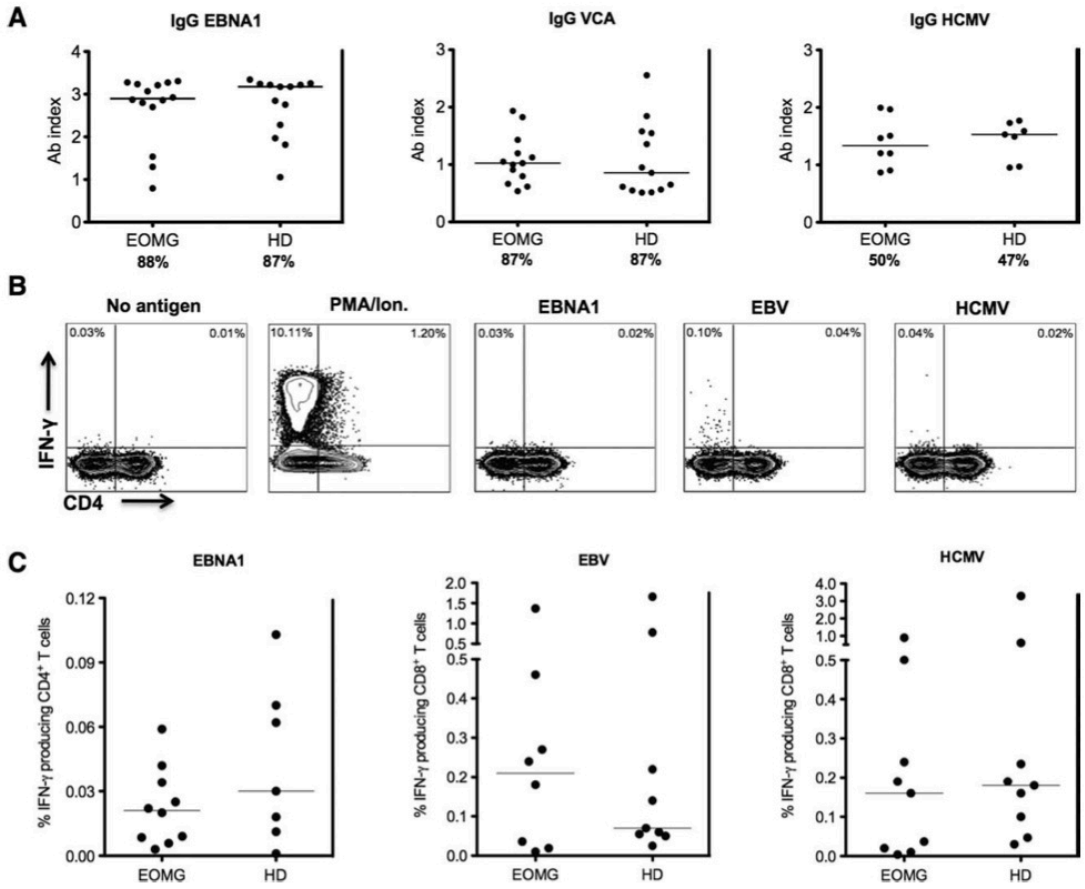

Figure 3.3.4. Epstein-Barr virus (EBV)-specific antibodies and T cell reactivity in patients with early onset myasthenia gravis (EOMG). (**A**) Circulating immunoglobulin IgG antibodies were determined in 16 patients, and 15 age- and gender-matched healthy controls, against EBV-encoded nuclear antigen 1 (EBNA1), the EBV-encoded viral capsid antigen (VCA), and human cytomegalovirus (HCMV). (**B**) Representative interferon IFN-γ intracellular cytokine staining dot plot data. Peripheral blood mononuclear cells were stimulated for 6 hours with a peptide library covering the immunogenic domain of the $CD4^+$ T cell antigen EBNA1, as well as with major histocompatibility complex (MHC) class I-restricted epitopes derived from lytic and latent EBV proteins and from the HCMV-derived pp65 protein or phorbol myristate acetate/ionomycin (PMA/Ion.) as positive control. (**C**) Frequencies of IFN-γ-producing EBV-specific T cells. The moderate elevation of $CD8^+$ T cell responses to MHC class I-restricted EBV peptides does not reach significance. Bars in A and C represent median values. (Figure copied from *Kakalacheva et al*. [1])

Table 3.3.2. Summary of Individual Results for all MG Patients. (Table copied from *Kakalacheva et al*. [1])

Patient	EBV DNA Positivity in:		Thymic Sections Positive for:			Antibody Indices Against:				% of IFNγ$^+$ T Cells Responding to Pooled Peptides From:		
	Total Cells	CD19$^+$ Cells	CD20	EBER	EBNA2	EBNA1 (IgG)	VCA (IgG)	VCA (IgM)	HCMV (IgG)	EBNA1	EBV	HCMV
MG1	+	–	nd	nd	nd	0.00	0.21	–	0.76	0.00	0.00	0.19
MG2	+	–	++	+/–	+/–	1.30	0.61	–	0.26	0.00	0.00	0.00
MG3	–	–	nd	nd	nd	0.79	0.54	–	1.47	0.01	0.24	0.16
MG4	–	–	nd	nd	nd	nd	nd	–	0.87	0.03	0.00	0.00
MG5	–	nd	nd	nd	nd	3.07	1.20	–	0.42	0.02	0.00	0.00
MG6	–	–	nd	nd	nd	0.00	0.12	–	0.34	0.01	0.02	0.00
MG7	+	–	++	+/–	nd	2.86	0.66	–	1.20	0.00	0.00	0.90
MG8	+	+	++	–	–	3.27	1.94	–	0.74	0.01	0.04	0.02
MG9	–	–	nd	nd	nd	2.92	0.80	–	0.70	0.03	0.27	0.00
MG10	–	nd	nd	nd	nd	3.23	1.43	–	0.44	0.00	0.00	0.04
MG11	–	nd	nd	nd	nd	2.87	1.02	–	0.35	0.00	0.00	0.00
MG12	–	nd	nd	nd	nd	2.70	nd	–	1.97	0.00	0.00	0.24
MG13	–	+	++	+/–	–	3.21	1.83	–	1.20	0.02	1.37	0.50
MG14	–	nd	++	–	–	2.80	1.00	–	0.90	0.00	0.01	0.00
MG15	–	+	++	+	+/–	3.27	1.05	–	1.51	0.04	0.46	0.00
MG16	–	nd	nd	nd	nd	1.54	0.91	–	1.99	0.06	0.18	0.01

Antibody indices ≥0.2, ≥0.4, and ≥0.8 were considered positive for EBNA1, VCA, and HCMV respectively.
++ denotes relative abundance of marker-positive cells.
+/– denotes rare occurrence of marker positive cells.

3.4. Identification of a Novel Inhibitor of Latent EBV Infection

3.4.1. Design of the High-Throughput Screening Assay

In order to be able to identify inhibitors of latent EBV infection, we chose to target EBNA1, an essential viral protein involved in the maintenance and replication of latent EBV. Since EBNA1 does not have enzymatic activity, we targeted the protein's ability to bind site-specifically to DNA and subsequently initiate viral replication at *OriP* in dividing latently infected cells. For that purpose together with an HTS company we designed an assay based on time-resolved fluorescence energy transfer (TR-FRET) that included histidine (His)-tagged C-terminal region of EBNA1 that is essential for the dimerization and DNA-binding function of the protein, and a 36-base pair biotinylated oligonucleotide with a sequence encoded on OriP that is specifically recognized by EBNA1. The His-tagged EBNA1 was recognized by anti-His mouse monoclonal antibody bound to Eu^{3+} Cryptate conjugate, while the biotinylated oligonucleotide was recognized by a streptavidin molecule bound to d2. In this assay format the Eu^{3+} Cryptate conjugate was the donor of the TR-FRET, while d2 functioned as the acceptor. If a small molecule disrupted the EBNA1/oligonucleotide complex, reduction in the TR-FRET signal would be observed. A schematic representation of the assay is shown in Figure 3.4.1A, while the sequence of the oligonucleotide is represented in Figure 3.4.1B. Since EBNA1 binds only to double-stranded DNA it was essential that the oligonucleotide formed a hairpin or dimerized.

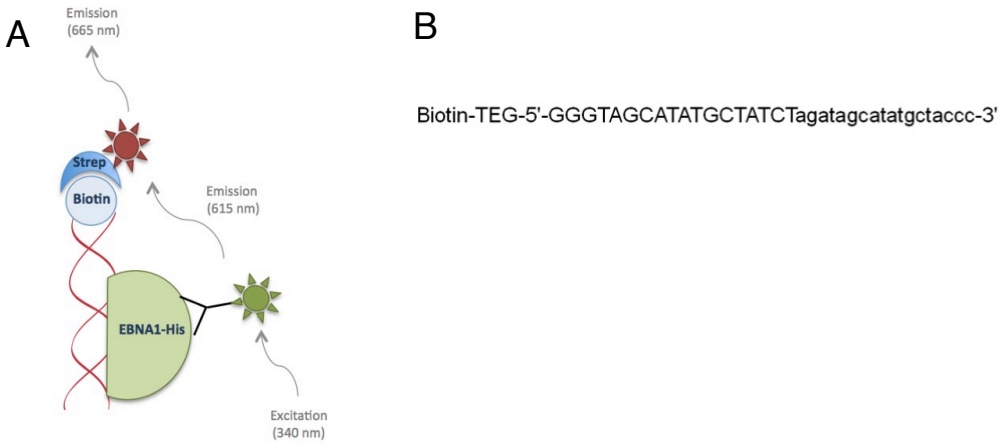

Figure 3.4.1 High-throughput screening assay for identification of EBNA1/oligonucleotide complex inhibitors. (**A**) Schematic representation of the time-resolved resonance screening assay including the biotinylated oligonucleotide and the His-tagged recombinant C-terminus of EBNA1 together with their respective binding partners: Streptavidin-d4 and anti-His mouse monoclonal antibody bound to Eu^{3+} Cryptate conjugate. The excitation and emission wavelengths are given in brackets. (**B**) Sequence of the oligonucleotide that is specifically recognized by EBNA1 and was used in the HTS.

3.4.2 Expression of Recombinant EBNA1

To perform the HTS assay, we expressed and purified the C-terminal region of EBNA1 (458-641) tagged to 6 histidine residues. Protein fractions from a representative purification process were run on an SDS-PAGE and a Silver stain is presented in Figure 3.4.2 A, where EBNA1 can be observed at the size of 21kDa. An overexpressed band at the size of 21 kDa can be observed in the pre-purification fraction (lane 2). Similar amount of the overexpressed band can be observed in the flow-through during loading (lane 3) which signifies that high amounts of the EBNA1 protein were not bound to the column and lost in the flow-through. To minimize the loss of recombinant EBNA1, the flow-through was re-run on the column. During the wash steps 40 mM Imidazole solution was used to remove weakly bound proteins to the His-Trap column. No EBNA1 loss was observed during the wash steps demonstrating that the recombinant EBNA1 was tightly bound to the column. EBNA1 could be eluted with Imidazole concentrations of 300 mM or higher. When EBNA1 was eluted with 500 mM of Imidazole, a faint line of a 75 kDa proteins was observed which contaminated the purified EBNA1 fractions. However, the concentration of the impurities was below 90%, which was considered acceptable for execution of the high-throughput screen (HTS) assay. Western blot analysis with specific 5F12 antibodies directed against the C-terminus region of EBNA1 was used to verify that the bands were positive for EBNA1 and that no degradation fragments were observed on the gel (Figure 3.4.2B).

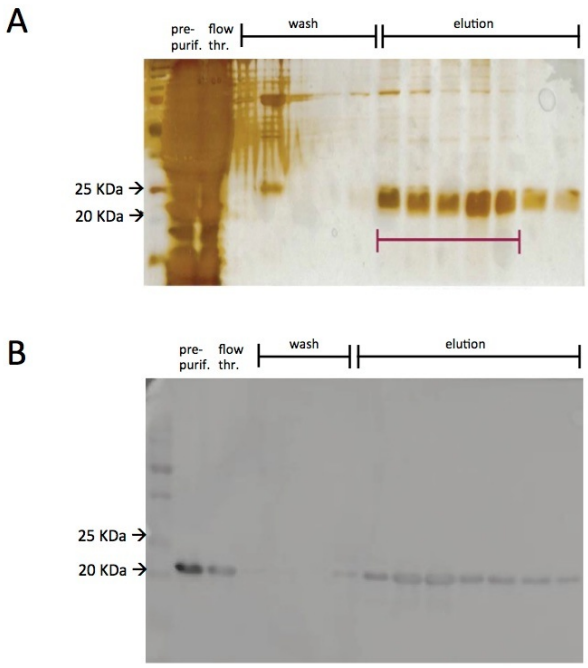

Figure 3.4.2. EBNA1 purification fractions (**A**) Silver stain post SDS-PAGE of recombinant EBNA1 purification fractions including marker (lane 1), pre-purification *E. coli* extract (lane 2), flow-through during His-Trap column loading (lane 3), flow-through during 40 mM Imidazole wash steps (lanes 4-8), elution fractions with 500 mM Imidazole (lanes 9-15). Elution fractions (lanes 9-13), designated with the purple line, were used for the high-throughput screening assay. (**B**) Western blot with 5F12 antibody specific for the C-terminal region of EBNA1.

3.4.3. High-Throughput Screening Outcome

A total number of 24 285 unique compounds (Class I group) were used for the primary screen (Table 3.4.1). While 636 compounds with intrinsic auto-fluorescence or quenching characteristics were identified and removed from the analysis, 103 compounds yielded an EBNA1/oligonucleotide complex displacement of more than 30% and underwent 11-point dose response hit profiling. Out of these 15 curves could be fitted using the curve-fitting module of the IDBS ActivityBase software. Counter assays for DNA intercalation and cytotoxicity identified respectively 6 and 4 compounds with more than 50% displacement.

Besides the Class I compounds, we investigated 8 783 compound mixtures generated from fermented fungi, termed HYPHA compounds (Class II group). 3.1% (266 compound mixtures) of the non-assay interfering 8 497 mixtures showed 30% displacement, while 1.3% (107 compound mixtures) presented with 50% HTS assay inhibition. This efficiency of hit finding is remarkably high compared to the efficiency observed for the Class I compounds, from which 0.7% of tested compounds had 30% HTS assay inhibition, while only 0.18%

yielded 50% inhibition. The top 5 best hits of the 50% displacement Class II compounds were selected for further fractionation since each mixture contained 20-30 different compounds. The fractionated samples were tested for activity through the HTS assay and the active fractions were further sub-fractionated. Several of these fractions were investigated *in vitro*. The one compound, P6, showed remarkable selective cytotoxicity to LCLs. Despite their great potential, the Class II compounds were not further investigated due to (1) complexity of the mixtures and need for identification of the component compounds, and (2) because of the complex legal issues concerning the intellectual property of the compounds. The following sections will only focus on the investigation of the Class I compounds with inhibitory potential.

Along with the HTS, we performed virtual screen of more than 1 x 10^6 compounds of which the top 50 hits were further investigated. Of these 32 were available for purchase and were subsequently used in the TR-FRET assay setup. However, from all 32 tested compounds only 2 had partial activity and were not pursued further.

Table 3.4.1 Class I and Class II compounds included in the primary high-throughput screening, hit profiling, and counter assays.

Screening phase	Class I compounds	Class II compounds
Primary screen	24 285	8 783
Removal of assay interfering compounds	23 649	8 497
>30% TR-FRET displacement	103	266
Hit profiling (11-point dose response curve fitting)	15	-
Counter assay for DNA intercalation	6/15	-
Counter assay for cytotoxicity	4/15	-

3.4.4. *In Vitro* Profiling of the HTS Hits

The chemical structure of the 15 top HTS hits is presented in Figure 3.4.3, while their activity on the HTS assay, cell viability and DNA intercalation counter assays is presented in Figure 3.4.4.

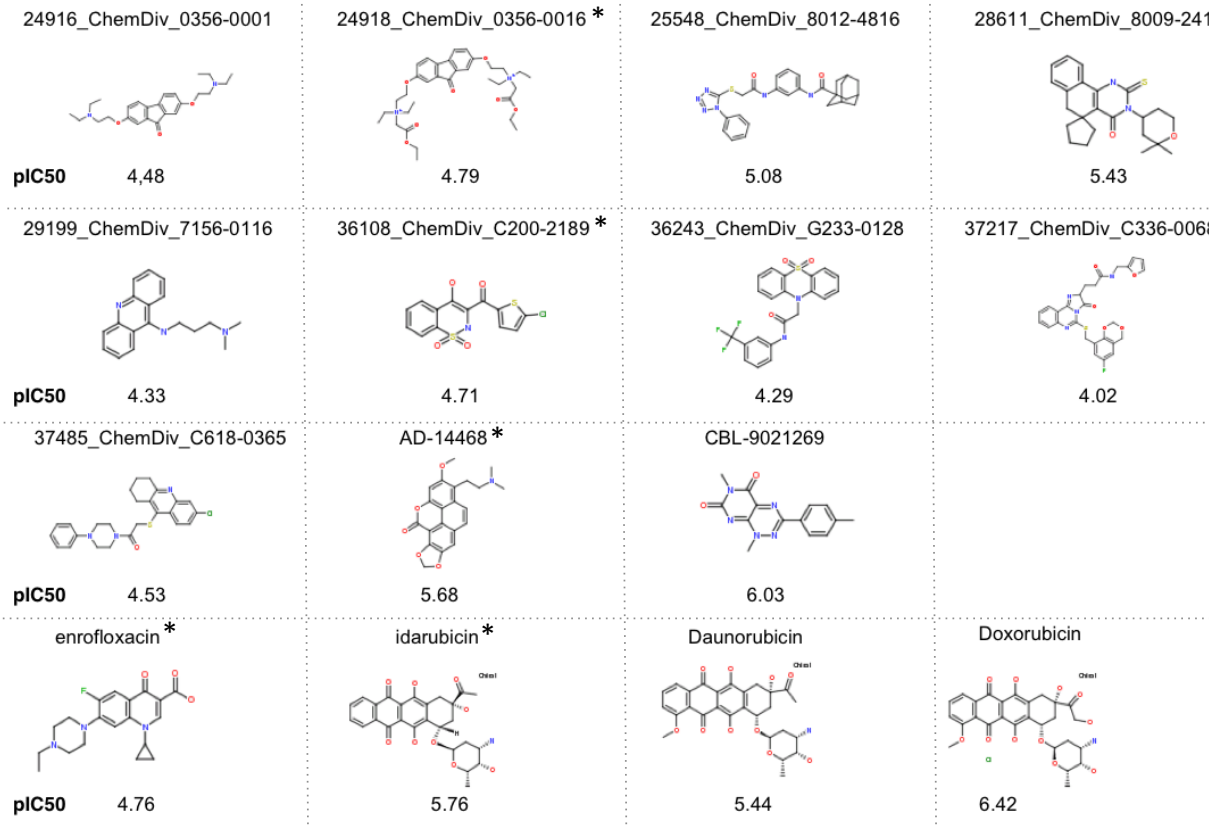

Figure 3.4.3. Chemical structure of all 15 top HTS hit compounds. The compounds marked with an asterisk (*) were not available for purchase.

Compound	Primary Assay		Cell Viability		DNA Intercalation	
	Primary		CellTiter-Glo		Pico green	
Compound Id	Chart	IC50 [μM]	Chart	IC50 [μM]	Chart	IC50 [μM]
24916_ChemDiv_0356-0001	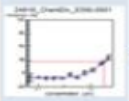	inactive	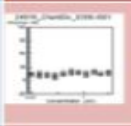	inactive	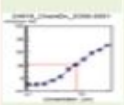	6.51
25548_ChemDiv_8012-4816	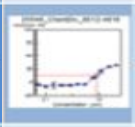	inactive	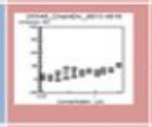	inactive	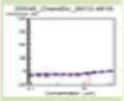	15.8
28611_ChemDiv_8009-2416	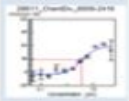	3.72	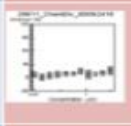	inactive	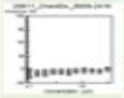	<0.09765625
29199_ChemDiv_7156-0116	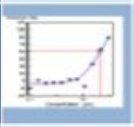	47.19	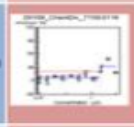	inactive	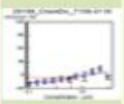	3.85
36243_ChemDiv_G233-0128	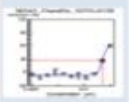	50	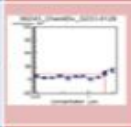	inactive	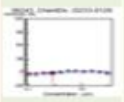	0.77
37217_ChemDiv_C336-0068	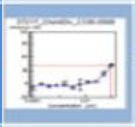	inactive	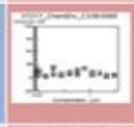	inactive	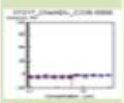	3.95
37485_ChemDiv_C618-0365	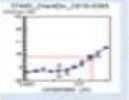	inactive		inactive	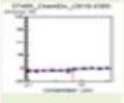	4.88
CBL_9021269	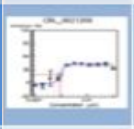	inactive	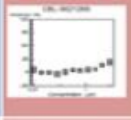	inactive	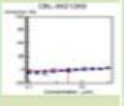	3.06
GR-318	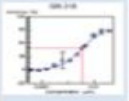	3.63	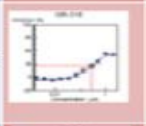	0.25	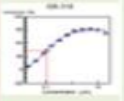	0.11
GR-319	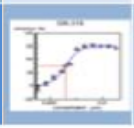	0.38	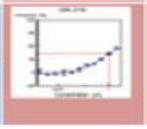	1.08	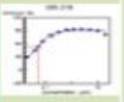	0.05

Figure 3.4.4. HTS assay results of the 10 available for purchase HTS hit compounds. The fitted displacement curves of the primary and the dose-response hit profiling HTS assays are shown together with the counter assays for cell viability to HEK cells and DNA intercalation.

10 of all 15 top HTS hit compounds were available for purchase and were screened *in vitro* in our laboratory for cytotoxicity to EBV-transformed lymphoblastoid cell lines (LCLs) and as a control to the EBV-negative Burkitt lymphoma cell line (Ramos). Three different

concentrations of the compounds were tested based on the inhibition curves obtained from the HTS. The majority of the tested compounds had either no effect on the viability of the LCLs or was cytotoxic to both the EBV-positive and EBV-negative cell lines.

Tilorone, a compound with 30% displacement of the EBNA1/oligonucleotide complex in the HTS assay at 33μM concentration, showed remarkable toxicity towards the LCLs, while it had limited effect on the Ramos cell line (Figure 3.4.5.). Based on this observation the compound was chosen as our top HTS hit and its thorough characterization was further undertaken.

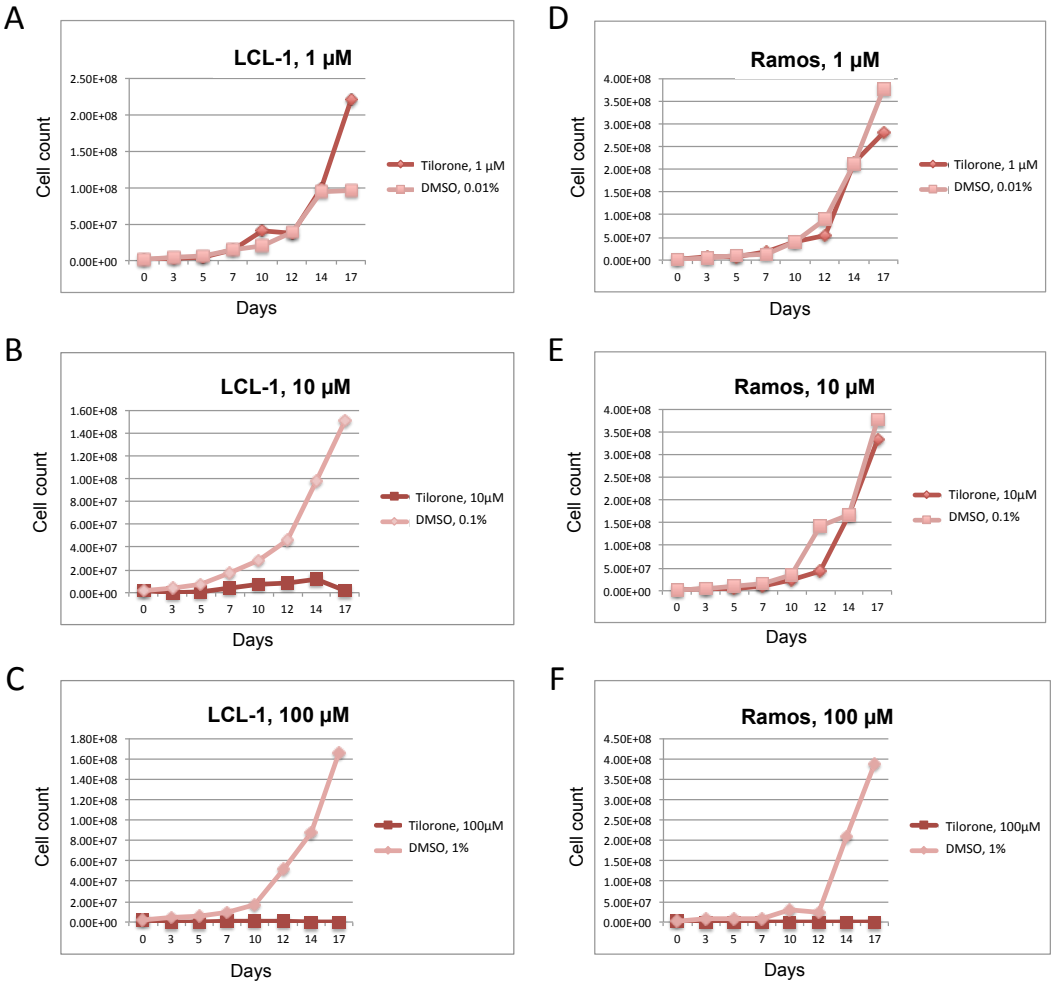

Figure 3.4.5. Cell cytotoxicity to LCLs (**A**-**C**) and Ramos cell line (**D**-**F**) as determined by total cell counts in the course of 17 days of incubation with 1 μM (**A** and **D**), 10 μM (**B** and **E**) or 100μM (**C** and **F**) of Tilorone.

3.4.5. Confirmation of Tilorone's Ability to Inhibit the EBNA1/DNA Interaction

Tilorone was identified as the top hit of a HTS that selected compounds that inhibited the ability of EBNA1 to bind to its cognate DNA sequence on *OriP*. In order to confirm this suggested mechanism of action of Tilorone, we designed an Electrophoretic mobility shift assay (EMSA) that independently determined the dissociation of the EBNA1/oligonucleotide complex. The biotinylated oligonucleotide was either incubated alone or in the presence of the C-terminal domain of EBNA1 together with no or increasing concentrations of Tilorone (0 μM-1000μM). The mixtures were then run on a non-denaturing polyacrylamide gel and blotted onto positively charged Nylon membrane (Figure 3.4.6.A). That allowed for the clear separation between oligonucleotide that is in unbound form and ran faster on the non-denaturing gel and the bound form of the oligonucleotide to EBNA1 that forms a complex with the protein that ran with a delay on the gel. Interestingly, we observed that two bands of EBNA1-bound oligonucleotide were present on the membrane, which might represent EBNA1 bound to the oligonucleotide in dimer and monomer forms. As expected we observed that Tilorone led to dose-dependent dissociation of the EBNA1/oligonucleotide complex that resulted in increasing concentrations of unbound oligonucleotide (Figure 3.4.6.). The EMSA and the HTS observation independently confirmed the ability of Tilorone to dissociate the EBNA1/oligonucleotide complex in a dose-dependent manner. Therefore, we decided to further characterize the compound in *in vitro* and *in vivo* models.

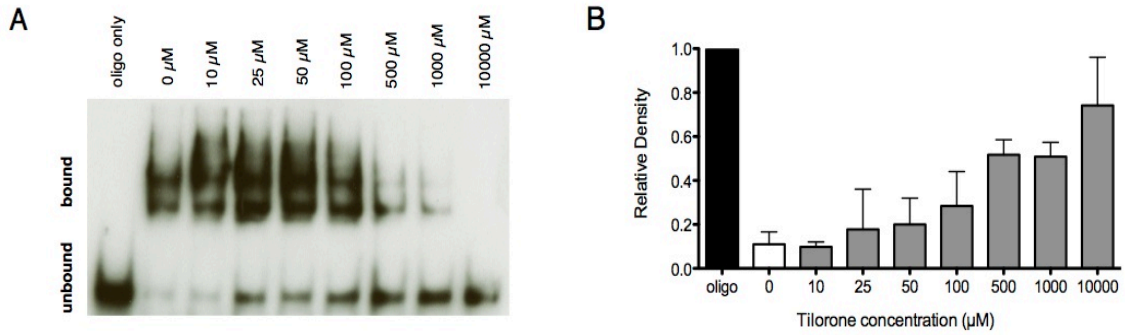

Figure 3.4.6. Electrophoretic mobility shift assay (EMSA) of the EBNA1/oligonucleotide complex incubated with increasing concentrations of Tilorone. (**A**) Representative EMSA blot of the oligonucleotide in a free form with no EBNA1 (lane 1), bound to EBNA1 in the presence of no Tilorone (lane 2), and in the presence of EBNA1 together with increasing concentrations of Tilorone (lanes 3-9). (**B**) Quantification of relative density of the unbound oligonucleotide band from three independent EMSA experiments.

3.4.6. Characterization of the Effect of Tilorone *In Vitro*

The EBV-transformed LCL cell line *in vitro* model system was chosen to further characterize the effect of Tilorone on EBV-infected cells. For that purpose we used distinct LCL types that were obtained from *ex vivo* EBV-transformed B cells from different healthy donors that were generated at different time points in our laboratory. These cells were considered suitable for our experiments since for their proliferation, the LCL require the persistence of the EBV genome. Four such LCL cell lines were used to quantify the cytotoxic effect of Tilorone. As a control we used the L428 EBV negative Hodgkin's lymphoma cell line, which was suggested to have similar activation and proliferation status as the LCLs. The cells were incubated for 7 days with various concentrations of Tilorone and the frequency of live cells as determined by flow cytometry was related to the frequency of live untreated cells at the respective time point. Tilorone reduced cell viability in a dose-dependent manner for all four types of LCLs. Incubation with 15 μM Tilorone led to reduction in cell viability of 35% on day 5 and 70% on day 7. This concentration had no effect on the L428 cell viability for the investigated time period. A Tilorone concentration of 20 μM led to reduction of LCL cell viability of 70% on day 5 and 94% at day 7. This Tilorone concentration had no effect on L428 cell viability on day 5 and only 12% cell viability reduction at day 7. However, while a concentration of 25 μM of Tilorone led to 89 and 99% reduction of LCL viability on day 5 and 7 respectively, it also resulted in 22 and 60% reduction of L428 viability on day 5 and 7 respectively (Figure 3.4.7.). This observation suggest that there is a limited range of concentrations at which Tilorone has a cytotoxic effect in an EBV-specific manner, however above a certain concentration the compound is cytotoxic also to EBV-negative cells.

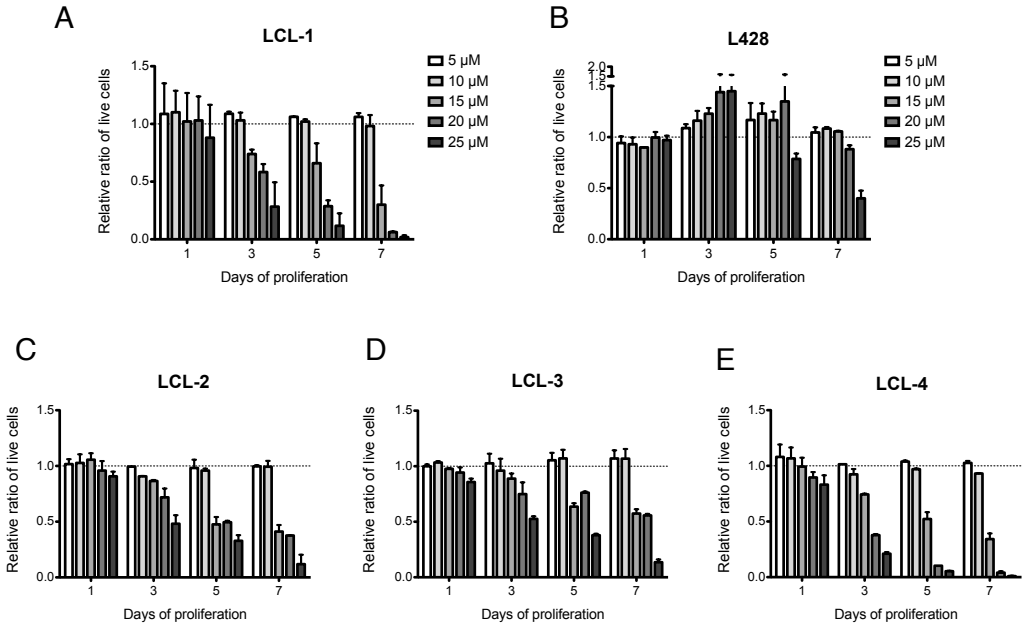

Figure 3.4.7. Tilorone exhibits cytotoxic effect on EBV-positive, but not on EBV-negative cell lines. Four types of LCLs (**A, C-E**) and one control cell line (**B**) were incubated with increasing concentrations of Tilorone (5, 10, 15, 20, and 25 μM) for 7 days. The cells were analyzed by flow cytometry and the frequency of live cells is presented as ratio of the live cells with 0 μM Tilorone at the respective time points.

Having seen that Tilorone exhibits cytotoxic effects on the LCLs, we decided to investigate whether that effect was due to reduction in cellular proliferation. In order to do that the LCL and L428 cell lines were stained with CellTrace Violet and incubated with increasing concentrations of Tilorone for 7 days. The dilution of the dye was used as a proliferation measure, and was analyzed by flow cytometry at 1, 3, 5, and 7 days of culture. Higher mean fluorescence intensity (MFI) signified less dye dilution that represented less cell proliferation. Tilorone led to dose-dependent inhibition of LCL proliferation that was observable as early as day 3 and was most pronounced at day 5 and 7 (Figure 3.4.8.A). The compound had little effect on the proliferation of the control cell line, L428. The only inhibition of L428 cell line proliferation was observed with the highest concentration of the compound (25 μM) at day 7 (Figure 3.4.8.B). This finding coincided with the abovementioned cytotoxic effect of Tilorone at high compound concentration that occurred in EBV-unrelated manner.

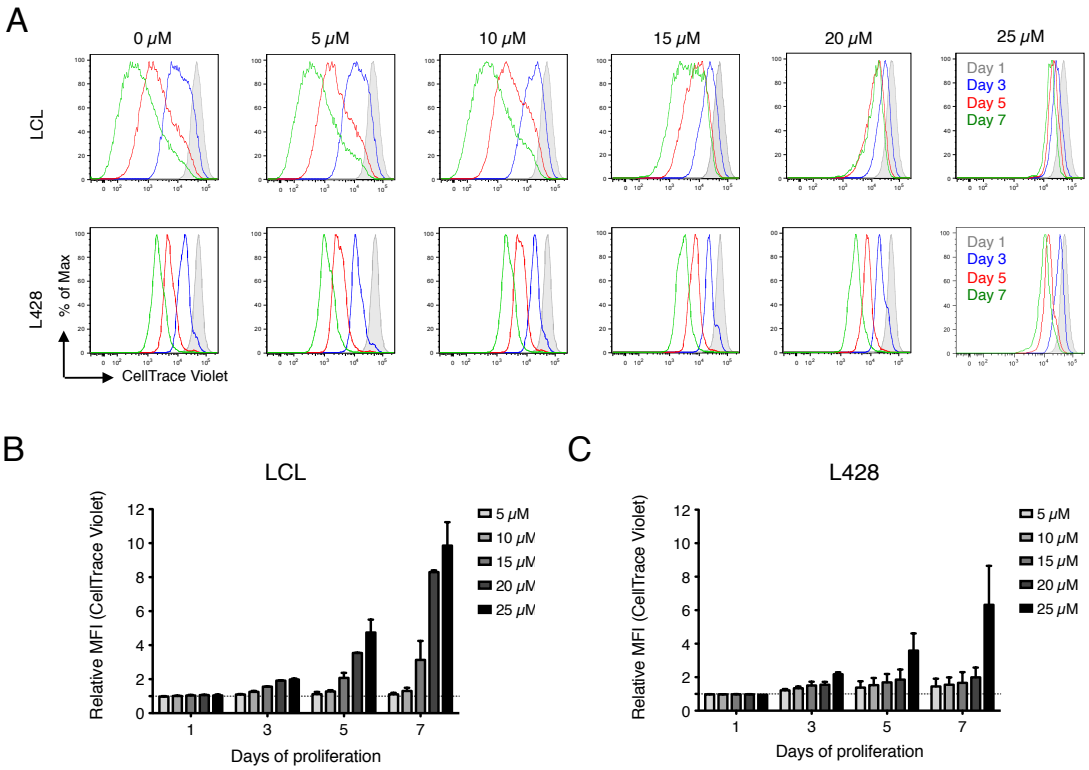

Figure 3.4.8. Tilorone inhibits proliferation of EBV-transformed LCLs. (**A**) EBV-positive cell line, LCL, and EBV-negative cell line, L428, were stained with CellTrace Violet and incubated with increasing concentrations of Tilorone for 7 days. The dilution of the dye, used as a proliferation measure, was analyzed by flow cytometry at 1, 3, 5, and 7 days of culture and presented as overlay of histograms. (**B**) Relative mean fluorescence intensity (MFI) of CellTrace Violet normalized to LCLs incubated with 0 μM Tilorone at the respective time point. (**C**) Relative mean fluorescence intensity (MFI) of CellTrace Violet normalized to L428 incubated with 0 μM Tilorone at the respective time point.

Moreover, we investigated whether the cytotoxic and anti-proliferative effect of Tilorone were due to apoptosis induction. For this purpose we analyzed the presence of Annexin V positive cells post incubation with increasing concentrations of Tilorone (Figure 3.4.9.A). In addition, we measured the activation of Caspase 3/7, as a direct marker of apoptosis initiation (Figure 3.4.9.B). The compound led to dose-dependent apoptosis induction as observed by both Annexin V expression and Caspase 3/7 activation.

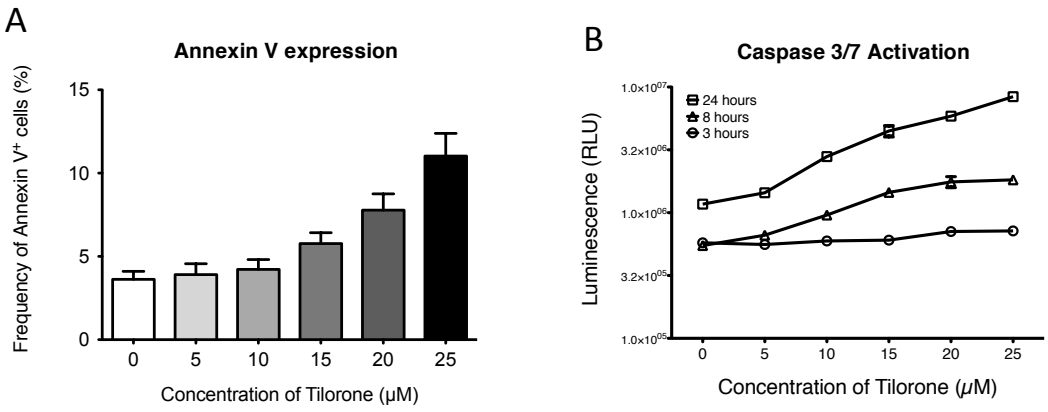

Figure 3.4.9. Induction of apoptosis as a result of Tilorone treatment. (**A**) Frequency of Annexin V-positive LCLs 24 hours post incubation with increasing concentrations of Tilorone. (**B**) Caspase 3 and 7 activation in LCLs 3, 8, and 24 hours post incubation with increasing concentrations of Tilorone.

Based on our *in vitro* findings we could conclude that Tilorone limited the proliferation and promoted cytotoxicity by inducing apoptosis in EBV-positive cell lines. These findings make the compound an interesting candidate for treatment of EBV-associated malignancies, therefore we decided to investigate it further with our mouse models.

3.4.7. *In Vivo* Effect of Tilorone on EBV-Associated Tumor Burden

Thanks to the abundant literature about the pharmacokinetics and pharmacodynamics of Tilorone in mice, we could determine that the compound would be well tolerated when applied through oral gavage or intraperitonealy (i.p.). The reported LD_{50} for oral application of Tilorone for mice was 959 mg/kg, while the LD_{50} for i.p. application was 145 mg/kg [152]. Since we had to apply the compound 3 times per week for the continuation of at least 4 weeks, we decided to apply Tilorone i.p. in order to minimize the risk of tissue scarring and animal loss due to repeated gavaging. The compound was applied at a concentration of 50 mg/kg 3 times per week and was well tolerated since no Tilorone-related weight loss was observed in our experiments (Figure 3.4.10.).

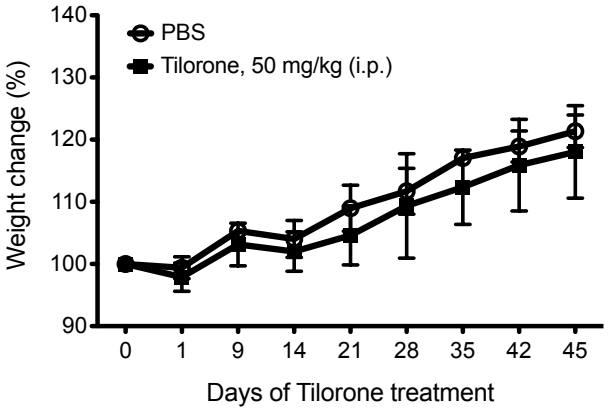

Figure 3.4.10. No weight changes observed due to treatment with Tilorone. Mouse weight change compared to initial weight in the course of 45 days of 3-times per week treatment with 50 mg/kg Tilorone. Representative experiment of three repeats including 5 mice in Tilorone-treated group and 4 mice in the PBS-treated group.

To test the efficacy of Tilorone against EBV-associated tumors *in vivo*, we injected i.v. $10x10^6$ luciferase-expressing LCLs (LCL-luc) or control (L428-luc) into NOD-SCID-gamma-chain-deficient (NSG) mice and monitored the luminescence signal as a measure of cancer cell line proliferation *in vivo* for four weeks. Representative luminescence measurements are presented in Figure 3.4.11.A. One to two days after injection the luminescence signal was localized mainly in the lungs and reproductive organs of the animals. During week one most of the signal localized to the liver, while from week two on increase in the luminescence signal and formation of high-signal foci in the area that localized with the spleen were observed.

Figure 3.4.11. summarizes the results obtained from one representative experiment from a total of 3 experiments per cell line. The mice, treated with Tilorone, showed significantly reduced tumor burden at week three and four post LCL injection compared to vehicle (PBS)-treated mice (Figure 3.4.11.B). Moreover, the percentage of mice presenting with spleen tumors was reduced from 100% (5/5 mice) in the vehicle-treated group to 14% (1/7 mice) in the Tilorone-treated group (Figure 3.4.11C). The compound had no effect on tumor proliferation (Figure 3.4.11C) or the tumor incidence (Figure 3.4.11.D) of an EBV-negative Hodgkin's lymphoma cell line, L428. It should be noted, however, that even though both cell lines have similar growth kinetic *in vitro*, the L428 cell line grew more aggressively in the NSG mice and led to tumor formations in the liver, rather than in the spleen as observed for the LCLs. In short, Tilorone successfully inhibited the proliferation and the

tumor incidence of an EBV-associated cancer cell line in immunodeficient mice, while it had no effect on the proliferation and tumor incidence of an EBV-negative cancer cell line.

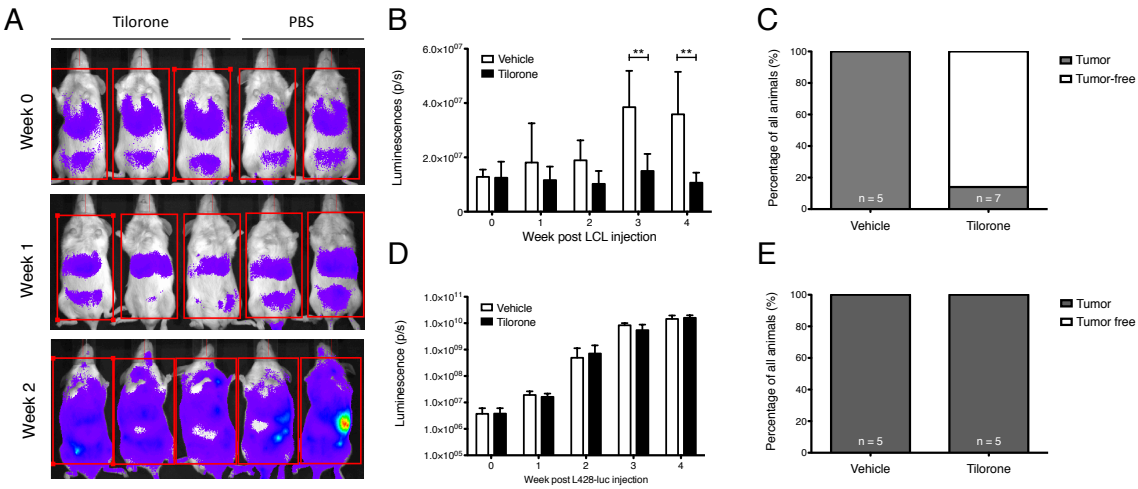

Figure 3.4.11. Tilorone effectively reduced EBV-associated tumor burden. NOD-SCID-gamma-chain-deficient (NSG) mice were injected with luciferase-expressing EBV-positive (LCL-luc) or EBV-negative (L428-luc) B cell lines. *In vivo* luciferase measurement was performed weekly to monitor tumor cell proliferation. (**A**) Representative luciferase measurements at week zero, one, and two post LCL-luc injection. (**B**) Luminescence measurement of vehicle- and Tilorone-treated mice post LCL-luc injection. One representative of three independent experiments with 5 mice in the control and 7 in the treatment group is shown. (**C**) Comparison between tumor incidences in the spleen of vehicle- and Tilorone-treated mice 4 weeks post LCL-luc injection. (**D**) Luminescence measurement of vehicle- and Tilorone-treated mice post L428-luc injection. One representative of three independent experiments with 5 mice in the control and 5 in the treatment group is shown. (**E**) Comparison between tumor incidences in the liver of vehicle- and Tilorone-treated mice 4 weeks post L428-luc injection.

3.4.8. Tilorone Inhibits *Ex Vivo* Transformation of Human B Cells by EBV

$CD19^+$ B cells were MACS-isolated from human PBMCs, stained with CellTrace Violet, and infected with EBV in the presence of increasing concentrations of Tilorone. The compound led to dose-dependent inhibition of proliferation of the B cells implying that Tilorone inhibited the capacity of EBV to transform B cells. Based on our observations, not only was Tilorone able to induce the death of EBV-positive cell lines, but also the compound was able to limit transformation of non-infected human B cells by EBV.

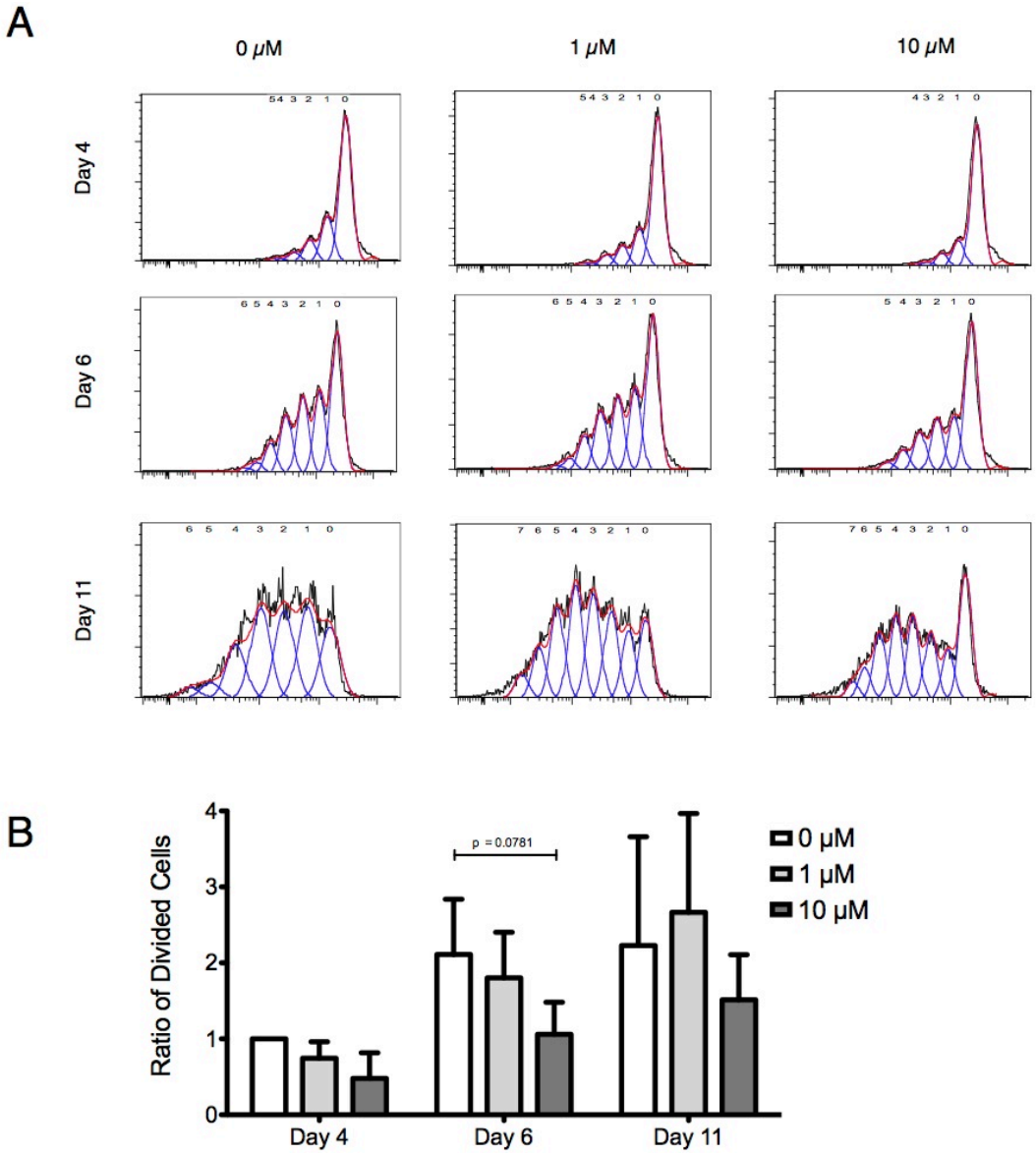

Figure 3.4.11. Tilorone inhibited *ex vivo* transformation of human B cells by EBV. Human CD19^{+} B cells were MACS-isolated from PBMCs and stained with CellTrace Violet, a cell proliferation dye. The cells were then infected with 0.5 MOI of EBV and cultured in the presence of increasing concentrations of Tilorone. (**A**) CellTrace Violet dye dilution at day 4, 6, and 11 post EBV infection. The numbers above the histograms represent the number of cell divisions as calculated by FlowJo cell proliferation analysis tool. Representative proliferation histograms of 1 donor out of 6 tested. (**B**) The frequency of divided cells was determined with the FlowJo cell proliferation analysis tool. The relative frequency of divided cells is presented normalized to the frequency of cells incubated with 0 μM of Tilorone for four days.

3.4.9. Tilorone Reduces Lytic EBV Reactivation in AKBM Cells

Having seen that Tilorone successfully reduces *ex vivo* transformation of B cells by EBV, we decided to investigate whether the compound has an effect on lytic reactivation. For that purpose we used the AKBM cell line, a cell line derived from the EBV-positive Burkitt's lymphoma cell line Akata. The cell line was transfected with a reporter to express an immuno-sortable surface (CD2) marker and GFP upon induction of the lytic cycle that was achieved through cross-linking of its BCR by anti-human IgG antibody. Upon induction of the lytic cycle the lytically switched cells would almost exclusively express CD2 and GFP and would upregulate the immediate early lytic EBV gene, BZLF1 [153].

AKBM cells were incubated with 0, 10, 15, 20, and 25 μM of Tilorone, while EBV lytic reactivation was induced through BCR cross-linking. The cells were harvested and analyzed for GFP expression by flow cytometry after 24 hours. 67% of the induced AKBM cells reactivated lytic EBV replication (Figure 3.4.12.A). The lytic reactivation was significantly reduced to 31% in the presence of 10 μM of Tilorone, while 25 μM of the compound led to nearly complete abrogation of lytic reactivation with only 3.6% GFP-positive AKBM cells. That reduction in lytic reactivation was not due to cytotoxic effect of Tilorone. Even though the induction of reactivation led to loss of about 60% of the AKBM cells both in the Tilorone treated and non-treated conditions, the compound itself did not lead to reduction in absolute cell counts (Figure 3.4.12.B).

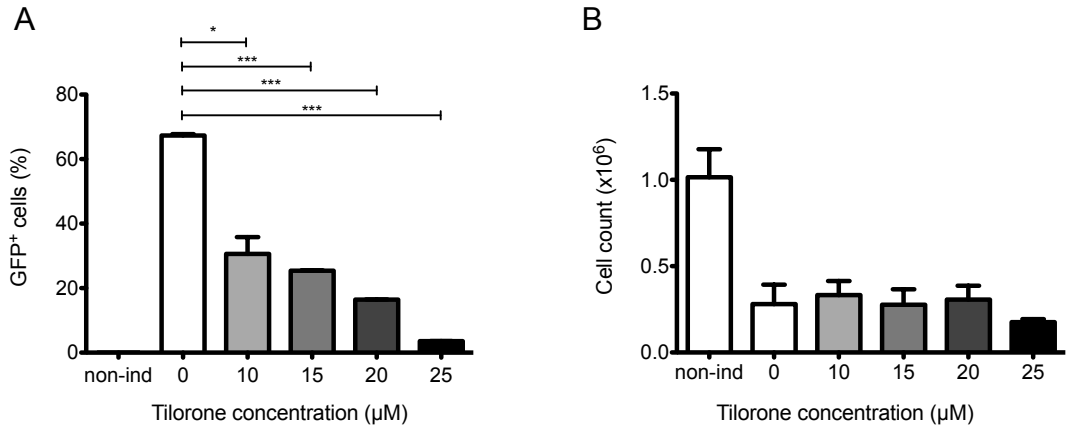

Figure 3.4.12. Tilorone reduces lytic EBV reactivation in AKBM cells. (**A**) Frequency of GFP positive AKBM cells as a result of lytic viral reactivation. (**B**) Absolute cell counts of live AKBM cells in non-induced and induced AKBM cells, treated with Tilorone.

3.4.11. Tilorone Leads to Marginal Reduction in Viral Load in EBV-Infected Humanized Mice

The next intriguing question that we wanted to answer was whether Tilorone could inhibit EBV infection *in vivo*. Since EBV is a species-specific pathogen and infects human B cells but not murine lymphocytes, we had to generate NOD-SCID-gamma-chain-deficient (NSG) mice with reconstituted human immune system components. NSG newborns were reconstituted with human fetal liver-derived $CD34^+$ cells. Three months later, the frequencies of the human lymphocytes were evaluated. The blood of the reconstituted mice typically comprised of 60-90% human $CD45^+$ cells, about 60% of which were human $CD19^+$, and 20-40% were $CD3^+$ with a 4:1 ratio of $CD4^+$ to $CD8^+$ T cells. $NKp46^+$ NK cells represented 1-4% of all human $CD45^+$ cells (Figure 3.4.13.).

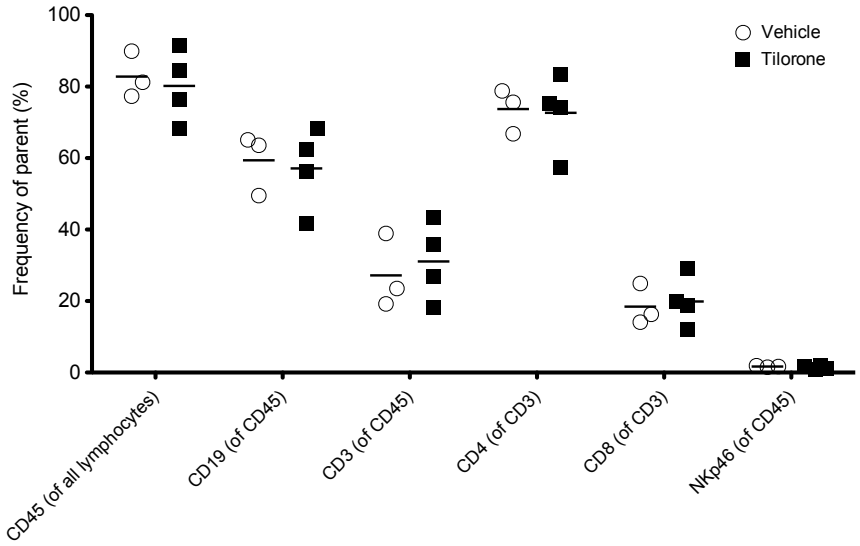

Figure 3.4.13. Reconstitution of human lymphocyte subsets in NOD-SCID-gamma-chain-deficient (NSG) mice from one representative cohort of humanized mice, split in subgroups for Tilorone or vehicle treatment.

The HLA-A2-transgenic or non-transgenic reconstituted NSG mice were infected with 10^5 RIU B95-8 EBV virus particles. One day before the infection and thrice a week thereafter, the mice were treated either with vehicle or 50 mg/kg Tilorone. The treatment dose and frequency was comparable to the one used for the non-reconstituted NSG mice (Section 3.4.7.). Similar to the non-reconstituted mice, the humanized NSG tolerated well the compound and responded with no treatment-specific weight loss (Figure 3.4.14.).

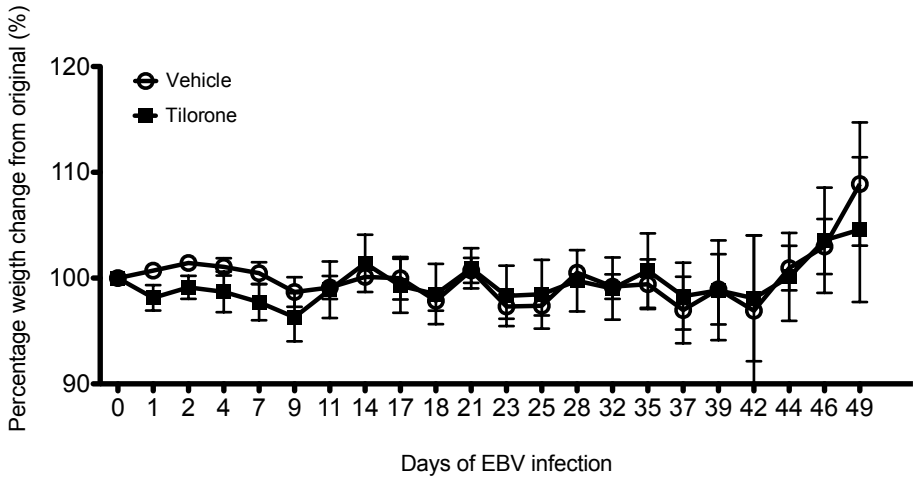

Figure 3.4.14. Tilorone does not lead to treatment-specific weight loss in humanized NSG mice. Weight changes compared to original weight in humanized NSG mice in the course of EBV infection with or without Tilorone treatment.

EBV viral load in the whole blood of the animals could be observed starting from week two and was measured weekly thereafter. We performed two independent experiments with HLA-A2 transgenic (experiment duration: 5 weeks) and two independent experiments with non-HLA transgenic humanized NSG mice (experiment duration: 7 weeks). In all four experiments we observed at least one time point when the Tilorone treated mice had reduced EBV viral load compared to the vehicle-treated mice (Figure 3.4.15.). However, that difference was significant only for two of the experiments (Figure 3.4.15.A-B), while when we combined all data points the significance was lost (Figure 3.4.15.E). However, we could observe a trend for reduced viral load in the Tilorone-treated group at weeks four, five, and six. This observation could be due to the variability between the individual mice both in reconstitution level and EBV viral load, but also due to diverse blood Tilorone levels.

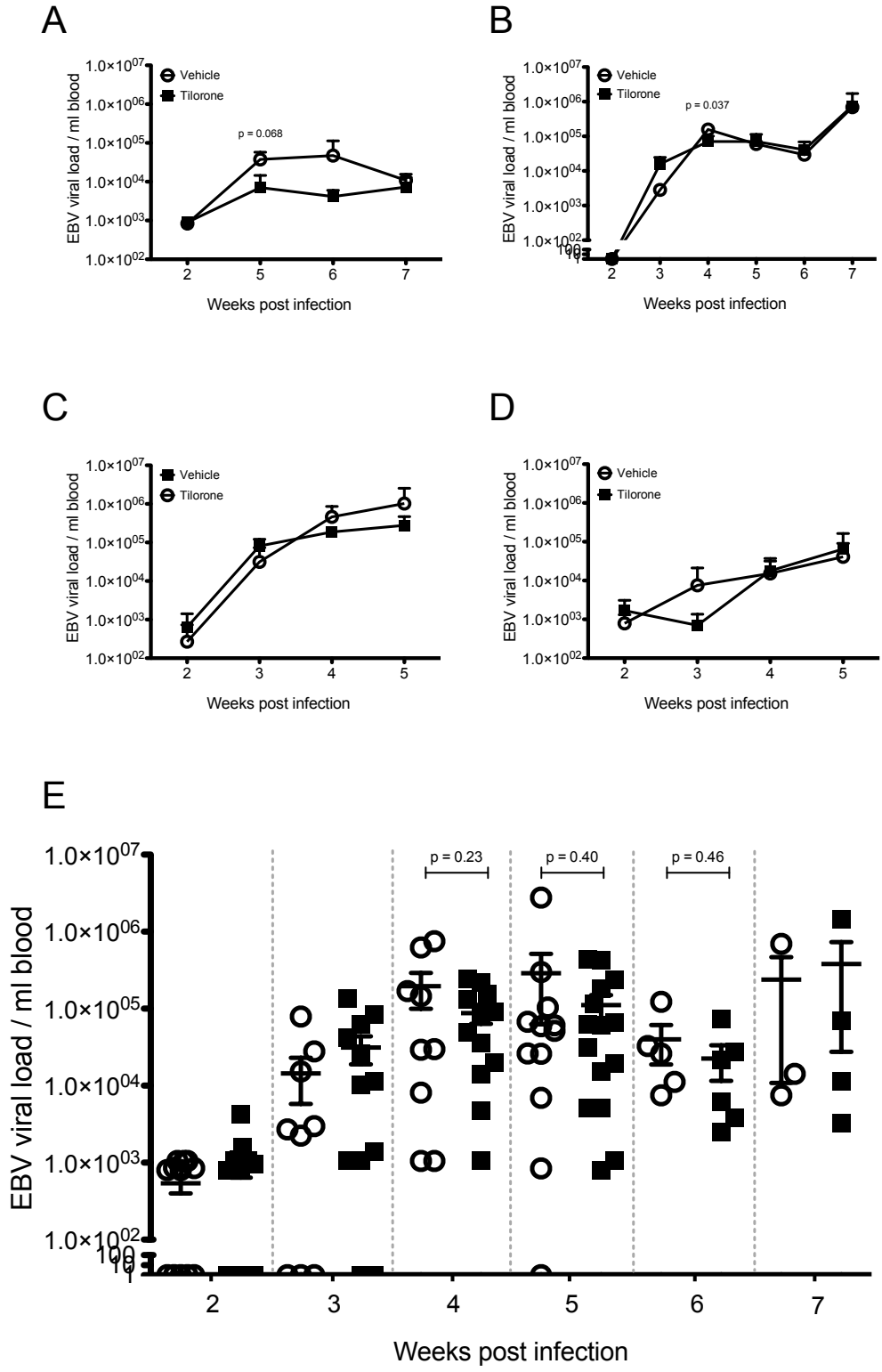

Figure 3.4.15. Tilorone led to marginally reduced EBV viral load in reconstituted humanized NSG mice. Two individual experiments conducted in non-HLA transgenic NSG mice (**A-B**) and two individual experiments in HLA-A2 transgenic NSG mice are presented (**C-D**). (**E**) EBV viral load changes as result of Tilorone treatment from all four experiments combined. The empty circles represent the vehicle-treated mice, while the filled squares represent the Tilorone-treated animals.

Despite the compound's strong cytotoxic and anti-proliferative effect *in vitro* and its ability to limit *ex vivo* B cell transformation, lytic reactivation, and tumor burden in non-reconstituted NSG mice, the complex environment of an NSG mouse reconstituted with human immune system components poses challenges to the efficiency of the treatment.

Encouraging, however, is the fact that Tilorone does not affect the composition, both in frequency and absolute numbers, of the reconstituted human immune system in the NSG mice (Figure 3.4.16.). Both vehicle and Tilorone treated mice showed no changes in absolute counts of the human $CD19^+$ cell subset (Figure 3.4.16.B), while the $CD3^+$ subset was expanding in the course of the infection due to increase in both $CD8^+$ (Figure 3.4.16.F) and $CD4^+$ T cells (Figure 3.4.16.H). Moreover, expansion of activated T cells, $CD3^+$ HLA-DR^+ subset (Figure 3.4.16.J), was observed in the course of the infection. However, as already mentioned the treatment with Tilorone did not lead to significant changed in the counts of B cells, or expansion and activation status of the human T cells.

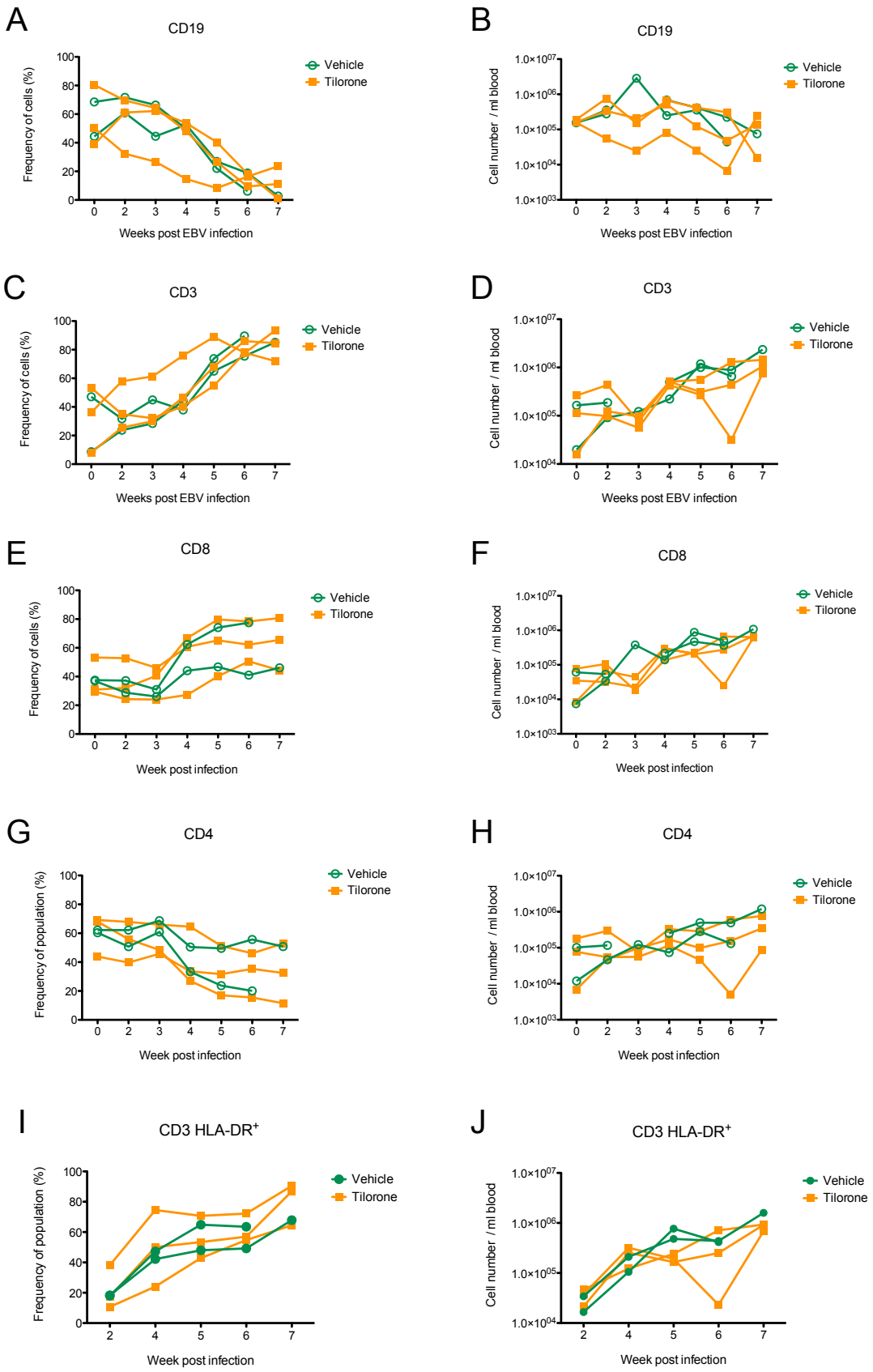

Figure 3.4.16. No change in reconstituted human lymphocyte subsets due to Tilorone treatment in humanized NSG mice. (**A**) Frequency and (**B**) absolute cell count of human $CD19^+$ cells. (**C**) Frequency and (**D**) absolute cell count of human $CD3^+$ cells. (**E**) Frequency and (**F**) absolute cell count

of human $CD8^+$ cells. (**G**) Frequency and (**H**) absolute cell count of human $CD8^+$ cells. (**I**) Frequency and (**J**) absolute cell count of human $CD3^+$ $HLA\text{-}DR^+$ cells. Data from one representative non-HLA-transgenic cohort of humanized NSG mice is shown here.

4. DISCUSSION

4.1. Generation of Autoreactive Humoral and Cellular Immune Responses during Infectious Mononucleosis

The aim of this study was to characterize the generation of autoreactive humoral and cellular immune responses during acute IM in order to better understand the well-described link between history of IM and autoimmune diseases such as multiple sclerosis. For that purpose we chose IM patients that underwent medical visit shortly after onset of IM symptoms. These patients were compared to age-matched patients that visited the same hospital however due to non-IM-related complaints. We considered this as the most appropriate control group as the patients in this group were not only matched for age, gender and demographic location, but also suffered from diverse conditions some of which were characterized by mild inflammation. Therefore, by comparing these two groups of patients one would be able to better eliminate autoimmune reactions that were rather due to not IM-specific inflammatory process, yet comparing the IM patients to other non-IM inflammatory disease patients would provide a more reliable control.

Moreover, in order to have only EBV carriers in the control and IM patient cohorts, in our control group we chose only patients who were latent EBV carriers based on presence of anti-VCA IgG antibodies. Interestingly, the IM patient group had reduced median level of anti-VCA IgG compared to the control group. That could be explained by the fact that anti-VCA IgG antibodies take about 2 weeks after onset of disease to develop [154]. 9 out of the 13 IM patients had their first doctor visit and blood drawing in the first week after onset of symptoms, therefore their IgG responses towards the VCA antigen were not as fully developed as in the latent EBV carriers in the control group.

4.1.1. Investigation of Humoral Autoreactive Immune Responses

Fulminant inflammation processes have been long known to stimulate the transient production of autoreactive antibodies. Myriad of studies were published during the 60s and 70s of the last century describing the occurrence of autoantibodies during acute IM. It was know that acute IM leads to augmented levels of immunoglobulins that persist for as long as 2 years post infection [155], [156]. These antibodies were usually of IgM isotype and rarely converted to IgG [157]. Such antibodies included antinuclear antibodies (ANA) [158], [157], anti-IgG [158], anti-I or cold-agglutinin antibodies [155], anti-smooth muscle antibodies [159], anti-cyroprotein antibodies [160], and anti-tubulin antibodies. Nevertheless, these autoantibodies were not strongly associated with disease pathologies except for the anti-I

antibodies, which are though to lead to hemolysis during IM. The other autoantibodies are thought to potentially contribute to liver damage and rare complications such as thrombocytopenia and agranulocytosis [161].

MS is a heterogeneous disease with complex pathology. Increasing evidence, however, points that antibody-mediated effector mechanisms could contribute to the immunopathogenesis of demyelination [143]. Such effector mechanisms include immunoglobulin deposition within white matter lesions [162], antibody-associated receptor mediated phagocytosis of myelin debris [163], and complement activation within the CNS [164], [143]. The CNS-confined MOG antigen was considered as a plausible target for the demyelinating immune response especially since animal models of MS, induced by immunization with CNS homogenates and complete Freund's adjuvant, were characterized by the generation of MOG-specific antibodies that contributed to the disease pathology [145], [165]. Additionally, MOG was shown to contain an encephalitogenic T cell epitope which together with the humoral immune responses against MOG contributed to the demyelination of CNS neurons in rat, mouse, and marmoset models of MS [166], [167], [168]. The role of anti-MOG antibodies in human MS is, nonetheless, controversial. Several studies have confirmed the persistent presence of anti-MOG antibodies, predominantly of IgM isotype, in MS patients and transiently in patients with other inflammatory neurological disorders [143], [144]. These anti-MOG antibodies were determined to occur early in the event of the disease progression as well as to be good predictors of MS conversion of patients with clinically isolated syndrome [143], [169]. The later observation was, however, contested by a different group [170].

Interestingly, not much is known about the presence of anti-MOG antibodies during infectious mononucleosis. One case report describes a patient with infectious mononucleosis who also developed post-EBV encephalopathy. The patient was negative for traces of active EBV infection in the CNS, suggesting no active role of EBV in the disease pathology, but had high humoral (predominantly IgM) and T responses against MOG that decreased after the encephalopathy was resolved [171]. Yet, the generation and prevalence of MOG antibodies during IM is poorly defined.

In our study we performed a novel assay for detection of anti-MOG antibodies by using human oligodendroglial cell line that stably expresses human MOG in its natural glycosylation form. We screened 13 IM and 13 control patient samples and detected anti-MOG antibodies in only one IM patient. One should note however that our assay used goat anti-human IgG as secondary detection antibody. Therefore, with this assay we screened only for presence of anti-MOG IgG antibodies in our cohorts. Since IgM MOG antibodies seem to

be the predominant isotype found in MS patients, it would be of high interest to optimize the assay for detection of IgM anti-MOG antibodies.

Besides through bystander activation in the course of fulminant inflammation, autoreactive antibodies can be produced due to EBV infection and immortalization of autoreactive B cells. We collaborated with Tracy *et al*. on a study that looked at autoreactivity of EBV-infected and EBV-negative B cells from acute IM patients. 56 EBV-positive and 69 EBV-negative memory B cells were single-cell sorted, and the antibodies of these B cells were cloned, expressed, and used for self- and poly-reactivity assays [172]. One of the assays performed was the MOG assay that we used for characterization of IM patient sera. Tracy *et al*. found that EBV does persist within self- and poly-reactive B cells; however, infection with the virus does not favor the survival of autoreactive B cells.

An interesting and unexpected finding from the HEp2 immunofluorescence analysis of the IM patient sera was the identification of vimentin-like autoantibodies in a large fraction of the patients. The cytoskeleton forms a complex network of filamentous proteins that are distributed throughout the cytoplasm. Autoantibodies against the three main types of filaments, microfilaments, microtubules, and intermediate filaments, have been described in numerous diseases such as anti-actin autoantibodies in liver diseases and anti-tubulin antibodies in infectious mononucleosis [173]. Vimentin is the most widely expressed intermediate filament protein. It is predominantly produced by mesenchymal cells and its main function is to facilitates cellular processes such as migration, protein trafficking and signal transduction by orchestrating protein complexes [174]. Antibodies against vimentin have been described in a number of diseases including connective tissue diseases such as SLE, RA, in Crohn's disease, and lymphoproliferative diseases such as angioimmunoblastic lymphadenopathy [175].

Our observations of high prevalence of anti-vimentin IgM antibodies in 69% of the IM patients compared to only 8% in control patients are not the first ones to describe the occurrence of cytoskeletal autoantibodies in IM. Kataaha *et al*. showed that 92.5% of 40 IM patients were positive for IgM autoantibodies against cytoskeletal intermediate filaments of pre-keratin or vimentin type [176]. Surprisingly, the group compared 72 RA patients and found that 81.9% of these patients also had high titers of the vimentin-like antibodies, while only 26% of the 93 healthy donors had low titers of the antibodies.

Interesting, several studies have shown that EBV infection led to upregulated expression of vimentin in the infected cells. Upon EBV infection vimentin was found to redistribute to patch-like inclusions in lipid rafts where it was associated with LMP1 [177]. When vimentin was chemically disrupted, LMP1 relocalized to the site where vimentin was redistributed, suggesting that the two proteins might form a complex [177]. A recent study by

Meckes *et al*. not only confirmed the association of the two proteins but also elucidated the functional significance of vimentin's activity. The researchers evaluated the function of vimentin by short hairpin RNA knockdown, expression of dominant-negative vimentin protein, and use of chemical inhibitor to reveal the role of the protein in LMP1 signal transduction and transformation [174].

Despite the low number of IM and control patients used in this study, we found positive correlation between the EBV viral load and MOG IgG and CCP reactivity. Curiously, the IM patient with the highest viral load (IM15) also presented with the highest humoral response to MOG, borderline positivity to citrullinated proteins (CCP2), and IgM but not IgG responses to vimentin. The IM patient with the second highest viral load (IM12), was the only patient from the IM cohort that was positive for ANA, had a high MOG reactivity, and IgM but not IgG responses to vimentin. Due to the high viral load and high levels of autoreactivity of the serum of these patients we decided to look closer into the T cell responses of these patients.

4.1.2. Investigation of Cellular Autoreactive Immune Responses

The acute phase of EBV infection is characterized by considerable activation and expansion of $CD8^+$ T cells. It is suggested that during this state of acute inflammation non-EBV-specific T cells also get activated through bystander activation or novel antigen availability due to release of cell material from copious cell death. Molecular mimicry could provide another mechanism for activation and expansion of autoreactive T cells. In the latter case, T cells that are reactive to viral epitopes have cross-reactivity potential to other antigens. The cross-reactivity to secondary antigens might be of lower affinity, however in the event of an acute inflammation, the reactivity of these cells could be augmented. Once generated, such cross-reactive T cells might convert to memory T cells and linger in the human body until they in combination with other environmental and genetic factors contribute to the development of autoimmune pathologies.

EBV-specific $CD8^+$ and $CD4^+$ T cells have been described to cross-react with allogeneic MHC molecules, self peptides, bacterial and other viral antigens [178], [179], [180], and [181]. In particular MBP-specific T cell clones isolated from MS patients have been shown to get activated by several viral and bacterial peptides, including common viruses such as EBV (peptide derived from the viral DNA polymerase) and influenza A, herpes simplex virus, and adenovirus [182]. A different study confirmed these findings by showing that MBP-specific T cell clones from MS patients can recognize a peptide from the EBV DNA polymerase protein, however in the context of a different MHC Class II molecule [183].

Crystal structures of the two peptides in complex with their respective MHC molecules were shown to have a very close similarity and nearly identical TCR contact surface [183].

Characteristic for MS patients is the presence of elevated humoral and cellular responses to certain EBV antigens. In particular, MS patients have been shown to possess enhanced T cell responses to EBNA1 owning to selectively expanded reservoirs of central memory $CD4^+$ T helper 1 precursors and T helper 1 polarized effector memory cells [98]. Interestingly, these EBNA1-specific T cells have been shown to cross-react with myelin antigens and to produce IFN-γ and IL-2, and were speculated as contributors of CNS immunopathology [184].

In this study we hypothesized that EBNA1-specific T cells that have the ability to cross-react to myelin antigens are generated during the acute phases of IM and can contribute to pathologies later in life.

To address this hypothesis, we first analyzed responses of total PBMCs to EBV, myelin, and pro-insulin peptide pools (Figure 3.1.7.). Post EBV lytic peptide pool stimulation on average 19 versus 3 IFN-γ SFU per $2x10^5$ PBMCs were detected from the IM patients compared to the controls, respectively. The higher response of the IM patients can be easily explained by the high availability of lytic antigens during active EBV infection. As expected, the controls were more reactive to the latent EBV peptide pool, than to the lytic ones, with an average of 8 SFU per $2x10^5$ PBMCs. The IM patients had an average of 21 SFU per $2x10^5$ PBMCs to the latent EBV peptide pool which we speculate could be due to the presence of latent antigen-reactive $CD8^+$ T cell clones, that were expanded during acute IM but decreased in numbers after resolution of the infection [138]. In general, one can see that the IFN-γ EBV peptide pool responses were rather close to the detection limit of the assay most probably due to the inflammatory state and the high activation status of the IM T cells. Such dysregulation of EBV-specific responses in IM patients has already been described [185]. Nevertheless, we could detect EBNA1 responses in the IM patient PBMCs. Presence of similar low but persistent EBNA1 $CD4^+$ and $CD8^+$ responses during acute IM have already been described by others [138]. On the other hand, myelin or pro-insulin IFN-γ responses could be detected neither in IM patients nor in control bulk PBMCs.

We next cloned EBNA1-reactive T cells from acute IM patients to test their cross-reactivity potential to autoantigens. For that purpose we chose the IM patients who presented with the highest level of serum autoimmunity and had the highest EBV viral load levels. 44 EBNA1-reactive CD4-positive clonal cultures could be outgrown from these two IM patients. None of these clones, however, had detectable reactivity neither to the myelin nor to the proinsulin peptides. Our inability to identify cross-reactive clones could be either due to the mere lack of such clones during IM or due to the fact that the patients from whom these

clones were generated were not carriers of HLA-DR1*15, which is the strongest genetic risk factor associated with MS.

In conclusion, despite the limited number of patients involved in this study, we observed enhanced autoreactivity to diverse self-antigens of the serum of IM patients. Moreover, this humoral autoreactivity correlated with the patient's cell-free EBV viral load. Currently, we are analyzing a new cohort of IM patients and non-IM inflammatory controls to determine whether our observations from the first cohort can be confirmed.

4.2. EBV-Specific Immune Responses in Patients with Multiple Sclerosis Responding to IFN-β Therapy

The following section is adapted from Comabella, Kakalacheva et al. Mult Scler. 2012 May;18(5):605-9.

Immune responses to EBNA1 are prominently increased in apparently healthy individuals who will develop MS, in patients with clinically isolated syndrome (CIS) suggestive of MS and in patients with clinically definite MS [99], [105], [102]. IgG responses to EBNA1 but not to lytic EBV antigens are reported to correlate with clinical and MRI-based markers of disease activity and progression, and to predict conversion to clinically definite MS in patients with CIS based on the 2005 revisions to the McDonald criteria [104], [102]. These changes in EBV-specific immunity appear not to be associated with an increase in viral replication or impaired immune control of EBV infection, since patients with clinically definite MS do not differ from healthy virus carriers in levels of cell-associated viral genomes in circulating blood cells and their ability to control EBV-infected B cell outgrowth in vitro [105], [106]. In line with these observations, we did not observe significant changes in T cell responses towards EBV-encoded antigens expressed during lytic infection and viral transformation in IFN-β-treated MS patients, further suggesting that the increase in EBNA1-specific immune responses in patients with MS and its downregulation during IFN-β therapy are not primarily driven by viral replication.

Elevated EBNA1-specific T cell responses in patients with MS display a phenotype indicative of frequent antigen recognition [184], and it has been suggested that these responses are maintained through restimulation by central nervous system-infiltrating and latently infected B cells or cross-reactivity with autoantigens [186], [106]. EBNA1 is the sole viral protein consistently expressed in latently infected proliferating B cells [187], and its transcription is regulated by IFN regulatory factors (IRFs) [188], [189], [190], [191], a family of transcription factors which is activated through IFN receptor signaling [192]. Thus, repression of EBNA1 transcription through IRFs leading to reduced antigen availability during systemic IFN-β treatment represents a hypothetical mechanism that could explain the observed downregulation of EBNA1-specific T cell responses. Due to the limited observation period of 1 year, we cannot exclude that IFN-β additionally affects immune responses to lytic EBV gene products or other viral antigens at later time points. Moreover, since T helper cell frequencies influence the generation and maintenance of IgG responses [193], we cannot exclude the possibility that antibody responses to EBNA1 decrease in patients responding to IFN-β therapy at a later time point. Nevertheless, our study shows that $CD4^+$ T cell responses to EBNA1 are consistently reduced early after treatment initiation, and thus supports the notion that EBNA1 is a target antigen of the pathological immune response in MS. Although

further investigations will be necessary to clarify whether these changes are causally related to MS development and progression, our study suggests, if replicated in larger cohorts of patients and controls, that the magnitude of EBNA1-specifc immune responses is not only associated with disease activity and disability progression [104], [102], but also with the clinical response to IFN-β in MS.

4.3. Intrathymic Epstein-Barr Virus Infection Is Not a Prominent Feature of Myasthenia Gravis

The following section is adapted from Kakalacheva et al., Ann Neurol. 2011;70:508–514.

We found that the majority of EOMG thymi had undetectable levels of EBV DNA, even after real-time PCR analysis of isolated thymic B cells. Cryosections of EOMG thymi contained large numbers of $CD20^+$ cells localized in foci, however, no EBER or EBNA2 positive cells were present where $CD20^+$ cells localized. Furthermore, no significant alterations in EBV-specific humoral or cellular immune responses were detected in EOMG patients versus healthy controls.

Investigating thymi from 17 MG patients including 12 with hyperplasia, Cavalcante *et al*. recently reported high frequencies of EBV-infected thymus-infiltrating B cells [120]. All their MG thymi showed evidence for active, i.e. replicative, EBV infection as defined by the presence of lytic and latent viral transcript and protein expression [120]. In sharp contrast, we could not confirm these high frequencies; even with highly sensitive and well established quantitative real-time PCR protocols for detecting genomic EBV [105], [194], [102], we found low viral DNA levels corresponding to single viral genomes in only 6 of 16 thymi. Nor could we detect presence of EBER or EBNA2 markers localizing with CD20-positive B cell foci in MG thymi.

The most obvious difference between these studies is that at least 14 of the 17 patients tested by Cavalcante *et al*. had been pre-treated with corticosteroids and/or other immunosuppressants (versus 1 of our 16) – which are known to impair immunosurveillance mechanisms of latent EBV infection [4]. In their remaining 3 cases, steroid or AChR antibody status is not reported, so they could derive from distinct MG subgroups. As suggested by Cavalcante *et al*., we checked for the systemic deregulation of host-EBV interactions reported for other autoimmune diseases such as MS [195]. Humoral as well as $CD4^+$ and $CD8^+$ T cell responses to immunodominant viral antigens expressed during B cell transformation, productive viral replication, and latent infection [4], [105], [141] proved to be unchanged in EOMG patients. These data are in line with the earlier screen for IgG antibody titers to EBV in patients with MG onset before age of 20 [196]. On the contrary, Csuka *et al*. claimed that EOMG patients are characterized by high titers of EBNA1 antibodies [197]. Their study compared the EBNA1 antibody levels in MG patients and controls and found no differences. However, when the authors quantified the frequency of high EBNA1 IgG producers, defined as more than 600AU/mL, they found that 16.3% of the healthy controls and 26.6% of the MG patients are positive ($p=0.024$), and therefore they deducted that high EBNA1 titers are characteristic of MG. Despite the high number of MG patients ($n=158$) included in their study, we believe that these percentages are too low to claim a strong association between the

disease and EBNA1 antibodies. Moreover, we found no difference in the level and titer of these antibodies in our cohort of EOMG patients.

Independently from our report two studies with similar findings were published in the last 2 years. Meyer *et al*. analyzed 25 EOMG thymi for histological signs of latent or lytic EBV infection and found no presence of EBV [198]. Moreover, Jing and colleagues analyzed 30 thymi from MG patients with Chinese origin and found no histological signatures of EBV infection [199]. Yet our study provided the most comprehensive analysis of EBV responses in EOMG patients as we not only looked at histological markers of EBV infection, but also compared viral load and humoral and cellular immune responses.

After the publication of our and Meyer *et al*.'s studies, Cavalcante and colleagues claimed that the discrepancies in our observations are most probably due to differences in the sensitivities of our assays. Therefore, we have established communication with the Italian researchers and initiated exchange of samples so that we can cross-analyze them. However, this initiative has yet not led to a conclusion since Cavalcante and colleagues have not yet provided us with their MG thymi samples for EBV DNA quantification.

In conclusion, in EOMG thymi taken before immunosuppressive therapy (mostly within a few months of MG-onset), we detected only very low levels of EBV signals, which are to be expected in tissues infiltrated by peripheral B cells. Furthermore, EBV-specific immune responses were unchanged in these patients. These findings do not support a role for EBV infection in the initiation of EOMG.

4.4. Identification of a Novel Inhibitor of Latent EBV Infection

With this study we aimed at identifying inhibitors of established EBV infection by targeting the essential interaction of EBNA1 with the viral episome. This protein/DNA complex has been well characterized as the crystal structure of the DNA-binding and dimerization domain of EBNA1 was solved in an unbound [38], and a form bound to a palindromic 18bp oligonucleotide encoded on OriP [39]. Curiously, the DNA binding domain of EBNA1 bares close structural similarity to the E2 protein of the papillomavirus despite their complete lack of sequence homology [39]. On the other side, the interaction of EBNA1 with the host DNA is less well characterized. Marechal *et al*. have identified the domains, CBS-1, -2, and -3, through which EBNA1 binds non-covalently to mitotic host chromosomes and therefore facilitates the almost equal separation of the viral episomes between the dividing daughter cells [200]. Since the interaction of EBNA1 with the episomal DNA sites has been much better characterized, we decided to use this interaction to design an HTS and screen for compounds that would dissociate the complex and subsequently would lead to abrogation of EBV infection. The sequence of the 36 bp oligonucleotide that we used in the HTS was constructed of the 18 bp nucleotide that *Bochkarev et al*. described joined to its 18 bp complementary strand. Inhibition of this interaction is supposed to interfere with the maintenance and the proliferation of the latent virus. This has been suggested by *Nasimuzzaman et al*. who substituted EBNA1 with a mutant EBNA1 form that could not bind to DNA. This mutant form exerted dominant negative effects on the maintenance of the viral episome and impaired the growth of a Burkitt lymphoma cell line [201]. Additionally, *Kariya et al*. showed that the presence of dominant-negative EBNA1 in the early stages of EBV infection led to inhibition of the positive feedback in the transcription of viral transforming genes and the subsequent eradication of EBV genomes in the sub-acute phases of the infection [202]. The observation that the abrogation of the functions of EBNA1 leads to reduced viral genome maintenance and decreased survival of EBV-infected cell lines has also been confirmed by *Hong et al*. who suppressed the expression of EBNA1 by RNA interference and observed reduced proliferation of Raji Burkitt lymphoma cell line [203]. Besides its essential role in episome maintenance and replication, EBNA1 is suggested to interact with other host factors and to support the survival of the infected cells as is the case for Burkitt's lymphoma [204]. Many studies have suggested a direct role of EBNA1 in host gene regulation, however no study has yet unequivocally and compellingly been able to prove that [205].

Recently, we were not the first ones to target EBNA1 in an attempt to inhibit EBV infection. Kang and colleagues used a cell-based HTS assay through which they screened 40 550 compounds for their ability to dissociate EBNA1 from OriP [206]. Roscovitine was

identified as an inhibitor of EBNA1 serine 393 phosphorylation that abrogated the interaction of the protein with OriP. This study elegantly elucidated the mechanisms of action of the compound, yet the authors evaluated the activity of the compound only against LCLs without providing an EBV-negative control cell line and did not at all look at the effect of roscovitine *in vivo*. Four other such reports have characterized EBNA1 inhibitors, however none of the studies has evaluated the efficacy of the identified compounds *in vivo* [207], [208], [209], [210]. Thompson *et al*. concluded that even though the HTS used in their study identified inhibitors of the EBNA1/DNA interaction, these compounds are unlikely to be clinically relevant unless the appropriate chemical modifications are made [207].

The abundant literature strongly supports our choice to target EBNA1 in order to inhibit latent EBV infection. However, one concern should be noted here. Our HTS was designed to screen for compounds that would dissociate the EBNA1/DNA interaction; however, a positive readout in this assay would be obtained with any strong DNA intercalator irrespective of its ability to bind specifically to EBNA1. Some of the strongest dissociators of the complex that appeared among our top 15 hits were DNA binding molecules that are currently used for cancer chemotherapy (Figure 3.4.3., bottom line). It is doubtful that these molecules recognize specifically EBNA1, but rather by binding strongly to the oligonucleotide they inhibit the formation of the complex. As expected these compounds showed cytotoxic activity to both the EBV-positive and the control EBV-negative cell line and were not investigated further. In order to exclude hits that promiscuously bind DNA, one could suggest that the hit compounds were run on a control TR-FRET screen that included a different DNA binding protein and its cognate oligonucleotide. One such control DNA-binding protein could be Proliferating cell nuclear antigen (PCNA). In order to determine which of our hit compounds interacted with DNA we used a PicoGreen counter-assay that identified dsDNA-binding compounds.

Tilorone, was among the top 15 hit compounds and was the only compound that showed LCL-specific cytotoxic activity *in vitro*. At higher concentrations, however, the compound would promote cell killing of EBV-negative cell lines (Figure 3.4.7.B). Therefore, based on our observations we cannot claim that Tilorone specifically inhibits EBV-positive cells, however, we do see an effect of the compound on the stability of the EBNA1/oligonucleotide complex (Figure 3.4.6.) and subsequent cytotoxic (Figure 3.4.7.) and anti-proliferative (Figure 3.4.7.) effect on EBV-positive cell lines. Therefore, we were confident to continue with the thorough characterization of the compound and to suggest it as a potential lead compound to develop an inhibitor of EBV infection. Interestingly, a chemical derivative of Tilorone was also among the top 15 HTS hits (Figure 3.4.3., top row, second column). Unfortunately, this compound was not available for purchase. Nevertheless, one

should consider in the future the potential optimization of Tilorone with medicinal chemistry techniques that would enhance its activity and biological availability. Such attempts by others have already led to the successful optimization of the activity of the compound by modification of its fluorenone skeleton and its side chains [211]. Zhou *et al*. generated 22 novel Tilorone analogs, 10 of which were shown to have better anticancer properties, defined as the compound's cytotoxicity to a number of cancer cell lines [211].

Curiously, our top hit, Tilorone, was first described in the early 70s as a broad-spectrum, orally active antiviral agent in mice [152]. The compounds was shown to effectively reduce the viral load of a number of RNA and DNA viruses including Semliki Forest virus, vesicular stomatitis virus, encephalomyocarditis, Mengo, vaccinia, herpes simplex virus and three strains of influenza among others [152], [212]. Yet, the efficaciousness of the compound in EBV infection has never been tested before.

Even though the compound can be administered orally, we chose to deliver it intraperitonealy in order to minimize injuries and complications as a result of repeated gavage applications. ^{14}C- and ^{3}H-tilorone pharmacokinetics studies have shown that the compound distributes rapidly throughout the body post intravenous, intraperitoneal, and oral administration [213], [214]. The highest concentration of the compound through either application route was found in the liver and the kidneys of the injected mice, while the lowest concentration was detected in the plasma of the animals. Therefore, all three routes of administration provide similar biological distribution of the compound, however while the LD_{50} dose of a single intraperitonealy injection is 145 mg/kg, the LD_{50} for a single oral dose is 959 mg/kg [152]. Therefore, one can apply orally 5 times higher concentration of Tilorone also taking into consideration that the hepatoportal system would eliminate about 21% of the orally administered Tilorone [214]. Hence, it would be of interested to explore the potential of application of a higher concentration of the compound through oral administration. Moreover, it would be advantageous to develop a chemical derivative of Tilorone that persist at higher concentrations in the blood if the compound is used for the treatment of EBV infection or EBV-associated lymphomas.

After the discovery of the broad anti-viral properties of Tilorone, the compound was approved for medical use and commercialized under the name Amixin in a limited number of countries such as Ukraine and Russia. The drug is currently being used as a prophylactic against a number of viral infections including influenza, hepatitis, and herpes. Curiously, even though not the primary standard of care, the drug is also suggested for the treatment of multiple sclerosis. However, we were not able to find any clinical study reports describing the efficacy of the drug. Interestingly, we performed 2 independent EAE experiments where oral treatment with the compound led to decrease in disease onset, incidence, and severity (data

not shown). We did not, however, further characterize the mechanism through which this occurs.

The mechanism of action described in the literature about the antiviral properties of Tilorone concerns the compound's ability to induce IFN-α [215]. High serum titers of IFN-α were reported in mice post oral administration of the compound, with a peak at 24 hours, however the compound had reduced capacity to induce IFN-α production in other organisms such as rabbits, hamsters, ferrets, cats, dogs, and humans [216]. Tilorone has been shown to form a reversible molecular complex with DNA with a predilection for AT-rich sequence motifs [212]. A poorly understood interaction with the promoter region of IFN-α is suggested to be involved in the compound's potential to induce the production of type I interferons. Nevertheless, the anti-proliferative effect of Tilorone on LCLs is most likely not due to the compound's ability to induce IFN-α since we were not able to detect presence of IFN-α protein in the supernatant of treated LCLs (data not shown) and LCLs were suggested to be irresponsive to IFN-α since they lack the respective receptors. Moreover, we were not able to find IFN-α protein in the serum of Tilorone treated humanized NSG mice both 17 hours post injection and at the time of termination of the experiment between week 5 and 7 (data not shown).

We hypothesis that due to its DNA intercalating abilities, Tilorone is able to bind to the AT-abundant sequence motif on *OriP* that EBNA1 recognizes and in doing so is able to interfere with the formation of the EBNA1/OriP complex which then leads to abrogation of the EBNA1 function to support the maintenance and the replication of latent EBV genomes. The activity of EBNA1 is mediated through binding of the protein on two distinct regions on *OriP* conveying two distinct functions (Figure 4.4.1.).

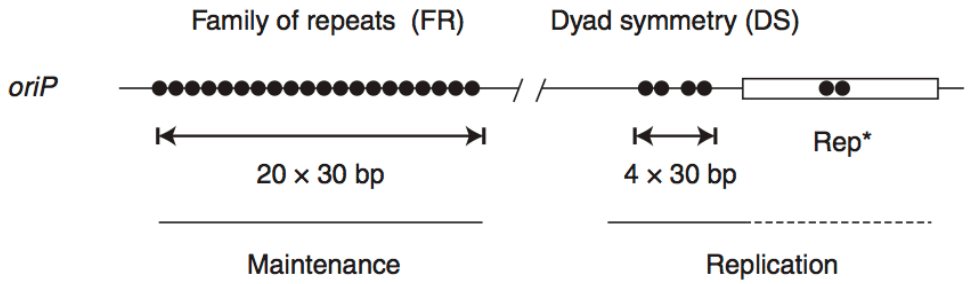

Figure 4.4.1. Depiction of OriP and its EBNA1 binding sites. (Figure drawn based on Hammerschmidt *et al*. [16].)

The family of repeats (FR) is an array of 20 non-conserved tandem repeats of 30bp size that is located on the *OriP* and is essential for episomal maintenance [12]. EBNA1 can bind with high affinity as a dimer to the 20 motifs in the FR; however, only seven of the 20 motifs need to be occupied by EBNA1 for efficient episomal maintenance to occur [12]. The dyad symmetry (DS), on the other hand, is a 65 bp region on *OriP* located about 1 kbps downstream of FR that is the minimal replicator element of episomal EBV. The region consists of two pairs of low affinity EBNA1-binding sites [12], [16]. The sites within one pair are spaced exactly 21 bp apart so that they fall in the same helical phase, a characteristic essential for their function as replicator that is not required for EBNA1 binding at the FR region [27]. Since the EBNA1 binding at the DS happens with low affinity and is highly sensitive to the helical turn of the DNA, we hypothesize that Tilorone is able to interfere with EBNA1 binding at the DS site due to the compound's ability to bind to AT-rich DNA sequences and to change the topological structure of the DNA when bound. We do not have yet data to prove this hypothesis; however, we have seen that when we treat LCL-injected non-reconstituted NSG mice with Tilorone, we observed an inhibition of the proliferation of the LCLs but not complete eradication of the injected LCLs (Figure 3.4.11.). One should note here that one limitation of this mouse model is that the treatment with the compound is started 2 days post intravenous injection of the LCLs and therefore this model is not a perfect representation of a solid tumor treatment in humans. Nevertheless, these data suggest that Tilorone inhibits strongly the proliferation of the latently infected cells, while it does not significantly influence the maintenance of the EBV episome. This differs from what we observed *in vitro*, where the compound not only inhibited the proliferation of latently infected cells, but also had cytotoxic effects and completely eradicated the LCLs (Figure 3.4.7. and 3.4.8.). This discrepancy could be explained by the higher concentrations of the compound reaching the cell *in vitro,* which could possible result in higher level of DNA intercalation of the compound and eventual interference with the DNA replication processes of the cell. However, we have also not seen a decrease in EBV episome number in Tilorone treated LCLs (data not shown).

Again we would propose that the compound should be optimized through medicinal chemistry in order to maximize its ability to dissociate the EBNA1/DNA complex not only at DS but also at the FR region. Then, we hypothesize that we would be able not only to interfere with the replication of latent EBV but also to efficiently abrogate EBV genome maintenance. That, however, raises the concern of EBV reinfection and subsequent IM-like complications of individuals who had cleared the infection post treatment. Since, however, EBV specific adaptive immune responses would be maintained after primary acute viral infections in memory T and B cell compartments, this would probably be less of a concern.

In conclusion, we have seen that Tilorone has strong cytotoxic and anti-proliferative effects on EBV-positive cells, while it significantly reduces *ex vivo* B cell transformation, lytic reactivation, and tumor burden in non-reconstituted NSG mice. The compound, however, has shown limited efficacy in reducing EBV viral load in EBV-infected humanized NGS mice. That most probably resulted from the potentially low Tilorone concentrations in the animal serum as suggested by pharmacokinetics studies with radio-labeled Tilorone [213], [214]. It would be interesting to evaluate the concentration of Tilorone in the mouse blood and correlate that to the viral load. More intriguing, however, would be to engineer the compound through medicinal chemistry to a form that is more readily available in the blood and efficacious against both EBV maintenance and proliferation. Further research and compound optimization could potentially lead to the development of a new treatment strategy against latent EBV infection and EBV-associated diseases.

5. REFERENCES

1. Kakalacheva, K., et al., *Intrathymic Epstein-Barr virus infection is not a prominent feature of myasthenia gravis*. Ann Neurol, 2011. **70**(3): p. 508-14.

2. de-The, G., *The Epstein-Barr virus (EBV): a Rosetta Stone for understanding the role of viruses in immunopathological disorders and in human carcinogenesis*. Biomed Pharmacother, 1985. **39**(2): p. 49-51.

3. Pellet P., R.B., *Herpesviridae: A Brief Introduction*. In Fields Virology. Vol. 5th edition, 2007.

4. Hislop, A., et al., *Cellular responses to viral infection in humans: Lessons from Epstein-Barr virus*. Annu Rev of Immunol, 2007. **25**: p. 587-617.

5. Baer, R., et al., *DNA sequence and expression of the B95-8 Epstein-Barr virus genome*. Nature, 1984.

6. Miller, G., et al., *Epstein-Barr virus: transformation, cytopathic changes, and viral antigens in squirrel monkey and marmoset leukocytes*. Proc Natl Acad Sci U S A, 1972. **69**(2): p. 383-387.

7. Parker, B.D., et al., *Sequence and transcription of Raji Epstein-Barr virus DNA spanning the B95-8 deletion region*. Virology, 1990. **179**(1): p. 339-346.

8. Zimber, U., et al., *Geographical prevalence of two types of Epstein-Barr virus*. Virology, 1986. **154**(1): p. 56-66.

9. Abdel-Hamid, M., et al., *EBV strain variation: geographical distribution and relation to disease state*. Virology, 1992. **190**(1): p. 168-175.

10. Fingeroth, J., *Epstein-Barr virus receptor of human B lymphocytes is the C3d receptor CR2*. Proc Natl Acad Sci U S A, 1984. **81**(14 I): p. 4510-4514.

11. Tugizov, S.M., J.W. Berline, and J.M. Palefsky, *Epstein-Barr virus infection of polarized tongue and nasopharyngeal epithelial cells*. Nat Med, 2003. **9**(3): p. 307-14.

12. Yates, J.L., *Epstein-Barr virus DNA replication*. DNA replication in eukaryotic cells. Cold Spring Harbor Laboratory Press, Cold Spring Harbor, NY, 1996: p. 751-773.

13. Bloss, T.A. and B. Sugden, *Optimal lengths for DNAs encapsidated by Epstein-Barr virus*. J Virol, 1994. **68**(12): p. 8217-8222.

14. Gibson, W. and B. Roizman, *compartmentalization of spermine and spermidine in herpes simplex virion*. Proc Natl Acad Sci U S A, 1971. **68**(11): p. 2818.

15. Hammerschmidt, W. and B. Sugden, *Identification and characterization of oriLyt, a lytic origin of DNA replication of Epstein-Barr virus*. Cell, 1988. **55**(3): p. 427-433.

16. Hammerschmidt, W. and B. Sugden, *Replication of Epstein-Barr Viral DNA*. Cold Spring Harbor Perspectives in Biology, 2013. **5**(1): p. a013029-a013029.

17. Liao, G.L., F.Y. Wu, and S.D. Hayward, *Interaction with the Epstein-Barr virus helicase targets Zta to DNA replication compartments*. J Virol, 2001. **75**(18): p. 8792-8802.

18. Liao, G.L., et al., *The Epstein-Barr virus replication protein BBLF2/3 provides an origin-tethering function through interaction with the zinc finger DNA binding protein ZBRK1 and the KAP-1 corepressor*. J Virol, 2005. **79**(1): p. 245-256.

19. Takagi, S., K. Takada, and T. Sairenji, *Formation of intranuclear replication compartments of Epstein-Barr-Virus with redistribution of BZLF1 And BMRF1 gene-products*. Virology, 1991. **185**(1): p. 309-315.

20. Nakayama, S., et al., *Epstein-Barr Virus Polymerase Processivity Factor Enhances BALF2 Promoter Transcription as a Coactivator for the BZLF1 Immediate-Early Protein*. J Biol Chem, 2009. **284**(32): p. 21557-21568.

21. Pfuller, R. and W. Hammerschmidt, *Plasmid-like replicative intermediates of the Epstein-Barr virus lytic origin of DNA replication*. J Virol, 1996. **70**(6): p. 3423-3431.

22. Daikoku, T., et al., *Postreplicative mismatch repair factors are recruited to Epstein-Barr virus replication compartments*. J Biol Chem, 2006. **281**(16): p. 11422-11430.

23. Kudoh, A., et al., *Homologous Recombinational Repair Factors Are Recruited and Loaded onto the Viral DNA Genome in Epstein-Barr Virus Replication Compartments*. J Virol, 2009. **83**(13): p. 6641-6651.

24. Sugimoto, A., et al., *Spatiotemporally Different DNA Repair Systems Participate in Epstein-Barr Virus Genome Maturation*. J Virol, 2011. **85**(13): p. 6127-6135.

25. Miyazaki, I., R.K. Cheung, and H.-M. Dosch, *Viral interleukin 10 is critical for the induction of B cell growth transformation by Epstein-Barr virus*. J Exp Med, 1993. **178**(2): p. 439-447.

26. Nanbo, A., A. Sugden, and B. Sugden, *The coupling of synthesis and partitioning of EBV plasmid replicon is revealed in live cells*. The EMBO Journal, 2007. **26**(19): p. 4252-4262.

27. Bashaw, J.M. and J.L. Yates, *Replication from oriP of Epstein-Barr Virus Requires Exact Spacing of Two Bound Dimers of EBNA1 Which Bend DNA*. J Virol, 2001. **75**(22): p. 10603-10611.

28. Yates, J.L., S.M. Camiolo, and J.M. Bashaw, *The Minimal Replicator of Epstein-Barr Virus oriP*. J Virol, 2000. **74**(10): p. 4512-4522.

29. Julien, M.D., Z. Polonskaya, and J. Hearing, *Protein and sequence requirements for the recruitment of the human origin recognition complex to the latent cycle origin of DNA replication of Epstein-Barr virus oriP*. Virology, 2004. **326**(2): p. 317-328.

30. Deng, Z., et al., *Telomeric proteins regulate episomal maintenance of Epstein-Barr virus origin of plasmid replication*. Molecular Cell, 2002. **9**(3): p. 493-503.

31. Lindner, S.E., et al., *The affinity of EBNA1 for its origin of DNA synthesis is a determinant of the origin's replicative efficiency*. J Virol, 2008. **82**(12): p. 5693-5702.

32. Kirchmaier, A.L. and B. Sugden, *Rep*: a viral element that can partially replace the origin of plasmid DNA synthesis of Epstein-Barr virus*. J Virol, 1998. **72**(6): p. 4657-4666.

33. Wang, J.D., et al., *Essential elements of a licensed, mammalian plasmid origin of DNA synthesis*. Mol Cell Biol, 2006. **26**(3): p. 1124-1134.

34. Wensing, B., et al., *Variant chromatin structure of the oriP region of Epstein-Barr virus and regulation of EBER1 expression by upstream sequences and oriP*. J Virol, 2001. **75**(13): p. 6235-6241.

35. Tempera, I. and P.M. Lieberman, *Chromatin organization of gammaherpesvirus latent genomes*. BBA - Gene Regul Mech, 2010. **1799**(3-4): p. 236-245.

36. Frappier, L. and M. Odonnell, *Overproduction, Purification, and Characterization of Ebna1, the Origin Binding-Protein of Epstein-Barr-Virus*. J Biol Chem, 1991. **266**(12): p. 7819-7826.

37. Chen, M.R., J.M. Middeldorp, and S.D. Hayward, *Separation of the Complex DNA-Binding Domain of EBNA-1 into DNA Recognition and Dimerization Subdomains of Novel Structure*. J Virol, 1993. **67**(8): p. 4875-4885.

38. Bochkarev, A., et al., *Crystal structure of the DNA-binding domain of the Epstein-Barr virus origin-binding protein EBNA 1*. Cell, 1995. **83**(1): p. 39-46.

39. Bochkarev, A., et al., *Crystal structure of the DNA-binding domain of the Epstein-Barr virus origin-binding protein, EBNA1, bound to DNA*. 1996. p. 791-800.

40. Hegde, R.S., et al., *Crystal-structure at 1.7-angstrom of the Bovine Papillomavirus-1 e2 DNA-binding domain bound to its DNA target*. Nature, 1992. **359**(6395): p. 505-512.

41. Altmann, M., et al., *Transcriptional activation by EBV nuclear antigen 1 is essential for the expression of EBV transforming genes*. Proc Natl Acad Sci U S A, 2006. **103**(38): p. 14188-14193.

42. Aras, S., et al., *Zinc Coordination Is Required for and Regulates Transcription Activation by Epstein-Barr Nuclear Antigen 1*. PLoS Pathogens, 2009. **5**(6).

43. Avolio-Hunter, T.M. and L. Frappier, *EBNA1 efficiently assembles on chromatin containing the Epstein-Barr virus latent origin of replication*. Virology, 2003. **315**(2): p. 398-408.

44. Middleton, T. and B. Sugden, *EBNA1 Can Link the Enhancer Element to the Initiator Element of the Epstein-Barr-Virus Plasmid Origin of DNA-Replication*. J Virol, 1992. **66**(1): p. 489-495.

45. Sears, J., et al., *The amino terminus of Epstein-Barr virus (EBV) nuclear antigen 1 contains AT hooks that facilitate the replication and partitioning of latent EBV genomes by tethering them to cellular chromosomes*. J Virol, 2004. **78**(21): p. 11487-11505.

46. Levitskaya, J., *Inhibition of ubiquitin/proteasome-dependent protein degradation by the Gly-Ala repeat domain of the Epstein-Barr virus nuclear antigen 1*. Proc Natl Acad Sci U S A, 1997. **94**(23): p. 12616-12621.

47. Yin, Y., B. Manoury, and R. Fahraeus, *Self-inhibition of synthesis and antigen presentation by Epstein-Barr virus-encoded EBNA1*. Science, 2003. **301**(5638): p. 1371-1374.

48. Paludan, C., et al., *Endogenous MHC class II processing of a viral nuclear antigen after autophagy*. Science, 2005. **307**(5709): p. 593-596.

49. Caldwell, R., *Epstein-Barr virus LMP2A drives B cell development and survival in the absence of normal B cell receptor signals*. Immunity, 1998. **9**(3): p. 405-411.

50. Gires, O., et al., *Latent membrane protein 1 of Epstein-Barr virus mimics a constitutively active receptor molecule*. EMBO Journal, 1997. **16**(20): p. 6131-6140.

51. Mosialos, G., et al., *The Epstein-Barr-virus transforming protein LMP1 engages signaling proteins for the tumor-necrosis-factor receptor family*. Cell, 1995. **80**(3): p. 389-399.

52. Kilger, E., et al., *Epstein-Barr virus-mediated B-cell proliferation is dependent upon latent membrane protein 1, which simulates an activated CD40 receptor*. EMBO Journal, 1998. **17**(6): p. 1700-1709.

53. Zimber-Strobl, U., et al., *Epstein-Barr virus latent membrane protein (LMP1) is not sufficient to maintain proliferation of B cells but both it and activated CD40 can prolong their survival*. EMBO J, 1996. **15**(24): p. 7070-8.

54. Beaufils, P., et al., *The (YXXL/I)2 signalling motif found in the cytoplasmic segments of the bovine leukaemia virus envelope protein and Epstein-Barr virus latent membrane protein 2A can elicit early and late lymphocyte activation events*. EMBO J, 1993. **12**(13): p. 5105-12.

55. Williams, H., et al., *The immune response to primary EBV infection: a role for natural killer cells*. Br J Haematol, 2005. **129**(2): p. 266-74.

56. Strowig, T., et al., *Tonsilar NK Cells Restrict B Cell Transformation by the Epstein-Barr Virus via IFN-γ*. PLoS Pathogens, 2008. **4**(2): p. e27.

57. Pappworth, I.Y., E.C. Wang, and M. Rowe, *The switch from latent to productive infection in Epstein-Barr virus-infected B cells is associated with sensitization to NK cell killing*. J Virol, 2007. **81**(2): p. 474-82.

58. Steven, N.M., et al., *Immediate early and early lytic cycle proteins are frequent targets of the Epstein-Barr virus-induced cytotoxic T cell response*. J Exp Med, 1997. **185**(9): p. 1605-17.

59. Steven, N.M., et al., *Epitope focusing in the primary cytotoxic T cell response to Epstein-Barr virus and its relationship to T cell memory*. J Exp Med, 1996. **184**(5): p. 1801-13.

60. Callan, M.F., et al., *CD8(+) T-cell selection, function, and death in the primary immune response in vivo*. J Clin Invest, 2000. **106**(10): p. 1251-61.

61. Hislop, A.D., et al., *Epitope-specific evolution of human CD8(+) T cell responses from primary to persistent phases of Epstein-Barr virus infection*. J Exp Med, 2002. **195**(7): p. 893-905.

62. Dunne, P.J., et al., *Epstein-Barr virus-specific CD8(+) T cells that re-express CD45RA are apoptosis-resistant memory cells that retain replicative potential*. Blood, 2002. **100**(3): p. 933-40.

63. Faint, J.M., et al., *Memory T cells constitute a subset of the human CD8+CD45RA+ pool with distinct phenotypic and migratory characteristics*. J Immunol, 2001. **167**(1): p. 212-20.

64. Hislop, A.D., et al., *EBV-specific CD8+ T cell memory: relationships between epitope specificity, cell phenotype, and immediate effector function*. J Immunol, 2001. **167**(4): p. 2019-29.

65. Keating, S., et al., *The lytic cycle of Epstein-Barr virus is associated with decreased expression of cell surface major histocompatibility complex class I and class II molecules*. J Virol, 2002. **76**(16): p. 8179-88.

66. Maini, M.K., et al., *Clonal expansions in acute EBV infection are detectable in the CD8 and not the CD4 subset and persist with a variable CD45 phenotype*. J Immunol, 2000. **165**(10): p. 5729-37.

67. Amyes, E., et al., *Characterization of the CD4+ T cell response to Epstein-Barr virus during primary and persistent infection*. J Exp Med, 2003. **198**(6): p. 903-11.

68. Precopio, M.L., et al., *Differential kinetics and specificity of EBV-specific CD4+ and CD8+ T cells during primary infection*. J Immunol (Baltimore, Md : 1950), 2003. **170**(5): p. 2590-2598.

69. Ressing, M.E., et al., *Interference with T cell receptor-HLA-DR interactions by Epstein-Barr virus gp42 results in reduced T helper cell recognition*. Proc Natl Acad Sci U S A, 2003. **100**(20): p. 11583-8.

70. Luzuriaga, K. and J.L. Sullivan, *Infectious mononucleosis*. New Engl J Med, 2010. **362**(21): p. 1993-2000.

71. Nagy, N. and E. Klein, *Deficiency of the proapoptotic SAP function in X-linked lymphoproliferative disease aggravates Epstein-Barr virus (EBV) induced mononucleosis and promotes lymphoma development*. Immunol Lett, 2010. **130**(1-2): p. 13-8.

72. Epstein, M.A., B.G. Achong, and Y.M. Barr, *Virus particles in cultured lymphoblasts from Burkitts lymphoma*. Lancet, 1964. **1**(733): p. 702.

73. Carbone, A., A. Gloghini, and G. Dotti, *EBV-associated lymphoproliferative disorders: classification and treatment*. Oncologist, 2008. **13**(5): p. 577-585.

74. Young, L.S. and A.B. Rickinson, *Epstein-Barr virus: 40 years on*. Nat Rev Cancer, 2004. p. 757-768.

75. Kennedy, G., J. Komano, and B. Sugden, *Epstein-Barr virus provides a survival factor to Burkitt's lymphomas*. Proc Natl Acad Sci U S A, 2003. **100**(24): p. 14269-14274.

76. Chou, J., et al., *Nasopharyngeal carcinoma—Review of the molecular mechanisms of tumorigenesis*. Head and Neck, 2008. **30**(7): p. 946-963.

77. Kakalacheva, K., C. Munz, and J.D. Lunemann, *Viral triggers of multiple sclerosis*. Biochim Biophys Acta, 2011. **1812**(2): p. 132-40.

78. Hemmer, B., et al., *Identification of high potency microbial and self ligands for a human autoreactive class II-restricted T cell clone*. J Exp Med, 1997. p. 1651-1659.

79. Hemmer, B., et al., *Identification of candidate T-cell epitopes and molecular mimics in chronic Lyme disease*. Nat Med, 1999. **5**(12): p. 1375-1382.

80. Hemmer, B., et al., *Contribution of individual amino acids within MHC molecule or antigenic peptide to TCR ligand potency*. of J Immunol, 2000. **164**(2): p. 861-871.

81. McRae, B.L., et al., *Functional evidence for epitope spreading in the relapsing pathology of experimental autoimmune encephalomyelitis*. J Exp Med, 1995. **182**(1): p. 75-85.

82. Yu, M., J.M. Johnson, and V.K. Tuohy, *A predictable sequential determinant spreading cascade invariably accompanies progression of experimental autoimmune encephalomyelitis: a basis for peptide-specific therapy after onset of clinical disease*. J Exp Med, 1996. p. 1777-1788.

83. Katz-Levy, Y., et al., *Endogenous presentation of self myelin epitopes by CNS-resident APCs in Theiler's virus-infected mice*. J Clin Invest, 1999. p. 599-610.

84. Kaufman, D.L., et al., *Spontaneous loss of T-cell tolerance to glutamic acid decarboxylase in murine insulin-dependent diabetes*. Nature, 1993. **366**(6450): p. 69-72.

85. Lurquin, C., et al., *Contrasting frequencies of antitumor and anti-vaccine T cells in metastases of a melanoma patient vaccinated with a MAGE tumor antigen*. J Exp Med, 2005. **201**(2): p. 249-257.

86. Miller, S.D., et al., *Persistent infection with Theiler's virus leads to CNS autoimmunity via epitope spreading*. Nat Med, 1997. p. 1133-1136.

87. Olson, J.K., J. Ludovic Croxford, and S.D. Miller, *Innate and adaptive immune requirements for induction of autoimmune demyelinating disease by molecular mimicry*. Mol Immunol, 2004. **40**(14-15): p. 1103-1108.

88. Longnecker, R., et al., *Deletion of DNA encoding the first five transmembrane domains of Epstein-Barr virus latent membrane proteins 2A and 2B*. J Virol, 1993. **67**(8): p. 5068-5074.

89. Pender, M., *Infection of autoreactive B lymphocytes with EBV, causing chronic autoimmune diseases*. Trends Immunol, 2003. **24**(11): p. 584-588.

90. Operskalski, E.A., et al., *A case-control study of multiple sclerosis*. Neurology, 1989. p. 825-829.

91. Lindberg, C., et al., *Epidemiological investigation of the association between infectious mononucleosis and multiple sclerosis*. Neuroepidemiology, 1991. **10**(2): p. 62-65.

92. Nielsen, T.R., *Multiple sclerosis after infectious mononucleosis*. Arch Neurol, 2007. p. 72-75.

93. Ramagopalan, S.V., et al., *Association of infectious mononucleosis with multiple sclerosis. A population-based study*. Neuroepidemiology, 2009. **32**(4): p. 257-262.

94. Nielsen, T.R., et al., *Effects of infectious mononucleosis and HLA-DRB1*15 in multiple sclerosis*. Mult Scler, 2009. **15**(4): p. 431-436.

95. Thacker, E., *Infectious mononucleosis and risk for multiple sclerosis: A meta-analysis*. Ann Neurol, 2006. **59**(3): p. 499-503.

96. Alotaibi, S., *Epstein-Barr Virus in Pediatric Multiple Sclerosis*. JAMA, 2004. p. 1875-1879.

97. Pohl, D., et al., *High seroprevalence of Epstein-Barr virus in children with multiple sclerosis*. Neurology, 2006. p. 2063-2065.

98. Lünemann, J.D., et al., *Broadened and elevated humoral immune response to EBNA1 in pediatric multiple sclerosis*. Neurology, 2008. p. 1033-1035.

99. Levin, L.I., et al., *Temporal relationship between elevation of Epstein-Barr virus antibody titers and initial onset of neurological symptoms in multiple sclerosis*. JAMA, 2005. p. 2496-2500.

100. Ascherio, A., et al., *Epstein-Barr virus antibodies and risk of multiple sclerosis: a prospective study*. JAMA, 2001. p. 3083-3088.

101. DeLorenze, G.N., et al., *Epstein-Barr virus and multiple sclerosis: evidence of association from a prospective study with long-term follow-up*. Arch Neurol, 2006. **63**(6): p. 839-844.

102. Lünemann, J.D., et al., *Elevated Epstein-Barr virus-encoded nuclear antigen-1 immune responses predict conversion to multiple sclerosis*. Ann Neurol, 2010. p. 159-169.

103. Jilek, S., et al., *Strong EBV-specific CD8+ T-cell response in patients with early multiple sclerosis*. Brain, 2008. **131**: p. 1712-1721.

104. Farrell, R.A., et al., *Humoral immune response to EBV in multiple sclerosis is associated with disease activity on MRI*. Neurology, 2009. **73**(1): p. 32-8.

105. Lünemann, J.D., et al., *Increased frequency and broadened specificity of latent EBV nuclear antigen-1-specific T cells in multiple sclerosis*. Brain, 2006. p. 1493-1506.

106. Lünemann, J.D., et al., *EBNA1-specific T cells from patients with multiple sclerosis cross react with myelin antigens and co-produce IFN-gamma and IL-2*. J Exp Med, 2008. **205**(8): p. 1763-1773.

107. Harkiolaki, M., et al., *T cell-mediated autoimmune disease due to low-affinity crossreactivity to common microbial peptides*. Immunity, 2009. **30**(3): p. 348-357.

108. Lang, H., *A functional and structural basis for TCR cross-reactivity in multiple sclerosis*. Nat Immunol, 2002. **3**(10): p. 940-943.

109. Olson, J.K., et al., *A virus-induced molecular mimicry model of multiple sclerosis*. J Clin Invest, 2001. **108**(2): p. 311-318.

110. Thorley-Lawson, D.A., *Epstein-Barr virus: Exploiting the immune system*. Nat Rev Immunol, 2001. p. 75-82.

111. Serafini, B., *Dysregulated Epstein-Barr virus infection in the multiple sclerosis brain*. The J Exp Med, 2007. **204**(12): p. 2899-2912.

112. Willis, S.N., et al., *Epstein-Barr virus infection is not a characteristic feature of multiple sclerosis brain*. Brain, 2009. **132**: p. 3318-3328.

113. Peferoen, L.A., et al., *Epstein Barr virus is not a characteristic feature in the central nervous system in established multiple sclerosis*. Brain, 2010. **133**: p. e137.

114. Sargsyan, S.A., et al., *Absence of Epstein-Barr virus in the brain and CSF of patients with multiple sclerosis*. Neurology, 2010. **74**(14): p. 1127-1135.

115. Vincent, A., *Unravelling the pathogenesis of myasthenia gravis*. Nat Rev Immunol, 2002. **2**(10): p. 797-804.

116. Hohlfeld, R. and H. Wekerle, *Reflections on the "intrathymic pathogenesis" of myasthenia gravis*. J Neuroimmunol, 2008. **201-202**: p. 21-7.

117. Shiono, H., et al., *Scenarios for autoimmunization of T and B cells in myasthenia gravis*. Ann N Y Acad Sci, 2003. **998**: p. 237-56.

118. Aoki, T., et al., *Attempts to implicate viruses in myasthenia gravis*. Neurology, 1985. **35**(2): p. 185-92.

119. Klavinskis, L.S., et al., *Attempted isolation of viruses from myasthenia gravis thymus*. J Neuroimmunol, 1986. **11**(4): p. 287-99.

120. Cavalcante, P., et al., *Epstein-Barr virus persistence and reactivation in myasthenia gravis thymus*. Ann Neurol, 2010. **67**(6): p. 726-738.

121. Esen, B.A., et al., *Serologic response to Epstein-Barr virus antigens in patients with systemic lupus erythematosus: a controlled study*. Rheumatol Int, 2012. **32**(1): p. 79-83.

122. Chen, D.Y., et al., *Polymyositis/dermatomyositis and nasopharyngeal carcinoma: the Epstein-Barr virus connection?* J Clin Virol, 2010. **49**(4): p. 290-5.

123. Yadav, P., et al., *Antibodies Elicited in Response to EBNA-1 May Cross-React with dsDNA*. PloS One, 2011. **6**(1).

124. Sundar, K., et al., *Expression of the Epstein-Barr virus nuclear antigen-1 (EBNA-1) in the mouse can elicit the production of anti-dsDNA and anti-Sm antibodies*. J Autoimmun, 2004. **23**(2): p. 127-140.

125. Kang, I., *Defective Control of Latent Epstein-Barr Virus Infection in Systemic Lupus Erythematosus*. J Immunol, 2004. p. 1287-1294.

126. Larsen, M., et al., *Exhausted Cytotoxic Control of Epstein-Barr Virus in Human Lupus*. PLoS Pathogens, 2011. **7**(10).

127. Ulff-Moller, C.J., et al., *Epstein-Barr virus-associated infectious mononucleosis and risk of systemic lupus erythematosus*. Rheumatology, 2010. **49**(9): p. 1706-1712.

128. Toussirot, E. and J. Roudier, *Epstein-Barr virus in autoimmune diseases*. Best Pract Res Clin Rheumatol, 2008. p. 883-896.

129. Baboonian, C., et al., *Cross reaction of antibodies to a glycine/alanine repeat sequence of Epstein-Barr virus nuclear antigen-1 with collagen, cytokeratin, and actin*. Ann Rheum Dis, 1991. **50**(11): p. 772-775.

130. Saal, J.G., et al., *Synovial Epstein-Barr virus infection increases the risk of rheumatoid arthritis in individuals with the shared HLA-DR4 epitope*. Arthritis Rheum, 1999. **42**(7): p. 1485-1496.

131. Epstein, M.A., et al., *Protection of cottontop tamarins against Epstein-Barr virus-induced malignant lymphoma by a prototype subunit vaccine*. Nature, 1985. **318**(6043): p. 287-289.

132. Cadavid, L.F., B.E. Mejía, and D.I. Watkins, *MHC class I genes in a New World primate, the cotton-top tamarin (Saguinus oedipus), have evolved by an active process of loci turnover*. Immunogenetics, 1999. **49**(3): p. 196-205.

133. Cohen, J.I., et al., *The need and challenges for development of an Epstein-Barr virus vaccine*. Vaccine, 2013. **31**: p. B194-B196.

134. Sashihara, J., et al., *Soluble Rhesus Lymphocryptovirus gp350 Protects against Infection and Reduces Viral Loads in Animals that Become Infected with Virus after Challenge*. PLoS Pathogens, 2011. **7**(10): p. e1002308.

135. Gu, S.Y., et al., *First EBV vaccine trial in humans using recombinant vaccinia virus expressing the major membrane antigen*. Dev Biol Stand, 1995. **84**: p. 171-177.

136. Sokal, E.M., et al., *Recombinant gp350 vaccine for infectious mononucleosis: a phase 2, randomized, double-blind, placebo-controlled trial to evaluate the safety, immunogenicity, and efficacy of an Epstein-Barr virus vaccine in healthy young adults*. J Infect Dis, 2007. **196**(12): p. 1749-1753.

137. Berger, C., et al., *Dynamics of Epstein‐Barr virus DNA levels in serum during EBV‐associated disease*. J Med Virol, 2001. **64**(4): p. 505-512.

138. Scherrenburg, J., et al., *Detailed analysis of EpsteinBarr virus-specific CD4 and CD8 T cell responses during infectious mononucleosis*. Clin Exp Immunol, 2008. **153**(2): p. 231-239.

139. Lünemann, J., et al., *Increased frequency of EBV-specific effector memory CD8+ T cells correlates with higher viral load in rheumatoid arthritis*. J Immunol, 2008. **181**(2): p. 991-1000.

140. Willcox, H.N., J. Newsom-Davis, and L.R. Calder, *Greatly increased autoantibody production in myasthenia gravis by thymocyte suspensions prepared with proteolytic enzymes*. Clin Exp Immunol, 1983. **54**(2): p. 378-86.

141. Lünemann, J.D., et al., *Increased frequency of EBV-specific effector memory CD8+ T cells correlates with higher viral load in rheumatoid arthritis*. J Immunol, 2008. **181**(2): p. 991-1000.

142. Strowig, T., et al., *Human NK cells of mice with reconstituted human immune system components require preactivation to acquire functional competence*. Blood, 2010. **116**(20): p. 4158-67.

143. Reindl, M., et al., *Antibodies against the myelin oligodendrocyte glycoprotein and the myelin basic protein in multiple sclerosis and other neurological diseases: a comparative study*. Brain, 1999. **122**: p. 2047-2056.

144. Egg, R., et al., *Anti-MOG and anti-MBP antibody subclasses in multiple sclerosis*. Mult Scler, 2001. **7**(5): p. 285-289.

145. Lebar, R., et al., *The M2 autoantigen of central-nervous-system myelin, a glycoprotein present in oligodendrocyte membrane*. Clin Exp Immunol, 1986. **66**(2): p. 423-434.

146. Baranzini, S., et al., *B cell repertoire diversity and clonal expansion in multiple sclerosis brain lesions*. J Immunol, 1999. **163**(9): p. 5133-5144.

147. Bielekova, B., et al., *Expansion and functional relevance of high-avidity myelin-specific CD4+ T cells in multiple sclerosis*. J Immunol, 2004. p. 3893-3904.

148. Comabella, M., et al., *EBV-specific immune responses in patients with multiple sclerosis responding to IFNbeta therapy*. Mult Scler, 2012. **18**(5): p. 605-9.

149. Currier, J.R., et al., *A panel of MHC class I restricted viral peptides for use as a quality control for vaccine trial ELISPOT assays*. J Immunol Methods, 2002. **260**(1-2): p. 157-72.

150. Münz, C., et al., *Human CD4(+) T lymphocytes consistently respond to the latent Epstein-Barr virus nuclear antigen EBNA1*. J Exp Med, 2000. **191**(10): p. 1649-1660.

151. Jones, M.D. and B.E. Griffin, *Clustered repeat sequences in the genome of Epstein Barr virus*. Nucleic Acids Res, 1983. **11**(12): p. 3919-37.

152. Krueger, R.E. and G.D. Mayer, *Tilorone hydrochloride: an orally active antiviral agent*. Science, 1970, **169**(951): p. 1213-1214.

153. Ressing, M.E., et al., *Impaired transporter associated with antigen processing-dependent peptide transport during productive EBV infection*. J Immunol, 2005. **174**(11): p. 6829.

154. Epstein, M.A. and B.G. Achong, *Pathogenesis of infectious mononucleosis*. Lancet, 1977. **2**(8051): p. 1270-1273.

155. Wollheim, F.A. and R.C. Williams, Jr., *Studies on the macroglobulins of human serum. I. Polyclonal immunoglobulin class M (IgM) increase in infectious mononucleosis*. N Engl J Med, 1966. **274**(2): p. 61-7.

156. Sutton, R.N., et al., *The occurrence of autoantibodies in infectious mononucleosis*. Clin Exp Immunol, 1974. **17**(3): p. 427-436.

157. Carter, R.L., *Antibody formation in infectious mononucleosis. I. Some immunochemical properties of the Paul-Bunnell antibody*. Br J Haematol, 1966. **12**(3): p. 259-67.

158. Holborow, E.J., et al., *Antinuclear factor and other antibodies in blood and liver diseases*. Br Med J, 1963. **1**(5331): p. 656-8.

159. Holborow, E.J., E.H. Hemsted, and S.V. Mead, *Smooth muscle autoantibodies in infectious mononucleosis*. Br Med J, 1973. **3**(5875): p. 323-5.

160. Kaplan, M.E. and E.M. Tan, *Antinuclear antibodies in infectious mononucleosis*. Lancet, 1968. **1**(7542): p. 561-563.

161. Carter, R.L., *Proceedings: Infectious mononucleosis. Immunopathology*. J Clin Pathol, 1973. **26**(12): p. 987-8.

162. Prineas, J.W., *The neuropathology of multiple sclerosis*. Handbook Clin Neurol. Vol. 47. 1985. 213-257.

163. Prineas, J.W. and J.S. Graham, *Multiple-sclerosis - capping of surface immunoglobulin-G on macrophages engaged in myelin breakdown*. Ann Neurol, 1981. **10**(2): p. 149-158.

164. Gay, D. and M. Esiri, *Blood-brain-barrier damage in acute multiple-sclerosis plaques - an immunocytological study*. Brain, 1991. **114**: p. 557-572.

165. Linington, C. and H. Lassmann, *Antibody-responses in chronic relapsing experimental allergic encephalomyelitis - correlation of serum demyelinating activity with antibody titer to the myelin oligodendrocyte glycoprotein (MOG)*. J Neuroimmunol, 1987. **17**(1): p. 61-69.

166. Adelmann, M., et al., *The N-terminal domain of the myelin oligodendrocyte glycoprotein (MOG) induces acute demyelinating experimental autoimmune encephalomyelitis in the Lewis rat*. J Neuroimmunol, 1995. **63**(1): p. 17-27.

167. Amor, S., et al., *Identification of epitopes of myelin oligodendrocyte glycoprotein for the induction of experimental allergic encephalomyelitis in SJL and Biozzi AB/H mice*. J Immunol, 1994. **153**(10): p. 4349-4356.

168. Genain, C.P., et al., *Antibody facilitation of multiple sclerosis-like lesions in a nonhuman primate*. J Clin Invest, 1995. **96**(6): p. 2966-2974.

169. Berger T., et al., *Antimyelin Antibodies as a Predictor of Clinically Definite Multiple Sclerosis*. N Engl J Med. 2003: p. 1-7.

170. Kuhle, J., *Lack of association between antimyelin antibodies and progression to multiple sclerosis*. New Engl J Med, 2007. **356**(4): p. 371-378.

171. Jilek, S., et al., *Severe post-EBV encephalopathy associated with myelin oligodendrocyte glycoprotein-specific immune response*. J Neuroimmunol, 2007. **192**(1-2): p. 192-197.

172. Tracy, S.I., et al., *Persistence of Epstein-Barr Virus in Self-Reactive Memory B Cells*. J Virol, 2012. **86**(22): p. 12330-12340.

173. Whitehouse, J.M., N. Ferguson, and G.A. Currie, *Autoantibody to microtubules in infectious mononucleosis*. Clin Exp Immunol, 1974. **17**(2): p. 227-35.

174. Meckes, D.G., Jr., N.F. Menaker, and N. Raab-Traub, *Epstein-Barr virus LMP1 modulates lipid raft microdomains and the vimentin cytoskeleton for signal transduction and transformation*. J Virol, 2013. **87**(3): p. 1301-11.

175. Alcover, A., et al., *Antibodies to vimentin intermediate filaments in sera from patients with SLE and RA: quantitation by solid phase radioimmunoassay*. J Rheumatol, 1985. **12**(2): p. 233-6.

176. Kataaha, P.K., et al., *Anti-intermediate filament antibodies, antikeratin antibody, and antiperinuclear factor in rheumatoid arthritis and infectious mononucleosis*. Ann Rheum Dis, 1985. **44**(7): p. 446-449.

177. Liebowitz, D., et al., *An Epstein-Barr virus transforming protein associates with vimentin in lymphocytes*. Mol Cell Biol, 1987. **7**(7): p. 2299-308.

178. Strang, G. and A.B. Rickinson, *Multiple HLA class I-dependent cytotoxicities constitute the "non-HLA-restricted" response in infectious mononucleosis*. Eur J Immunol, 1987. **17**(7): p. 1007-13.

179. Burrows, S.R., et al., *An alloresponse in humans is dominated by cytotoxic T lymphocytes (CTL) cross-reactive with a single Epstein-Barr virus CTL epitope: implications for graft-versus-host disease*. J Exp Med, 1994. **179**(4): p. 1155-1161.

180. Misko, I.S., et al., *Crossreactive recognition of viral, self, and bacterial peptide ligands by human class I-restricted cytotoxic T lymphocyte clonotypes: implications for molecular mimicry in autoimmune disease*. Proc Natl Acad Sci U S A, 1999. **96**(5): p. 2279-2284.

181. Clute, S.C., *Cross-reactive influenza virus-specific CD8+ T cells contribute to lymphoproliferation in Epstein-Barr virus-associated infectious mononucleosis*. J Clin Invest, 2005. **115**(12): p. 3602-3612.

182. Wucherpfennig, K. and J. Strominger, *Molecular mimicry in T cell-mediated autoimmunity: Viral peptides activate human T cell clones specific for myelin basic protein*. Cell, 1995. **80**(5): p. 695-705.

183. Lang, H.L.E., et al., *A functional and structural basis for TCR cross-reactivity in multiple sclerosis*. Nat Immunol, 2002. **3**(10): p. 940-943.

184. Lünemann, J.D., et al., *EBNA1-specific T cells from patients with multiple sclerosis cross react with myelin antigens and co-produce IFN-gamma and IL-2*. J Exp Med, 2008. p. 1763-1773.

185. Borysiewicz, L.K., et al., *Epstein Barr virus-specific immune defects in patients with persistent symptoms following infectious mononucleosis*. Q J Med, 1986. **58**(226): p. 111-121.

186. Lünemann, J. and C. Münz, *EBV in MS: guilty by association?* Trends Immunol. 2009. 30(**6**): p.243-248.

187. Hochberg, D., *Demonstration of the Burkitt's lymphoma Epstein-Barr virus phenotype in dividing latently infected memory cells in vivo*. Proc Natl Acad Sci U S A. 2004. 101(**1**): p.239-244.

188. Zhang, Q., et al., *The Epstein-Barr virus (EBV) DNA polymerase accessory protein, BMRF1, activates the essential downstream component of the EBV oriLyt*. Virology, 1997. **230**(1): p. 22-34.

189. Nonkwelo, C., I.K. Ruf, and J. Sample, *Interferon-independent and -induced regulation of Epstein-Barr virus EBNA-1 gene transcription in Burkitt lymphoma*. J Virol, 1997. **71**(9): p. 6887-6897.

190. Zhang, L. and J.S. Pagano, *Interferon regulatory factor 2 represses the Epstein-Barr virus BamHI Q latency promoter in type III latency*. Mol Cell Biol, 1999. **19**(4): p. 3216-3223.

191. Zang, Y.C., et al., *Immunoregulation and blocking antibodies induced by interferon beta treatment in MS*. Neurology, 2000. **55**(3): p. 397-404.

192. Tamura, T., et al., *The IRF family transcription factors in immunity and oncogenesis*. Annu Rev Immunol, 2008. **26**: p. 535-84.

193. Freer, G., et al., *Role of T helper cell precursor frequency on vesicular stomatitis virus neutralizing antibody responses in a T cell receptor beta chain transgenic mouse*. Eur J Immunol, 1995. **25**(5): p. 1410-6.

194. Strowig, T., et al., *Priming of protective T cell responses against virus-induced tumors in mice with human immune system components*. J Exp Med, 2009. **206**(6): p. 1423-1434.

195. Münz, C., et al., *Antiviral immune responses: triggers of or triggered by autoimmunity?* Nat Rev Immunol, 2009. **9**(4): p. 246-258.

196. Klavinskis, L.S., et al., *Antivirus antibodies in myasthenia gravis*. Neurology, 1985. **35**(9): p. 1381-4.

197. Csuka, D., et al., *High anti-EBNA-1 IgG levels are associated with early-onset myasthenia gravis*. Eur J Neurol, 2012. **19**(6): p. 842-846.

198. Meyer, M., et al., *Lack of evidence for epstein‐barr virus infection in myasthenia gravis thymus*. Ann Neurol, 2011. **70**(3): p. 515-518.

199. Jing, F., et al., *Lack of Epstein-Barr virus infection in Chinese myasthenia gravis patients*. Acta Neurol Scand, 2013.

200. Marechal, V., et al., *Mapping EBNA-1 domains involved in binding to metaphase chromosomes*. J Virol, 1999. **73**(5): p. 4385-4392.

201. Nasimuzzaman, M., et al., *Eradication of Epstein-Barr virus episome and associated inhibition of infected tumor cell growth by adenovirus vector-mediated transduction of dominant-negative EBNA1*. Mol Ther, 2005. **11**(4): p. 578-590.

202. Kariya, Y., et al., *Dominant-negative derivative of EBNA1 represses EBNA1-mediated transforming gene expression during the acute phase of Epstein-Barr virus infection independent of rapid loss of viral genome*. Cancer Sci, 2010. **101**(4): p. 876-81.

203. Wang, H., et al., *EBV latent membrane protein 2A induces autoreactive B cell activation and TLR hypersensitivity*. 2006. p. 2793-2802.

204. Kennedy, G. and B. Sugden, *EBNA-1, a bifunctional transcriptional activator*. Mol Cell Biol, 2003. **23**(19): p. 6901-6908.

205. Smith, D. and B. Sugden, *Potential Cellular Functions of Epstein-Barr Nuclear Antigen 1 (EBNA1) of Epstein-Barr Virus*. Viruses, 2013. **5**(1): p. 226-240.

206. Kang, M.S., et al., *Roscovitine inhibits EBNA1 serine 393 phosphorylation, nuclear localization, transcription, and episome maintenance*. J Virol, 2011. **85**(6): p. 2859-68.

207. Thompson, S., et al., *Development of a high-throughput screen for inhibitors of Epstein-Barr virus EBNA1*. J Biomol Screen, 2010. **15**(9): p. 1107-1115.

208. Li, N., et al., *Discovery of selective inhibitors against EBNA1 via high throughput in silico virtual screening*. PLoS One. 2010 **5**(4).

209. Kim, S.Y., et al., *Small molecule and peptide-mediated inhibition of Epstein-Barr virus nuclear antigen 1 dimerization*. Biochem Bioph Res Co, 2012: p. 1-6.

210. Arvey, A., et al., *An Atlas of the Epstein-Barr Virus Transcriptome and Epigenome Reveals Host-Virus Regulatory Interactions*. Cell Host Microbe, 2012. **12**(2): p. 233-245.

211. Zhou, D., et al., *Synthesis and activity evaluation of tilorone analogs as potential anticancer agents*. Eur J Med Chem, 2013. **64**(C): p. 432-441.

212. Chandra, P. and G.J. Wright, *Tilorone hydrochloride: the drug profile*. *Top Curr Chem* , 1977. **72**: p. 125-148.

213. Wacker, A., et al., *Distribution of C-14 Tilorone in Mice*. Naturwissenschaften, 1972. **59**(11): p. 520.

214. Zinkovsky, V.G., O.V. Zhuk, and S.K. Sumriy, *Pharmacokinetics of a synthetic interferon inducer amixin in mice*. Pharmacol Rep, 2007. **59**(6): p. 739-751.

215. Kleinschmidt, W.J., *Biochemistry of interferon and its inducers*. Ann Rev Biochem, 1972. **41**(10): p. 517-542.

216. Mannering, G.J. and L.B. Deloria, *The pharmacology and toxicology of the interferons: an overview*. Ann Rev Pharmacol Toxicol, 1986. **26**: p. 455-515.

ACKNOWLEDGEMENTS

First and foremost, I would like to thank my supervisor, Jan Lünemann, for giving me the opportunity to perform my doctoral studies in his laboratory. That enabled me to contribute to a variety of projects, many of which were successfully published, to establish international collaborations, and to participate at local and international conferences and student programs, all of which have provided a tremendous boost to my professional as well as personal development.

I would also like to thank Christian Münz for the constant support, scientific advice, supervision, and inspiration throughout the last four years.

For the invaluable opportunity to work with the humanized mouse model I would like to express my gratitude to all people involved in the arduous task of generating and taking care of the mice: Sonja Meixlsperger-Rämer, Patrick Rämer, Obinna Chijioke, Carol Leung, Olga Antsiferova, Ana Raykova, Donal McHugh, Cornelia Gujer, Vanessa Landtwing, Bithi Chatterjee, Debora Häfeli, and the rest of the mouse house team.

My warmest gratitude to our collaborators who contributed to the experimental data used in this thesis: Fabienne Brilot-Turville (University of Sydney) for providing us with complete protocols and materials for the MOG serum reactivity assay; Walter Bossart and Riccarda Capaul (Medical Virology, UZH) for EBV quantification; Stefan Regenass (Clinical Immunology, USZ) for HEp2 staining, CCP and SS-A detection, Nick Willcox (University of Oxford) and Björn Tackenberg (University of Marburg) for MG patient samples; Manuel Comabella (Hospital Universitari Vall d'Hebron) for MS patient samples; Silke Wiesmayr and Kevin Rostasy (University Hospital Innsbruck), Tarik Azzi and David Nadal (Experimental Infectious Diseases and Cancer Research, UZH) for IM and control patient samples; Silvia Behnke (Sophistolab) for tissue histology, European Screening Port for HTS assay expertise.

I would also like to thank Burkhard Becker and Burkhard Ludewig for agreeing to take part in my PhD committee and for providing me with scientific guidance and encouragement.

My four years at the Institute of Experimental Immunology would have not been the amazing time they were without the great friendships that I made. Most importantly, thanks to Michael Maurer, Patrick Weber, Christina Sina, Isaak Quast, Christian Keller, Flavio Cueni, and Deeqa Osman for the great time in the Lünemann lab and the advice, support and help with experimental troubleshooting. Many thanks to Heike Nowag, Olga Antsiferova, Rosa Barreira, Ana Raykova, Vanessa Landtwing, and Donal McHugh for their friendship and support through the common PhD ups-and-downs. Credits to Carol Leung, Susana Romao,

Sonja Meixlsperger-Rämer, Patrick Rämer, Monique Ghannage, Obinna Chijioke, Bithi Chatterjee, and Cornelia Gujer for their expert advice on experiments and life in general; and to Patrick Weber, Anne Müller, Danusia Vanoaica, and Brady Messmer for keeping the lab up and running. Greatly appreciated are also all the other members of the Institute of Experimental Immunology, and all the born and born-to-be lab babies who kept the rumors and excitement in the institute alive.

Next, I would like to express my tremendous gratitude to my family for encouraging me to pursue my dreams away from my home country, for their invaluable support and motivation throughout the years.

Last but not least, I would like to thank Christian Beeler for making my time in Switzerland an unforgettable and life-changing experience, and for providing the balance that made it possible to successfully surmount the difficulties I am encountering on my way.

CURRICULUM VITAE

Name:	Kristina Kakalacheva
Work Email:	kristina.kakalacheva@uzh.ch
Private Email:	k.kakalacheva@gmail.com
Date of Birth:	May 16th, 1986
Nationality:	Bulgarian

EDUCATION

10/2009 – to date	**University of Zurich, Switzerland** PhD in Immunology
09/2008 – 09/2009	**University of Oxford, UK** MSc in Integrated Immunology
09/2005 – 05/2008	**Jacobs University Bremen, Germany** BSc in Biochemistry and Cell Biology
09/2001 – 05/2005	**High School Vasil Levski, Bulgaria** Graduated with diploma in Natural Sciences and Mathematics

PRACTICAL EXPERIENCE

10/2009 – to date	**Institute of Experimental Immunology, University of Zurich, Zurich, Switzerland** Doctoral thesis conducted in the laboratory of Prof. Jan Lünemann on *Epstein-Barr virus: environmental trigger and therapeutic target in autoimmune diseases*. Member of the Microbiology and Immunology track of the Life Sciences Graduate School.
04/2009 – 09/2009	**Jenner Institute, Oxford, UK** Master thesis conducted in the group of Prof. Adrian Hill on the *Induction of Indoleamine 2,3-dioxygenase by tuberculosis vaccines and its impact on vaccine immunogenicity*.
07/2008 – 09/2008	**Swiss Federal Institute of Technology (ETH), Zurich, Switzerland** Participant in the International Biology Undergraduate Summer School, including a two-month research project in the group of Prof. Martin Lössner on the *Characterization of recombinase protein of a novel L. monocytogenes bacteriophage*.
01/2008 – 02/2008	**Max Planck Institute for Marine Microbiology, Bremen, Germany** Guided research in the group of Prof. Antje Boetius on the *Identification of the phylogeny of giant sulfide-oxidizing bacteria*.
09/2007 – 12/2007	**Jacobs University Bremen, Bremen, Germany** Guided research in the group of Prof. Klaudia Brix on the *Determination of the role of lipoprotein receptor-related protein 1 in binding cathepsin B on the surface of migrating keratynocytes*.
07/2007 – 09/2007	**Wellcome Trust Centre for Human Genetics, University of Oxford, Oxford, UK** Internship in the group of Dr. Zoia Larin Monaco on the *Development of human artificial chromosomes for gene therapy*.
06/2006 – 09/2006	**Applied Biocatalysis Research Center, Graz, Austria** Internship in the group of Prof. Anton Glieder on *Cloning and expression of bacterial cytochrome P450 enzymes*.

AWARDS AND HONORS

08/2012	**Merck Serono Innovation Cup** Winner of competition for most innovative business plan on a novel autoimmune disease treatment strategy
06/2012	**RIKEN Research Center for Allergy and Immunology** Awarded funding to attend a summer research program for young scientists in Japan
09/2008 – 09/2009	**Integrated Immunology Bursary Fund** Granted to pursue a Master's degree at the University of Oxford
05/2007 – 05/2008	**Annual Academic Life Steps Financial Grant, American Standard Foundation** Awarded for outstanding academic performance
09/2005 – 05/2008	**Merit-Based Academic Scholarship from Jacobs University Bremen** Granted to pursue a Bachelor's degree

COURSES AND ACTIVITIES

08/2013	**Science and Technology Leadership Association (STeLA) Forum** Workshop aiming at developing leadership skills for students in science and engineering, and facilitating multicultural dialogue on global issues
02/2013 – 06/2013	**Challenges in Drug Discovery and Development, Swiss Biotech Association** Six-module course taught by leaders in the pharmaceutical and biotech industries
08/2012	**Merck Serono Innovation Cup** Challenging competition for development of an innovative business plan involving collaborative teamwork, successful presentation, and proposal defense in front of Merck Serono managers
02/2012 – 06/2012	**Entrepreneurship Course Venture Challenge, ETH Zurich** Lectures by leading entrepreneurs and start-up coaches involving extensive teamwork on the founding of a biotech start-up
08/2011	**Novartis International Biotechnology Leadership Camp (BioCamp)** Workshop on the trends and challenges facing the pharmaceutical industry including teamwork and presentation of a case study on transforming a research finding into a start-up idea

CONFERENCES

04/2013	**Roche Nature Medicine Immunology Symposium, Buonas, Switzerland** Poster presentation
03/2013	**Young Investigators Meeting, Grindelwald, Switzerland** Oral presentation
04/2013	**RIKEN RCAI International Summer Program, Yokohama, Japan** Poster and oral presentation
04/2013	**7th ENII Immunology Spring School, Sardinia, Italy** Poster presentation
01/2012	**Swiss Academy of Sciences Workshop on "How to Improve Animal Experimentation", Rigi Kulm, Switzerland** Poster and oral presentation

04/2011 **XXII Meeting of the Swiss Immunology PhD Students, Schloss Wolfsberg, Switzerland**
Oral presentation

03/2011 **Young Investigators Meeting, Crans-Montana, Switzerland**
Oral presentation

09/2010 **Microbiology and Immunology Life Sciences Graduate School PhD Program Retreat, Ascona, Switzerland**
Oral presentation

PUBLICATIONS

Tracy SI, Kakalacheva K, Lünemann JD, Luzuriaga K, Middeldorp J, Thorley-Lawson DA. **Persistence of Epstein-Barr virus in self-reactive memory B cells.** *J Virol*. 2012 Nov;86(22):12330-40.

Jelcić I, Hsu KC, Kakalacheva K, Breiden P, Dupont B, Uhrberg M, Martin R, Münz C, Lünemann JD. **Killer immunoglobulin-like receptor locus polymorphisms in multiple sclerosis.** *Mult Scler*. 2012 Jul;18(7):951-8.

Comabella M, Kakalacheva K, Río J, Münz C, Montalban X, Lünemann JD. **EBV-specific immune responses in patients with multiple sclerosis responding to IFNβ therapy.** *Mult Scler*. 2012 May;18(5):605-9.

Kakalacheva K, Maurer MA, Tackenberg B, Münz C, Willcox N, Lünemann JD.**Intrathymic Epstein-Barr virus infection is not a prominent feature of myasthenia gravis.** *Ann Neurol*. 2011 Sep;70(3):508-14.

Kakalacheva K, Lünemann JD. **Environmental triggers of multiple sclerosis.** *FEBS Lett*. 2011 Dec 1;585(23):3724-9.

Kakalacheva K, Comabella M. **Epstein-Barr virus and multiple sclerosis: causation or association?** *Future Microbiol*. 2010 Nov;5(11):1617-9.

Kakalacheva K, Münz C, Lünemann JD. **Viral triggers of multiple sclerosis.** *Biochim Biophys Acta*. 2011 Feb;1812(2):132-40.

Comabella M, Montalban X, Kakalacheva K, Osman D, Nimmerjahn F, Tintoré M, Lünemann JD. **B cell expression of the inhibitory Fc gamma receptor is unchanged in early MS.** *J Neuroimmunol*. 2010 Jun;223(1-2):135-7.

Comabella M, Montalban X, Horga A, Messmer B, Kakalacheva K, Strowig T, Caballero E, Münz C, Lünemann JD. **Antiviral immune response in patients with multiple sclerosis and healthy siblings.** *Mult Scler*. 2010 Mar;16(3):355-8.